corewind

Exploration of innovations and breakthroughs of station keeping systems for FOWT

USTUTT, INNOSEA, DTU

August 2022

Disclaimer:

This project has received funding from the European Union's Horizon 2020 Research and Innovation programme under grant agreement No 815083

Project details:

Duration:
1 Sep 2019 - 28 Feb 2023
Grant agreement:

Document information

Deliverable number	D2.3
Deliverable name	Exploration of innovations and breakthroughs of station keeping systems for FOWT
Reviewed by	Pau Trubat (UPC), Climent Molins (UPC), Tim Habekost (UL), Jean-Christophe Gilloteaux (INNOSEA)
Date	August 2022
Work Package and Task	WP2 - Design and optimization of station keeping systems Task 2.3 – Exploration of innovations and breakthroughs of station keeping systems for FOWT
Lead Beneficiary for this Deliverable	USTUTT

Authors

Name	Organisation	E-mail
Lucas Méchinaud	INNOSEA	lucas.mechinaud@innosea.fr
Maxime Chemineau	INNOSEA	maxime.chemineau@innosea.fr
Florian Castillo	INNOSEA	florian.castillo@innosea.fr
Mohammad Youssef Mahfouz	USTUTT	mahfouz@ifb.uni-stuttgart.de
Qi Pan	USTUTT	pan@ifb.uni-stuttgart.de
Leonard Willeke	USTUTT	willeke@ifb.uni-stuttgart.de
Henrik Bredmose	DTU	hbre@dtu.dk
Ozan Gözcü	DTU	ozgo@dtu.dk
Nicolò Pollini	DTU	nipol@dtu.dk

Version control

Version	Date	Author	Description of Changes
00	[12-08-2022]	See above listing	Issued for Internal Review
01	[30-08-2022]	See above listing	First Issuance

Table of contents

1 ABBREVIATION LIST

Abbreviation	Description
AHV	Anchor Handling vessel
ALS	Accidental Limit State
BEM	Blade Element Momentum
BoQ	Bill of Quantities
CA	Consortium Agreement
CAPEX	Capital Expenditure
CFS	Certificate on Financial Statement (audit report)
DEL	Damage Equivalent Load
DLC	Design Load Case
EC	European Commission
EC - GA	(European Commission)-Grant Agreement
EIB	Exploitation and Innovation Board
EU	European Union
FLS	Fatigue Limit State
FOWT	Floating Offshore Wind Turbine
GAGA	General Assembly / Grant Agreement
GC	Gran Canaria
IAB	International Advisory Board
IMS	Intelligent Mooring System
IPB	In-plane Bending
IPR	Intellectual Property Right
LCOE	Levelized Cost of Energy
LRFD	Load and resistance factor design
MB	Morro Bay
MBL	Minimum Breaking Load
NDT	Non-Destructive Testing
OPB	Out of Plane Bending
OPEX	Operational Expenditure
PC	Project Coordinator
PMO	Project Management Office
PR	Periodic Report
ROV	Remotely Operated Vehicle
SF	Safety Factor
SLS	Service Limit State
T&I	Transport and Installation
TDP	Touchdown Point
TFI	Technology From Ideas

TLP	Tension Leg Platform
ULS	Ultimate Limit State
WoB	West of Barra
WP	Work package
WT	Wind turbine
WTG	Wind turbine generator

2 EXECUTIVE SUMMARY

Corewind is a Horizon 2020 project funded and supported by the European Commission, that focuses on cost reduction of floating wind technology through research and optimization of the mooring and anchoring systems, dynamic cables, as well as the improvement of installation, operation and maintenance activities. WP2 of the project focuses on optimization of mooring and anchoring system, from both cost and global performance perspectives. To achieve these objectives, four tasks were identified, and the present report constitutes deliverable 2.3: Innovation and breakthroughs of station keeping systems explored for FOWT. Four subtasks were identified to improve design and optimize systems. This report follows Deliverable D2.2 [1] which focused on designing and optimizing mooring systems for the three sites and the two floaters of the project. Several comparisons with this deliverable are done in this report, as well as useful references to avoid repetition.

To improve the design of mooring systems and optimize it from an economic perspective, subtask 2.3.1 focused on peak load reduction systems. Two systems were studied, one acting as a spring, and the other one as a damper. Mooring systems including those devices were compared to initial moorings to evaluate their potential benefices. . Analysis revealed that those systems allow to reduce up to 50% the tension in the line, allowing to reduce lines sizes. Conversely, the unit costs of those systems tend to reduce benefits from a cost perspective, leading to either increase or decrease of overall costs depending on the platform and site. FLS analysis was also performed with those systems, to assess benefit on the lifetime of a single line of the mooring, but results were not satisfying at this stage, and further studies would be required.

To propose a cost-effective and low-footprint mooring configurations, subtask 2.3.2 focused on the impact of three parameters: the ratio pretension over MBL, the ratio laying line length over hanging line length, and the use of clump weights. The use of clump weights showed a good improvement regarding mooring footprint, as well as for mooring tensions, particularly under extreme conditions, but it implies an increase of both motions and fatigue damage. The tension ratio shows promising results with respect to floater motions but tends to increase line length and mooring footprint. Eventually, length ratio does not show significant impact.

Fatigue analysis, performed as part of D2.2 [1] and in this report, shows that it could drive mooring designs for some sites. As a consequence, subtask 2.3.3 investigates the possibility of tuning the controller to reduce the fatigue. Different approaches are studied: First by keeping PI controller and by adapting Kp, Ki and both of them at the same time. In a second time, PI controller is changed to include the feed-in of the nacelle fore-aft velocity. The analysis shows how blade pitch controller influences drastically the resulting Damage Equivalent Load (DEL) . The most promising result from first test is the change of both Kp and Ki, leading to up to 6% DEL reduction, even though a power loss of 7% is observed. Individual increase of these gains provides ambivalent effect. Second approach with feed-in of the nacelle fore-aft velocity shows a DEL reduction of up to 5% in the main line, with a power loss of only 2%. In both case side line DEL slightly increased.

Eventually, innovative mooring layouts, such as shared anchor and shared mooring lines, were studied in subtask 2.3.4. It was found that shared anchor layouts were technically feasible, but did not improve the total mooring system costs, due to spacing constraints forcing to increase line lengths. Nevertheless, installation costs were not taken into account, and further studies could be considered to improve those results. Shared mooring lines layout was found to largely decrease global costs compared to the optimized mooring found in D2.2 [1], by decreasing the number of anchors and buoys needed to respect the criteria. Moreover, an ALS study showed that no risks of domino effect was expected after a shared line failure. A simple modal analysis was also carried out and showed that several mode frequencies of the system can correspond to wave frequencies, but not 1P frequencies of the turbines.

The shared mooring line design optimization by means of a surrogate model in Morro Bay site is studied in subtask 2.3.4. The surrogate model is generated using HAWC2 simulation results where equilibrium points and response analyses are performed. Results showed that tension forces at the mooring lines in fore-aft direction is affected most by the length of shared mooring lines. The surrogate model is able to estimate the responses very accurately and suitable for optimization purposes.

3 INTRODUCTION

3.1 Introduction

Floating offshore wind is still a nascent technology and its LCOE is substantially higher than onshore and bottom-fixed offshore wind, and thus requires to be drastically reduced.

The COREWIND project aims to achieve significant cost reductions and enhance performance of floating wind technology through the research and optimization of mooring and anchoring systems and dynamic cables. These enhancements will be assessed and validated by means of simulations and experimental testing both in the wave basin tanks and the wind tunnel by taking as reference two concrete-based floater concepts (semi-submersible and spar) supporting large wind turbines (15 MW), installed at water depths greater than 100 m and 200 m for the semi-submersible and spar concept, respectively.

Within this project, Work Package 2 (WP2) main objective is to optimize mooring and anchoring systems from both costs and performances perspectives. At the end, partners will deliver guidelines and recommendations from lessons learned, key findings and new knowledge accumulated during the different tasks, to improve cost competitiveness of floating wind. The present report is dedicated to task 2.3 of the WP2, focusing on exploration of innovations and breakthroughs of station keeping systems for FOWT. It follows deliverable D2.1 [2], which addressed a review of the state of the art of mooring and anchoring designs, technical challenges and identification of relevant DLCs, and D2.2[1] dedicated to the design analysis and optimization of mooring and anchoring system for floating wind turbines. It will be followed by another deliverable summarizing works carried out during the project, addressing design practices and guidelines (D2.4).

The work presented in this deliverable focused on two types of foundations, the semisubmersible ActiveFloat developed by COBRA Esteyco, and the spar-buoy WindCrete developed by UPC. Three sites were investigated, with different environmental conditions, West of Barra (Scotland), Gran Canaria (Canaria Islands, Spain) and Morro Bay (California, USA). Some works presented below focus on some cases only.

3.2 Objective

The goal of the report is to satisfy task 2.3 as part of the WP2 of the Corewind project. The objective of this task is to investigate innovative and disruptive technologies, in order to mitigate obstacles identified for mooring systems (regarding components, systems and processes). This report follows report D2.2 [1], refers to it and uses tools defined in it. To achieve this objective, four topics of interest were identified.

Subtask 2.3.1 aims at studying the use of peak load reduction systems. These devices are designed to reduce peak load tensions observed within mooring lines. This analysis aims at evaluating their benefits, mainly for Ultimate Limit State (ULS) and additionally for Fatigue Limit State (FLS), from an economic point of view. It is expected that their use will allow a reduction of mooring system size (chain grade and Minimum Breaking Load) and to improve lifetime. The dynamic of the floater is also assessed to ensure respect of design criteria established (maximum offset).

To reduce overall mooring lines costs, subtask 2.3.2 investigates various solutions to reduce mooring footprint. These solutions consist in the use of different size clump weight, the modification of the ratio pretension over MBL, and the change of the ratio between the length of the line laying on the seabed and the hanging part of the line. In addition to the footprint, the dynamic of the floater with these changes is assessed.

As underlined in the results presented in deliverable D2.2 [1], fatigue could drive mooring designs in some conditions. Hence, subtask 2.3.3 investigates the benefit of tuning of the controller, to reduce mooring fatigue. To do so, different types of control strategy are investigated, and their impact of mooring damage is assessed.

In addition, fatigue damage of other components (blade, tower) is also analysed to ensure that what benefits to the mooring will not prejudicate other parts of the system.

To reduce the total anchor costs, subtask 2.3.4 investigates innovative layout such as shared anchor and shared mooring lines configurations. An optimization on mooring lines materials is carried out in order to explore costs benefits of these layouts. For the shared mooring lines configuration, an Accidental Limit State analysis is conducted in order to evaluate the risks of a line failure. Finally, through a modal analysis, mode frequencies of the shared mooring lines system are compared with exterior loads frequencies.

4 REFERENCE FRAMES

4.1 Global reference frame

The global reference frame is defined as follows:

- Origin O is defined at the intersection of the floater centreline and the Mean Sea Level (MSL);
- X-axis is directed in the wind, wave and current direction at an angle of 0° as defined in Figure 4-1
- Z-axis is directed vertically upwards;
- Y-axis is defined so that the global reference frame is a Cartesian direct coordinate system.

The angle of the wave (β), current (δ) and wind (γ) directions are illustrated in Figure 4-1.

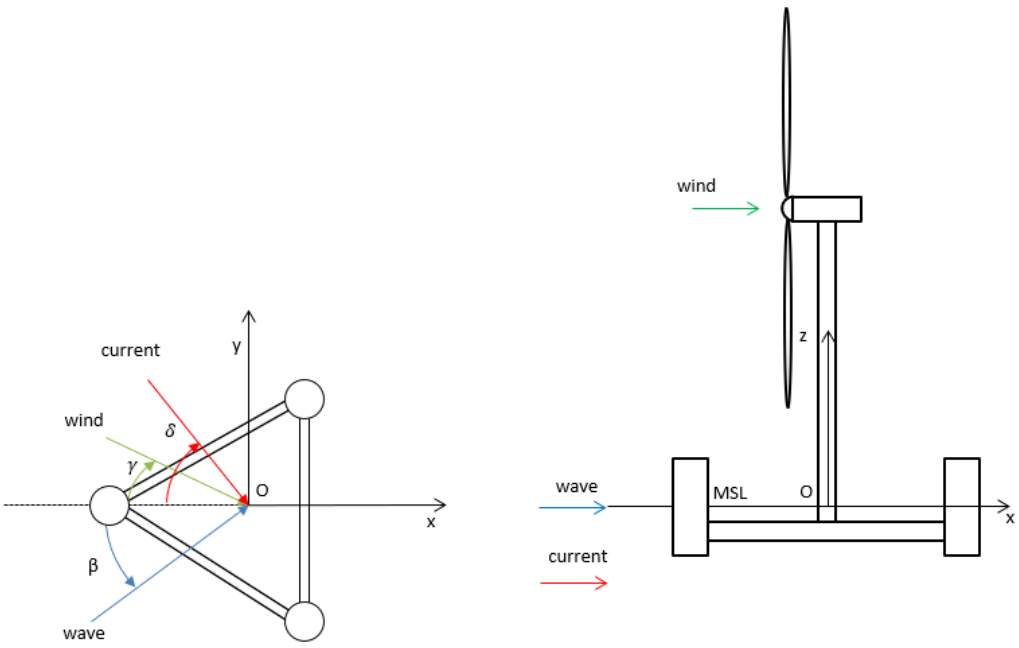

Figure 4-1: Illustration of the global reference frame

It must be noted that the direction 0 deg in OrcaFlex does not necessary corresponds to the geographic north. Indeed, it was assumed that the main line is aligned with the main environmental direction.

4.2 Local reference frame

The local reference frame xyz before launching simulation is identical to the global reference frame, i.e.:

- Origin O is defined at the intersection of the floater centerline and the Mean Sea Level (MSL);
- x-axis is directed in the wind, wave and current direction at an angle of 0° as defined in Figure 4-1;
- z-axis is directed vertically upwards;
- y-axis is defined so that the global reference frame is a Cartesian direct coordinate system.

When external forces are applied to the floater, the local reference frame does no longer coincide with the global reference frame. The local reference frame follows the FOWT motions but moves with the floater.

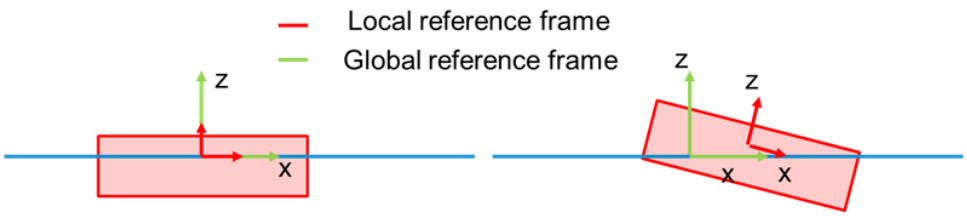

Figure 4-2: Difference between global reference frame and local reference frame

5 SOFTWARES

5.1 Coupled analysis softwares

5.1.1 OrcaFlex

OrcaFlex is a software developed by Orcina [3], that allows to perform dynamic analysis for offshore marine systems. It is often preferred to OpenFAST to model the mooring systems of offshore floating wind turbines for its versatility and different features. In addition, OrcaFlex has a python interface – OrcFxAPI – that is very useful for pre-processing and post-processing, aside of the development of a routine for the optimization of the mooring systems (more details in section 5.2.).

Major feature of OrcaFlex is for the composition of the lines, that can be divided in different sections that are modeled using a *Line Type*. Such object gathers the line properties: mass, axial stiffness, diameters, etc. A *Line Type* can be completely set by the user, or created using a Wizard. It is an interface integrated to OrcaFlex that has its own database to be able to set up a *Line Type* based on a selected material and diameter.

OrcaFlex also offers an integrated tool to perform fatigue analysis either time-domain analysis, based on usual rainflow counting algorithm, or frequency-domain analysis. Inputs required are a T-N curve and a list of exposure times per load case analysed. Outputs are the damage values per arclength, and estimations of total damage and total lifetime.

For production load cases simulations, it is now possible to model the turbine in OrcaFlex. This update features a model of the tower as a *Line Type* and a new object dedicated to the *Turbine*. Blades can be set as rigid or flexible, and can be added an external controller for the blade pitch and generator torque.

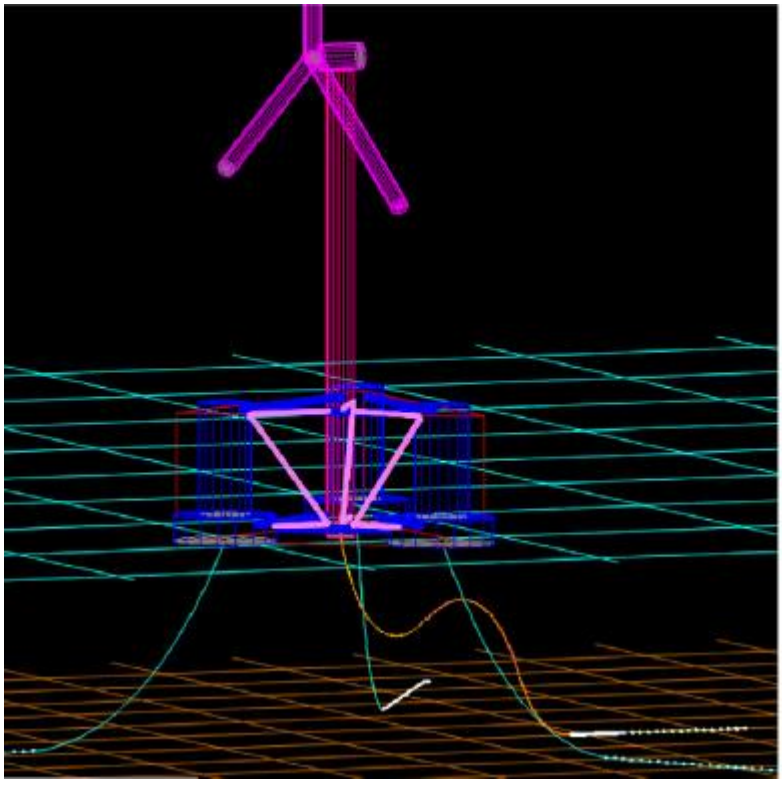

Figure 5-1: View of OC4 model set-up with Orcaflex

5.1.2 OpenFAST

OpenFAST code is an opensource code developed by the National Renewable Energy Laboratory (NREL) that allows to model land-based, fixed-bottom offshore and floating offshore wind turbine. OpenFAST offers the possibility to perform coupled analyses with aero-servo-hydro and elastic modules. Information can be found on NREL website and OpenFast Github [4,5]. In this project, OpenFAST is used to generate time-series representing aerodynamic loads applied in OrcaFlex. Results from OpenFAST models defined by partners are also used to be compared with those obtained with OrcaFlex.

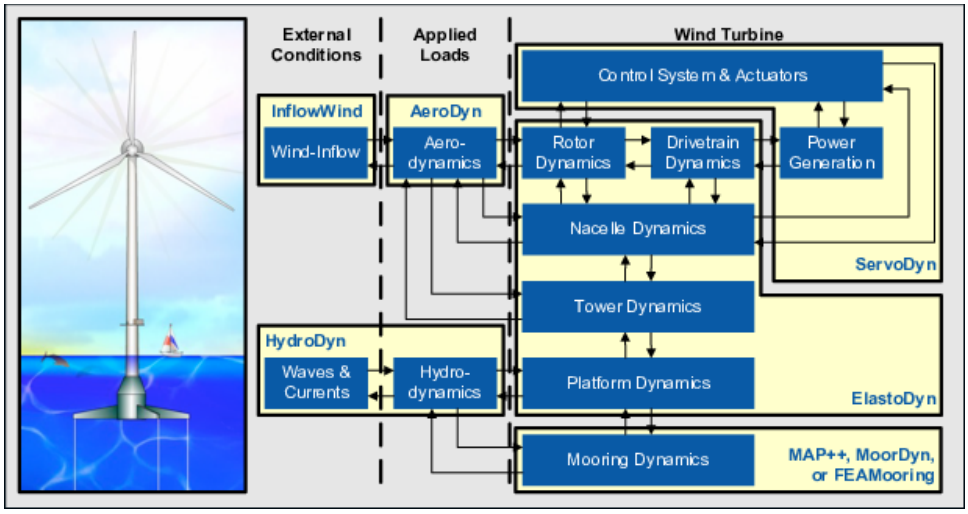

Figure 5-2: OpenFAST Modules desciption

OpenFAST is based on different modules responsible for different parts of the simulations:

- **AeroDyn** is an aerodynamics software library (module) for use by designers of horizontal-axis wind turbines. It is designed to be interfaced with FAST for aero-elastic analysis of wind turbine models. The aerodynamics model in AeroDyn is based on Blade Element Momentum (BEM) theory (with modifications to improve accuracy in yawed flow).
- **InflowWind** is a FAST module that allows to process wind-inflow, either steady wind model internally calculated or using various types of input files (uniform, binary TurbSim full-field, binary bladed-style FF, binary HAWC wind files).
- **Elastodyn** is a structural-dynamic model for horizontal-axis wind turbines based on modal superposition theory. It includes structural models of the rotor, drivetrain, nacelle, tower and platform.
- **HydroDyn** is a time-domain hydrodynamics module that has been coupled with FAST to enable aero-hydro-servo-elastic simulation of offshore wind turbines. HydroDyn allows for multiple approaches for calculating the hydrodynamic loads on a structure: a linear potential-flow theory solution, a strip-theory solution, or a combination of both. Hydrodyn requires importing the hydrodynamic database in frequency domain obtained by a potential flow solver (e.g., NEMOH).
- **ServoDyn** is a control and electrical-drive model for wind turbines. It includes control and electrical-drive models for blade pitch, generator torque, nacelle yaw, high-speed shaft brake and blade-tip brakes. ServoDyn can use an external controller defined by a DLL, so-called “Bladed-style” because it uses the same communication scheme as DNV GL’s Bladed.
- MoorDyn is a lumped—mass mooring line model that could be coupled with OpenFast. It allows to perform dynamic analysis of moorings for floating offshore structures. It accounts for internal axial stiffness, damping forces, weight and buoyancy. Hydrodynamic loads are applied using Morison equation. .
- The **TurbSim** stochastic inflow turbulence tool has been developed by NREL to enable the numerical

simulation of a full-field flow that contains coherent turbulence structures. The purpose of TurbSim is to provide the wind turbine designer with the ability to drive FAST simulations of advanced turbine designs with simulated inflow turbulence environments that incorporate many of the important fluid dynamic features known to adversely affect turbine aero-elastic response and loading. TurbSim is used in pre-processing, before FAST simulations.

BModes is a finite-element code that provides dynamically coupled modes for a beam. The beam can be a rotor blade, rotating or non-rotating, or a tower. Both the blades and tower can have a tip attachment. The tip attachment is assumed to be a rigid body with mass, six moments of inertia, and a mass centroid that may be offset from the blade or tower axis. In addition to the tip inertia, the tower can also have tension-wire supports. Both the tip inertias and tension-wire support can substantially influence the coupled modes mentioned earlier, especially for a tower. BModes is used in pre-processing, before FAST simulations.

OpenFAST will be used for the station keeping simulations coupled with Orcaflex in particular for the floater global performance and part of the software package to evaluate the floater excursions.

5.1.3 HAWC2

HAWC2 [6] is an aero-servo-hydro-elastic wind turbine analysis code developed by DTU Wind and Energy Systems. It can model general structures such as turbines with multiple rotors, any floater or tower shape therefore any turbine type can be modeled in HAWC2. Below figure shows the different levels of the wind turbine models starting from bottom fixed turbine (aero-servo-elasticity) to floating wind turbine (aero-hydro-servo-elasticity) and the required HAWC2 modules to model them.

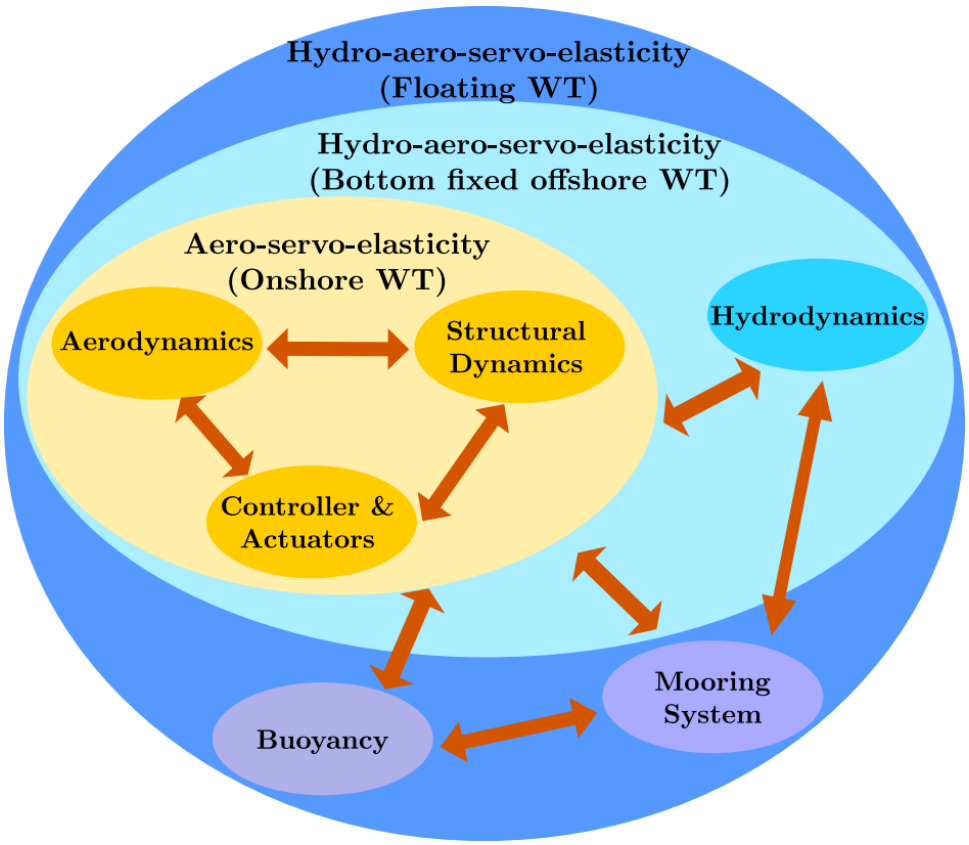

Figure 5-3: Wind turbine load computation sub-modules for different turbine configurations.

Important features of HAWC2 modules can be listed as:

Aerodynamic: It uses Blade Element Momentum theory [7] and extended from the classic approach to handle dynamic inflow, dynamic stall, skew inflow, shear effects on the induction and effects from large deflections. It can also include some corrections for swept effects [8]. Users can use higher fidelity aerodynamic solvers such as Ellipsys or MIRAS when they couple their aerodynamic solvers with HAWC2 multibody solver.

Structure: It uses multibody dynamic formulation [9] with linear Timoshenko beams for turbine structures. It can capture geometrically non-linear effects and can model material coupling effects. External super-elements can also be called by HAWC2 to represent structures modeled outside of HAWC2.

Control: The controller, generator and servo systems are defined as an external dynamic link library (dll).

Hydrodynamic: The hydrodynamic loads are computed either through the Morison equation in its full form, or by using the WAMIT [10] frequency response functions for the radiation and diffraction forces combined with the Morison drag.

Mooring system: Mooring line dynamics are computed by an external dll developed by DTU Wind and Energy Systems. They are modelled as truss structures for load carrying mooring lines and the cables are modeled by including both axial and bending stiffness.

Environmental conditions: HAWC2 uses different wind and hydro conditions, some of them are computed in HAWC2 and some are read from an external file such as Mann turbulence box. It can model turbines under turbulent wind with wind shear, yaw, gust and at sea states with irregular waves and current.

5.2 Optimization screening tool

5.2.1 Python optimization library

To perform the optimization of the moorings equipped with peak loads reduction systems, a tool was developed on python. The benderopt library is used. It is a black box optimization library, generally used to optimize a function whom gradient cannot be computed. More information regarding this library can be found online [11].

The multiprocessing library was used to perform parallel computations. This is allowed by the construction of the benderopt library, new sample of mooring parameters being chosen based on past results stored in a vector. As a consequence, several samples can be run in parallel before being added simultaneously in the result vector. Additionally, a user interface has been developed using the PySimpleGUI library [12]. Eventually, several usual libraries were used (numpy, scipy, time, etc.).

6 BREAKTHROUGH ANALYSIS / TECHNOLOGICAL BENEFITS REGARDING PEAK LOADS REDUCTION

In this first subtask, two different peak loads reduction systems have been selected in order to investigate potential benefits for the mooring system cost. Indeed, those systems should allow to reduce the size of the mooring lines as a consequence of the peak loads reductions. TFI and IMS systems have been selected because the technology owners accepted to share all the data needed to perform mooring optimizations with OrcaFlex and the optimization screening tool developed, using cost functions and variable stiffnesses both depending on the size of the system implemented.

In this section, are briefly presented the two peak load reduction systems properties, then the optimization strategy is detailed, as well as the modelling of the system. To proceed, the optimized mooring designs are presented for each floater and site. Finally, is presented a brief investigation of the fatigue in the moorings equipped with TFI or IMS.

6.1 Peak loads reduction systems presentation

6.1.1 TFI Spring system

The TFI spring system is a technology developed by Irish company Technology From Ideas. It is a tailored shaped plastic spring with a steel structure that can be added on the mooring lines of a floating platform, to change the mooring system response and reduce the peak loads. It features a variable axial stiffness and that acts as a shock absorber. Figure 6-1 is an illustration of the technology. It fits in any mooring type (catenary, semi-taut, TLP) and works with any line material (chain, rope, synthetic fibre).

Figure 6-1: TFI system.

The following figure is an example of load-extension curve of the TFI. It depends on its MBL, that increases with the size and weight of the system.

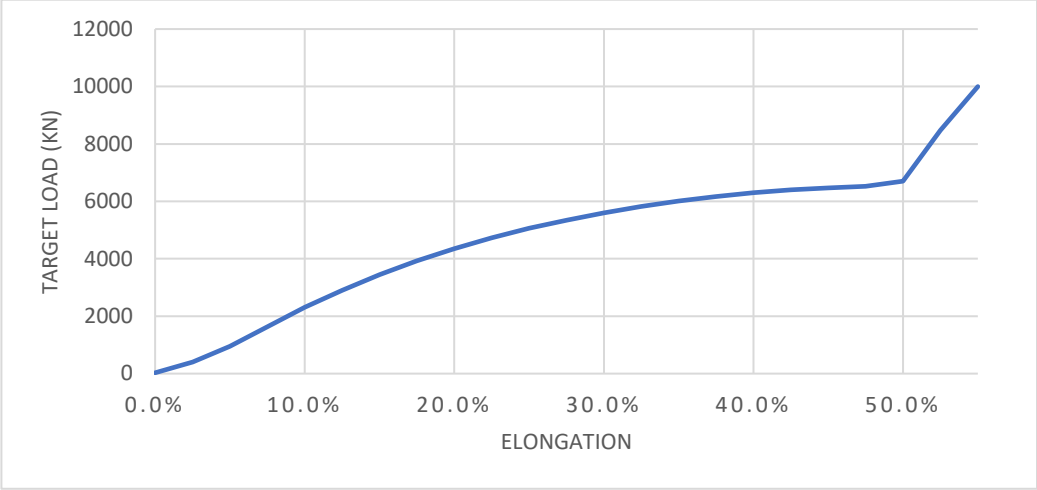

Figure 6-2: Example of load-extension curve of TFI.

6.1.2 Intelligent Mooring System

The Intelligent Mooring System or IMS is a more complex system developped by the British company Intelligent Moorings Limited. Detailed information about the technology can be found in [13]. Figure 6-3 shows a prototype of IMS at a reduced scale.

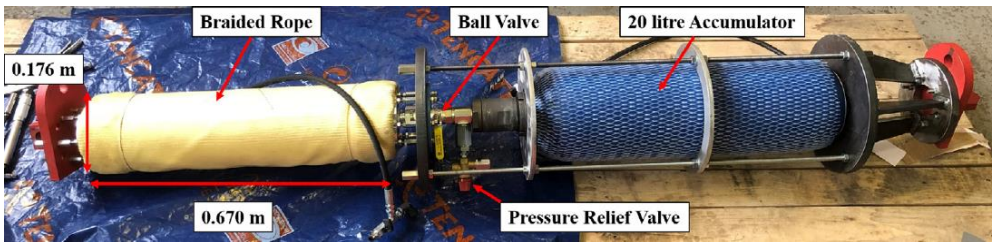

Figure 6-3: IMS prototype.

The system is divided into two parts: a hollow braided rope housing a pressurized water filled bladder, and an accumulator charged with gas. When the rope extends under tension the volume in the bladder compresses, so that the water is transferred to the accumulator. This acts as a shock absorber, with the particularity that the pressure in the accumulator can be pre-set at different levels. This allows for one system to have numerous load-extension curves.

Naturally, this system has also a variable axial stiffness. Figure 6-4 is an example of load extension typical curve for the IMS.

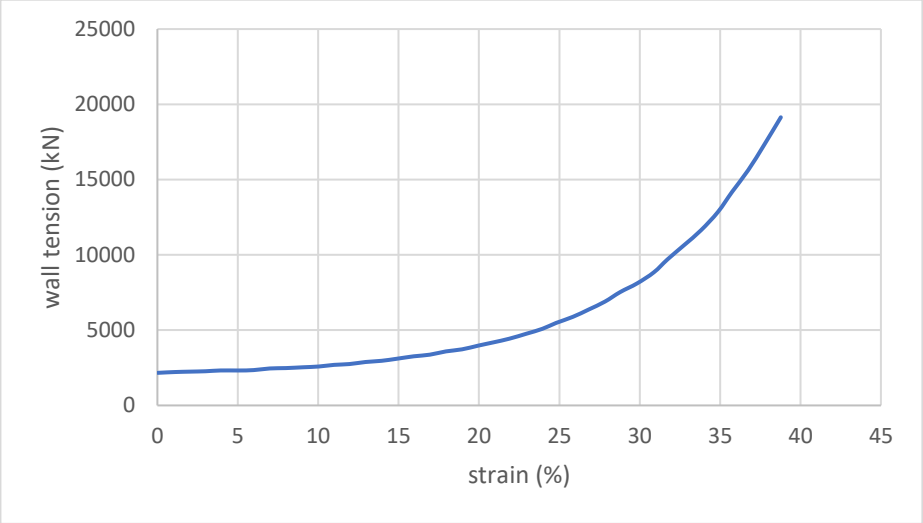

Figure 6-4: Example of load-extension curve of IMS

6.2 Optimization strategy

Design of mooring system is a complex and time-consuming task. Usually, a design phase will consist of several iterations between which mooring parameters (diameter, materials) will be updated to obtain a reliable and cost-effective mooring system.

Therefore, the automatization of this screening process should allow mooring designers to cover a larger design space while reducing time and costs allocated to this task, besides making sure to find an optimized mooring system within the design space. It is particularly useful for sensitivity analysis of the peak loads mooring systems.

The following section aims at presenting the methodology developed to automatize this process. In addition, section 6.4 of deliverable D2.2 [1] is dedicated to a simple mooring design case that aims to verify the accuracy of the optimization screening tool.

6.2.1 Global approach

The mooring system is validated through the analysis of DLCs 6.1 and 6.2 (ULS) as defined in [14]. The most critical load case in term of design tensions in the mooring lines is identified by performing simulations of all DLCs 6.1 and 6.2 and is then used for the mooring optimization.

Different parameters can be optimized such as materials used, materials properties, line length, etc. To simplify the optimization, the layout and the type of materials (chain or synthetic) composing the mooring system are set and fixed before optimization.

The OrcaFlex model used during this task is a simplified one. Only the substructure is modelled, and the aerodynamic loads are OpenFast time-series applied to the RNA. Tower and RNA lump masses and inertias are considered.

One iteration of the optimization is composed of two analyses: one based on start-of-life hypothesis, and one on end-of-life hypothesis (marine growth and corrosion are accounted for on the mooring lines). Both are required for validation of the mooring, the first being usually limiting regarding maximum offset of the platform, and the other limiting regarding maximum tension criterion in the mooring lines. To save time, all design criteria and constraints are checked after the start of life simulation, and the end-of-life simulation is run only if all criteria and constraints are met.

A python script uses the OrcaFxAPI to set up the OrcaFlex models, modify the mooring lines for the end-of-life simulations, extract the results for verification of the criteria and constraints, and estimate the total cost of the mooring system. If one of the criteria or constraints isn't met, the total cost is set to 99999999$. Then, the Benderopt black box library is used to iterate and generate a new sample of mooring parameters.

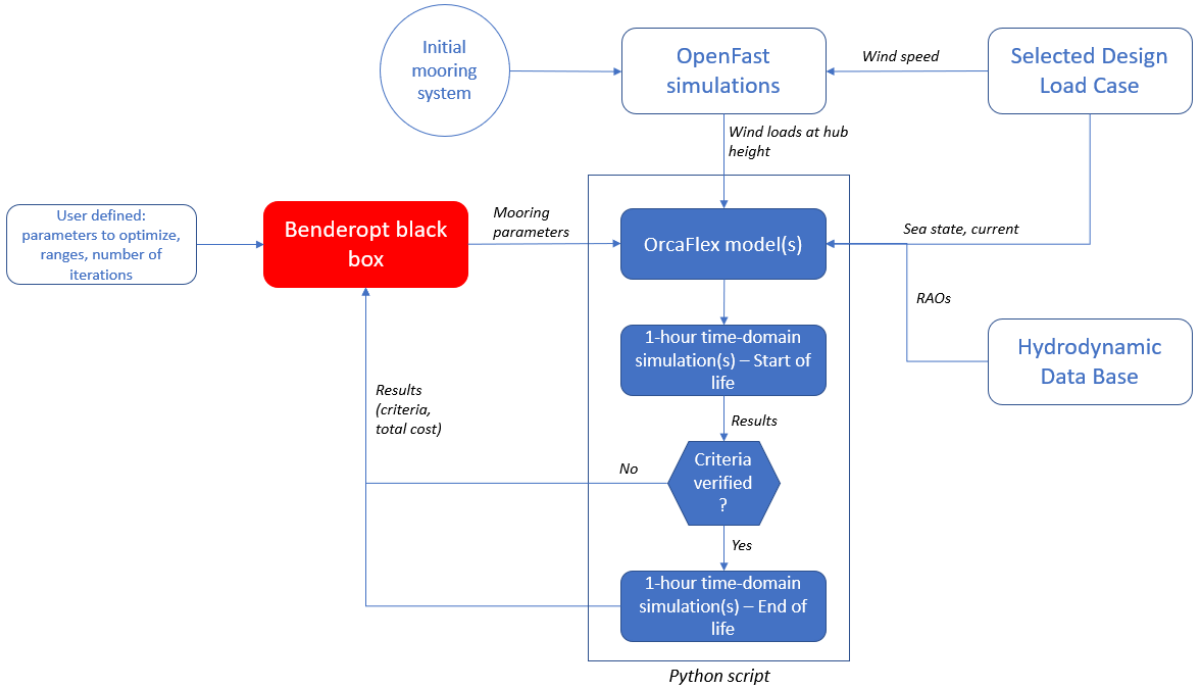

Figure 6-5: Optimization screening tool routine.

Once optimized, the integrity of the new mooring system is verified for each case of the DLC 6.1 and 6.2 using this simplified model, before being assessed using an OpenFAST fully coupled model.

6.2.2 Design parameters

The design variables are:

- Diameters,
- Chain grade,
- Line length,
- Section lengths,
- Anchor radius coefficient (find more details in Report D2.2),
- Number of peak loads reduction systems (TFI or IMS),
- MBL of the peak loads reduction systems,
- For IMS, the pressure in the accumulator.

A user interface has been developed within the python script to make the optimization tool easier to manipulate.

Depending on sites and environmental conditions, it is possible to optimize independently each line to avoid oversizing it. The tool developed during the project has the capability to treat independently each line by defining some groups of lines. Parameters presented in this section are then optimized for each group. During the project up to three groups have been used.

For each optimized parameter considered, the range of values to be tested is set in-between a lower and a higher bound, as well as the step.

More details are available in deliverable D2.2 [1].

6.2.3 Cost functions

The cost function used within this project is based on material procurement costs. It includes chain, synthetic materials, peak loads reduction systems, eventual clump weights and anchors. The cost function does not include installation costs which is a limiting hypothesis when comparing different layouts.

To sum costs a conversion rate of 0.93€/$ is applied, corresponding to conversion rate from March 2020 [15].

Chain cost is a function of the minimum breaking load (MBL). This approach allows to optimize the grade of the mooring chain. At equivalent diameter, the MBL increases with the grade.

Two synthetic materials have been tested during the project, polyester, and nylon fibres. Costs for these two materials are function of the MBL.

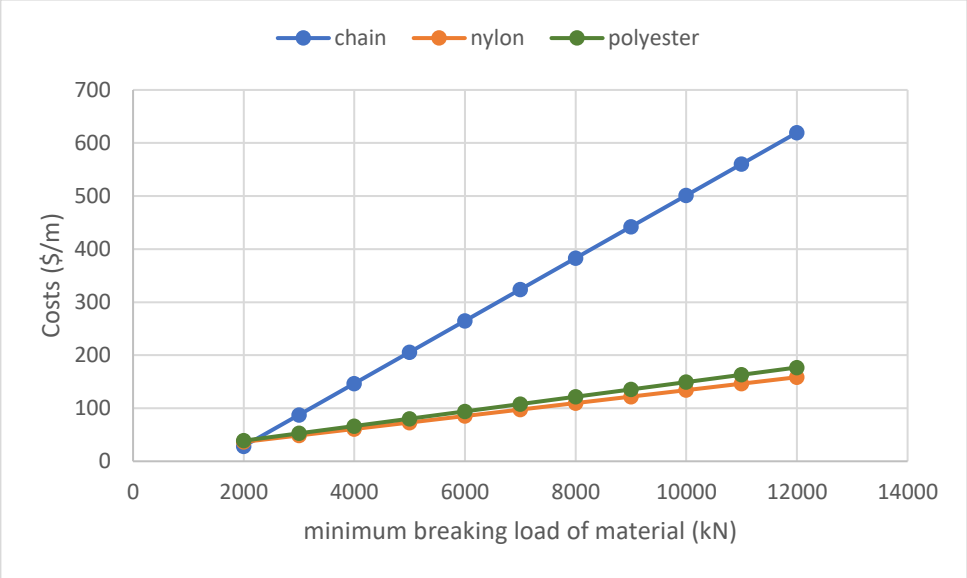

Figure 6-6: Cost functions for the chain, nylon and polyester line sections

Details about the anchors and clump weights cost estimation is available in deliverable D2.2 section 6.2.3 [1]. Anchors cost is based on drag-embedded anchors and is a function of the MBL of Chain connected to the anchor.

Cost functions of the TFI and IMS cannot be communicated, but it can be said that the cost function of the TFI is MBL dependent, and the cost of the IMS is MBL-independent.

6.2.4 Constraints

The mooring system directly influences platform motions, and a certain amount of design limits must be defined.

The following constraints are used. The first ones are defined in the Design Basis [16].

The offset criteria are based on excursion restrictions.

Horizontal offset (WTG shutdown). Maximum during parked conditions	
DoF / Limit typology	**Limit**
Excursion restrictions (100 m)	30 m
Excursion restrictions (200 m)	60 m
Excursion restrictions (870 m)	104 m

Table 6-1: Maximum horizontal offsets as function of water depth.

In addition, pitch and roll maximum angles are checked.

Limit for	Windcrete	Activefloat
OPERATION		
Yaw (10 min. max)	<15º	
Yaw (10 min. std)	<3º	
Pitch (max.)	[-5.5º, +5.5º]	[-5.0º, +5.0º]
Pitch (10 min. average)	[-4.0º, +4.0º]	[-2.0º, +2.0º]
Roll (max.)	[-3.5º, +3.5º]	[-2.0º, +2.0º]
Pitch (10 min. std)	<1º	
Roll (10 min. std)	<1º	<0.4º
IDLING CONDITION		
Pitch (10 min. average)	[-5º, +5º]	
Pitch (10 min. max)	[-7º, +7º]	
EMERGENCY STOP		
Max. pitch	[-15º, +15º]	

Table 6-2: Roll and pitch limits in cases of operation, idling and emergency stop.

Accelerations are evaluated at RNA CoG.

ACCELERATIONS LIMITS		
	Windcrete	**Activefloat**
Operation (acc. XY / acc. Z)	2.94 m/s^2 (0.3 g)	2.94 m/s^2 (0.3 g)
Survival (acc. XY / acc. Z)	4.41 m/s^2 (0.45g)	4.41 m/s^2 (0.45g)

Table 6-3: Maximum horizontal accelerations for the two floaters.

In addition, the mooring line integrity is assessed following recommendations from the DNVGL-ST-0119 [17]. Design criteria on the tensions is detailed in deliverable D2.2, section 6.2.4 [1]. The formula for the design tension is given by:

$$T_d = \gamma_{mean} \times T_{mean} + \gamma_{dyn} \times (T_{dyn} - T_{mean})$$

Where γ_{mean} and γ_{dyn} are respectively the mean and dynamic load factor and T_{dyn} and T_{mean} respectively the dynamic and mean characteristic tension. In ULS and consequence class 1, $\gamma_{mean} = 1.3$ and $\gamma_{mean} = 1.75$ [17].

To fullfill standard requirements, the design tension must respect:

$$T_d < 0.95 \times MBL$$

Where MBL is the minimum breaking load of the material composing the line.

Some additional constraints were added, though not defined within standards or in the design basis, regarding minimum line length laying on the seabed, minimum yaw mooring stiffness, seabed clearance in case of synthetic materials. Detailed information is available in deliverable D2.2 section 6.2.4 [1].

6.2.5 End-of-life analysis

A lifetime of 27 years is required for ActiveFloat, and 25 years for WindCrete. During the entire life of the FOWT, the mooring system must withstand extreme environmental conditions. The lines are subjected to corrosion (diminution of the chain diameters) and marine growth (increase of lines weights and corresponding drag coefficients). Such analysis must be done, they are called End-of-life analysis.

Corrosion allowance requirements as well as marine growth recommendations are specified in the DNVGL-OS-E301 [18]. More detailed information about the End-of-life analysis is available in deliverable D2.2 section 6.2.5 [1].

6.3 Modelling

6.3.1 Floater modelling

The floater is modelled using 6D buoys with drag coefficients attached on the columns, and using a hydrodynamic database for the wave loads and hydrodynamic coefficients. All data was shared by Corewind partners from Cobra and UPC.

6.3.2 Turbine modelling

The tower and RNA are modelled in OrcaFlex as *6D buoys* lump masses. Hub, rotor and tower masses and inertias are specified. The transition piece is considered part of the floater model.

6.3.3 Mooring lines modelling

The mooring lines are modelled using *Line Types* in OrcaFlex. Lines can be divided into different sections of different materials and refinement.

Chain sections are modelled using the wizard module from OrcaFlex. From the chain bar diameter, OrcaFlex calculates all the line properties (weight in air, axial stiffness, equivalent diameter, etc).

Nylon sections are modelled using the variable axial stiffness and weight values of the Viking Braidline developed by Bridon [19].

Polyester sections are modelled with a constant axial stiffness. The polyester used is the DeepRope polyester Acordis Polyester 855TN, developed by Bexco [20].

Both TFI and IMS are modelled as *Line Types* featuring a variable axial stiffness that depends on the MBL of the system. IMS concept designer has shared load-extension curves (in %MBL) for different pre-charge pressures and pre-loading, notes for weight and length estimations, and examples of *Line Types*. TFI concept designer has shared a spreadsheet that contains formulas to get the axial stiffness, weight and length of the system in function of its MBL.

6.3.4 Loads modelling

Wind loads are modelled using time-series applied at the tower top. These loads are computed using OpenFAST. OpenFAST models used are based on those presented in deliverable D1.3 [21]. However, floating substructure degrees of freedom were blocked, and the turbine was considered as a rigid body. More information about the models is available in section 6.3.

Irregular sea state is modelled in OrcaFlex with a JONSWAP spectrum. Hs, Tp, main direction and wave seeds number are specified. Wave-structure interactions are modelled with the potential flow theory. It considers first order wave loads by solving a linearized boundary value problem for inviscid, incompressible flow about a rigid body. Both Froude-Krylov Forces and Diffraction Forces are included in the potential flow model.

Potential flow theory is applicable to floating bodies which have a large characteristic length in comparison to the incoming wavelength. A drag coefficient has been attached to the columns to account for the viscous effects that are not negligible. It complete the HDB attached to the full hull of the floater.

Current loads are modelled using a specified current speed profile as detailed in the Corewind Design Basis [16].

6.4 Optimized mooring designs

For each site and floater, the TFI and IMS systems were implemented on the top sections of each line of the optimized mooring systems presented in deliverable D2.2 [1]. Then, a new loop of optimization using the screening tool presented in section 6.2 was performed to obtain another optimized mooring system equipped with TFI or IMS.

For both TFI and IMS-equipped mooring systems of all three sites and two floaters, simulations corresponding to DLC 6.1 and DLC 6.2 were performed. For each case, maximum design tensions (as defined in DNVGL-ST-0119 [17]) were extracted and compared to the line materials minimum breaking loads. In addition, maximum dynamic offsets (platform displacement relatively to static position without wind, waves and current) in each degree of freedom were calculated. Also, maximum horizontal nacelle accelerations were extracted, as well as the maximum pitch and yaw movements of the platform. Both start of life and end of life analysis (including corrosion and marine growth as defined within the design basis) were performed.

In addition, for Windcrete, maximum pretensions of 2,0MN at the fairleads of the lines and minimum yaw mooring stiffness of the mooring (370,0 MN.m/rad for site B Gran Canaria and 570,0 MN.m/rad for site C Morro Bay) have been set as limiting parameters for the optimization, to make sure that the yaw constraint will not be reached in other DLCs.

Mooring costs calculations are simple estimations used for comparison between tested configurations. Final costs estimations will be performed within WP6. It has to be noted that a conversion rate of 0.93 between dollar and euro has been used (conversion rate from 23/03/2020) [15].

6.4.1 ActiveFloat site A – West of Barra

- TFI-equipped mooring system

For this site, it was chosen to keep the number of 12 lines, nylon section lengths and clump weights arrangement from the optimized mooring system described in deliverable D2.2 [1]. The nylon is also the nylon Viking Braidline developed by Bridon [19].

Table 6-4 summarizes the physical properties of the chain and nylon sections used for all 12 mooring lines. The lines are separated in two groups: six upwind lines and six downwind lines.

Group of lines	Material	diameter [mm]	Equivalent diameter [mm]	Line Length [m]	Dry mass per meter length [kg/m]	Axial stiffness [kN]	Steel Grade
Upwind lines	Chain	114,00	225,00	227,50	310,94	1,334e6	R4
	Nylon	240,00	198,75	147,50	35,20	Variable	-
Downwind lines	Chain	100,00	225,00	333,00	310,94	1,334e6	R4S
	Nylon	240,00	198,75	87,00	35,20	Variable	-

Table 6-4: ActiveFloat West of Barra: Physical properties of the material used in the optimized mooring system.

Figure 6-8 and Figure 6-9 are 3D views from OrcaFlex of the mooring system in the static position. In green are the nylon sections, in red the chain sections. The clump weights are represented in purple. White sections represent the chain sections laying on the seabed.

Nylon is used here because of its interesting properties, especially its low weight per unit length, low axial stiffness, and low cost when compared to MBL-equivalent chain. But as a consequence, slacking is more likely to appear in the mooring lines. TFI systems are located at 15 meters from the fairleads, in the nylon sections of the mooring lines. Two spring systems per line are used, with a spacing of 3 meters between each, as shown in the figure below in blue.

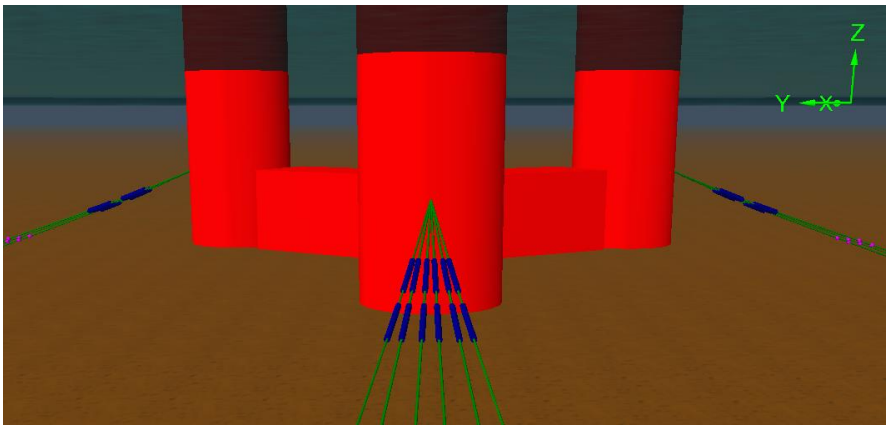

Figure 6-7: OrcaFlex representation of the TFI spring systems on the mooring lines of ActiveFloat WoB

Two clump weights were positioned between the fairleads and the Touchdown Points (TDPs). The length of the nylon section was set to limit slacking. More clump weights were positioned between the TDPs and the anchors to reduce the uplift of the lines in this zone, and limit the excursions of the platform and the peak loads in the mooring lines.

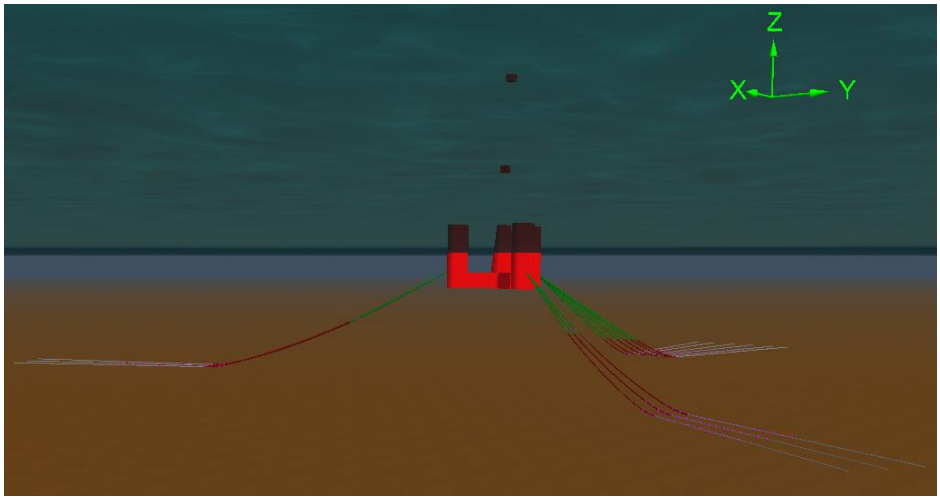

Figure 6-8: ActiveFloat site A. OrcaFlex 3D view of the mooring system.

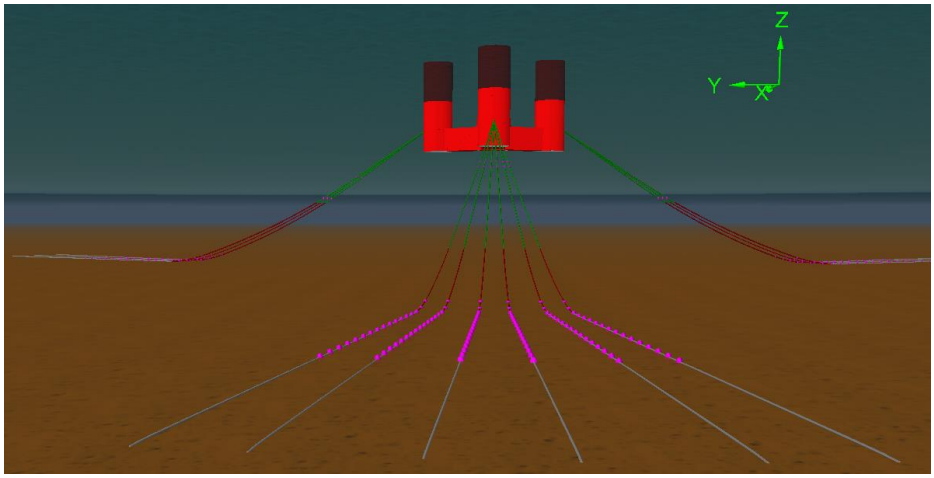

Figure 6-9: ActiveFloat West of Barra: OrcaFlex front view of the mooring system.

Table 6-5 presents the maximum values obtained from the complete analysis of DLCs 6.1 and 6.2, as well as the peak load reduction when compared to the originally optimized mooring system.

DLC61 & 62 (SOL&EOL) results	Upwind	Downwind
Max tension criterion | chain (-)	0,974	0,927
Max tension criterion | nylon (-)	0,822	0,676
Max tension criterion | TFI (-)	0,861	0,776
Minimum touchdown point (m)	14	10
Max offset (m)	32,407	
Max pitch (°)	8,942	
Max yaw (°)	6,629	
Max horizontal acceleration (m/s2)	2,908	
Max peak load [kN]	4898	
Peak load reduction	**32%**	

Table 6-5: ActiveFloat West of Barra: Main results of the start of life and end of life analysis of DLC 6.1 and 6.2.

The maximum tension criterion is the defined in section 6.2.4. It is the ratio between the design tension and 95% of the MBL of the material, and must be less than 1.

- Conclusions

The design criteria on the maximum tensions admissible in the mooring lines is respected, as well as the constraints of maximum pitch and yaw of the platform, maximum horizontal accelerations of the RNA, and the minimum of 10 meters length of chain laying on the seabed required for catenary lines. However, the platform offset limit of 30 meters is not respected. Maximum offset of the platform reaches 32 meters in the case of DLC 6.1 with a main wind direction of 270° (0° = north), a main wave direction of 240°, an extreme sea state with Hs = 15,6m and Tp = 12s, and a yaw misalignment of 0°. The offset constraint could not be respected here but was drastically reduced when compared with the maximum offset of 42 meters reached with the optimized mooring system of phase 1 (see deliverable D2.2 [1] optimized mooring system equipped with nylon and TFI).However, the nylon sections are modelled with a quasi-static stiffness, which leads to larger offsets when compared to dynamic stiffness modelling. Also, as detailed in deliverable D2.2 [1], the fully coupled simulations that USTUTT ran with OpenFast showed that offset results from OrcaFlex-non coupled simulations with the models used for mooring optimizations are conservative.

Using formula provided in the deliverable D2.1 [2], costs were estimated to be about 5651 k€. These costs correspond to materials costs for both mooring lines and anchors, including the costs per unit of the TFI systems and the clumps, but not considering the costs related to the connection links. It has to be noted that a conversion rate of 0.93 between dollar and euro has been used to perform this calculation (from Banque de France, 23/03/2020) [15].

ActiveFloat Site A	Chain sections	Nylon sections	TFI	Clumps	Anchors	Total
Cost (k€)	1634,5	224,1	2164,5	266,0	1362,3	**5651,4**
% of total	*28,9%*	*4,0%*	*38,3%*	*4,7%*	*24,1%*	

Table 6-6: ActiveFloat West Of Barra: Cost detail of the optimized mooing system.

Interesting is to observe that the chain sections are responsible for almost 30% of the total cost of the mooring, when the nylon sections are responsible for only 4% of it. Since 33% of the total line length of the mooring is made of nylon, the benefit of the use of such material is significant for cost reduction. Also, it is not surprising to see that the anchors are responsible for 24% of the total cost of the mooring, as a number of twelve lines is composing the mooring system here. For the same reason, the total cost estimated for the implementation of 24 TFI systems (2 per line) is responsible for more than 38% of the total cost of the mooring system.

ActiveFloat site A	Phase 1	TFI
Chain sections cost (k€)	3123,4	1634,5
Difference (%cost of phase 1)		*-26,7%*
Nylon sections cost (k€)	224,1	224,1
Difference (%cost of phase 1)		*+0,0%*
TFI cost (k€)	0,0	2164,5
Difference (%cost of phase 1)		*+38,9%*
Clumps cost (k€)	266,0	266,0
Difference (%cost of phase 1)		*+0,0%*
Anchors cost (k€)	1952,9	1362,3
Difference (%cost of phase 1)		*-10,6%*

Total cost (k€)	**5566,3**	**5651,4**
Difference (%cost of phase 1)		***+1,5%***

Table 6-7: ActiveFloat West of Barra: Comparison of the detailed costs of the mooring systems.

Finally, the total cost of the mooring equipped with chain, nylon and TFI systems is 85k€ more expensive than the chain and nylon configuration. The TFI systems showed that they could reduce the peak loads to 32% and hence allow to reduce the chain diameters and grades, as well as the size of the anchors.This led to more than 37% of total cost reduction, but could not compensate for the cost increase due to the implementation of the 24 TFI systems. However, the maximum offset of the platform has been reduced to 32 meters. Since offsets results are conservative as the fully-coupled simulations run by USTUTT (detailed in deliverable D2.2 [1]) have revealed, it is possible to assume that the mooring system equipped with TFI satisfies all the design criteria. It is not the case for the nylon and chain mooring system; therefore, it can be concluded that the TFI system improved the mooring system, keeping the costs at globally the same level.

6.4.2 ActiveFloat site B – Gran Canaria

On this site, TFI and IMS systems were tested. Both layouts are similar to the one from the originally optimized mooring described in deliverable D2.2 [1]. The mooring systems are composed of three catenary mooring lines, equipped with chain from the fairleads to the anchors. Gentle environmental loads combined with higher water depth makes the use of synthetic rope or clump weights unnecessary on this site. Two types of chain are used, so that the mooring is not symmetrical. The mooring systems have been designed with respect to all the design criteria established within the design basis and to avoid uplifting forces at the anchors.

The following figure is a 3D view of the layout of the optimized mooring system described in deliverable D2.2 [1], without peak loads reduction systems.

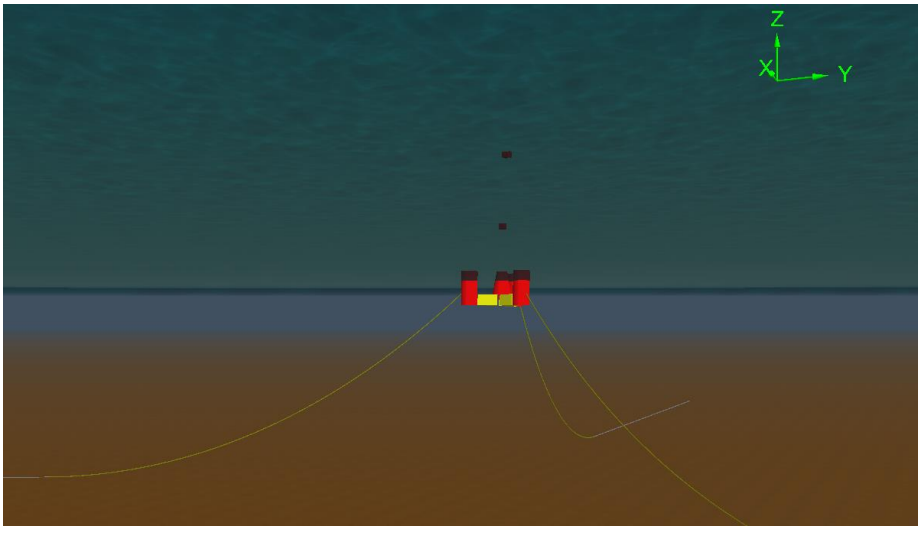

Figure 6-10: ActiveFloat Gran Canaria: OrcaFlex 3D view of the mooring system.

- **TFI-equipped mooring system**

Table 6-8 summarizes the physical properties of the chain used, upwind (1 line) and downwind (2 lines).

Group of lines	Chain bar diameter [mm]	Equivalent diameter [mm]	Line Length [m]	Dry mass per meter length [kg/m]	Axial stiffness [kN]	Steel Grade

Upwind lines	90,00	162,00	990,00	161,19	691,74e3	R4
Downwind lines	56,00	100,80	865,00	62,41	267,81e3	R3

Table 6-8: ActiveFloat Gran Canaria: Physical properties of the material used in the optimized mooring system (TFI-equipped).

Table 6-9 presents the maximum values obtained from the complete analysis of DLCs 6.1 and 6.2, as well as the peak load reduction when compared to the originally optimized mooring system.

DLC61 & 62 (SOL&EOL) results	Upwind	Downwind
Maximum tension criterion | chain (-)	0,960	0,936
Maximum tension criterion | TFI (-)	0,949	0,696
Minimum touchdown point (m)	12,00	11,00
Maximum offset (m)	58,216	
Maximum pitch (°)	1,653	
Maximum yaw (°)	4,968	
Maximum horizontal acceleration (m/s²)	0,682	
Maximum peak load (kN)	3856	
Peak load reduction	**28%**	

Table 6-9: ActiveFloat Gran Canaria, TFI: main results of start of life and end of life analysis of DLCs 6.1 & 6.2.

- **IMS-equipped mooring system**

Table 6-10 summarizes the physical properties of the chain used, upwind (1 line) and downwind (2 lines).

Group of lines	Chain bar diameter [mm]	Equivalent diameter [mm]	Line Length [m]	Dry mass per meter length [kg/m]	Axial stiffness [kN]	Steel Grade
Upwind lines	94,00	169,20	950,00	175,84	754,59e3	R3S
Downwind lines	56,00	100,80	900,00	62,41	267,81e3	R3

Table 6-10: ActiveFloat Gran Canaria: Physical properties of the material used in the optimized mooring system (IMS-equipped).

Table 6-11 presents the maximum values obtained from the complete analysis of DLCs 6.1 and 6.2, as well as the peak load reduction when compared to the originally optimized mooring system.

DLC61 & 62 (SOL&EOL) results	Upwind	Downwind
Maximum tension criterion | chain (-)	0,971	0,999
Maximum tension criterion | IMS (-)	0,800	0,578
Minimum touchdown point (m)	16,00	14,00
Maximum offset (m)	57,166	
Maximum pitch (°)	2,147	
Maximum yaw (°)	4,029	
Maximum horizontal acceleration (m/s2)	1,464	
Maximum peak load (kN)	4064	
Peak load reduction	**24%**	

Table 6-11: ActiveFloat Gran Canaria, IMS: main results of start of life and end of life analysis of DLCs 6.1 & 6.2.

- **Conclusions**

For both TFI and IMS-mooring systems, the design criteria on the maximum tensions admissible in the mooring lines is respected, as well as the constraints of maximum pitch, yaw and offset of the platform, maximum horizontal accelerations of the RNA, and the minimum of 10 meters length of chain laying on the seabed required for catenary lines.

Using formulas detailed in section 6.2.3, the total cost of the optimized mooring system was estimated to be about 712,8k€ with TFI, and 765,7k€ with IMS. These costs include material costs for mooring chains and anchors as detailed in Table 6-11 and Table 6-12 below.

ActiveFloat Site B	Chain sections	TFI	Anchors	Total
Cost (k€)	480,3	102,6	130,0	**712,8**
% of total	*67,4%*	*14,4%*	*18,2%*	

Table 6-12: ActiveFloat Gran Canaria, TFI: Cost detail of the optimized mooing system.

ActiveFloat Site B	Chain sections	IMS	Anchors	Total
Cost (k€)	463,1	174,0	128,5	**765,7**
% of total	*60,5%*	*22,7%*	*16,8%*	

Table 6-13: ActiveFloat Gran Canaria, IMS: Cost detail of the optimized mooing system.

Costs of the originally optimized mooring system was 865,1k€. Detailed mooring costs are compared in the following table.

ActiveFloat site B	Chain cost (k€)	*Difference (%cost of phase 1)*	TFI/IMS cost (k€)	*Difference (%cost of phase 1)*	Anchors cost (k€)	*Difference (%cost of phase 1)*	Total Cost (k€)	*Difference (%cost of phase 1)*
Chain	680,7	-	0	-	184,4	-	**865,1**	-
Chain + TFI	480,3	*-23,2%*	102,6	*+11,9%*	129,9	*-6,3%*	**712,8**	***-17,6%***
Chain + IMS	463,1	*-25,2%*	174,0	*+20,1%*	128,5	*-6,5%*	**765,7**	***-11,5%***

Table 6-14: ActiveFloat Gran Canaria: Comparison of the detailed costs of the mooring systems.

With TFI attached on the top sections of the mooring lines, the total cost of the mooring has been decreased of 17,6% when compared to the chain-only mooring system, for a 28% reduction of the maximum peak load observed among all the load cases simulated.

With IMS attached, a cost reduction of 11,5% has been reached for a 24% reduction of the maximum peak load observed among all the load cases simulated.

6.4.3 ActiveFloat site C – Morro Bay

On this site, TFI and IMS systems were implemented in ActiveFloat's optimized mooring described in deliverable D2.2 [1]. For the comparison, layouts are similar: mooring systems are composed of three semi-taut mooring lines, equipped with chain at the top and bottom sections and polyester in-between. Mooring buoys are attached at the top sections of each line to increase the yaw stiffness, which is necessary to limit the yaw movements of the platform. Two types of chain and two types of polyester are used in this system. The mooring system is designed to respect design criteria established within the design basis.

The following figure is a 3D view of the originally optimized mooring system as represented in OrcaFlex, in the static position, as described in deliverable D2.2 [1]. In green are represented the polyester sections, in red the chain sections. The mooring buoys are represented in purple.

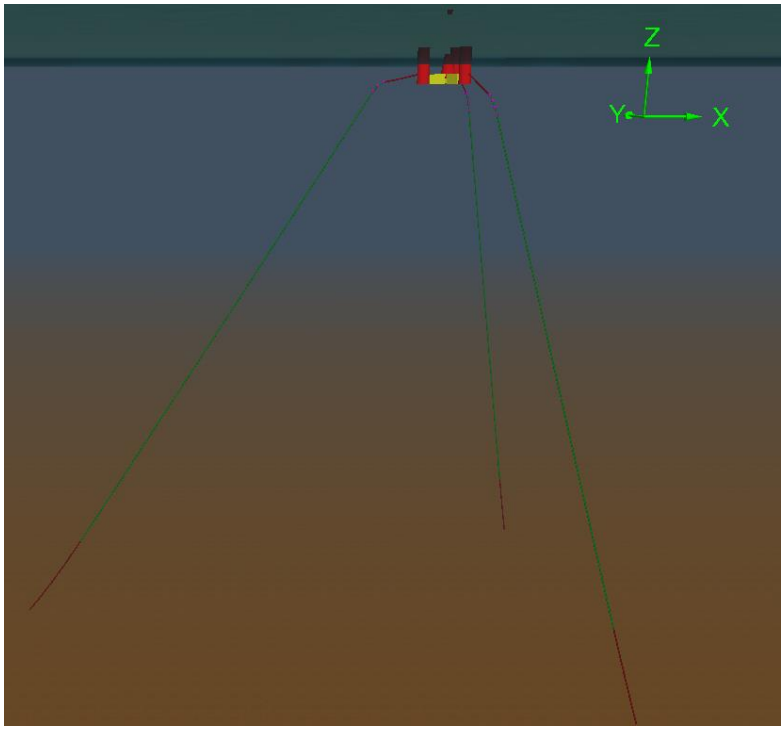

Figure 6-11: ActiveFloat Morro Bay: OrcaFlex 3D view of the mooring system.

The polyester had been chosen for its lower weight and cost. Indeed, the water depth of 870 meters requires line lengths of at least around 900 to 1000 meters. Lines fully made of chain would have very high vertical weight and axial stiffness, and consequently very high tensions.

- **TFI-equipped mooring system**

Table 6-15 summarizes the physical properties of chains and polyester used in the mooring system featuring TFI.

Group of lines	Material	diameter [mm]	Equivalent diameter [mm]	Line Length [m]	Dry mass per meter length [kg/m]	Axial stiffness [kN]	Steel Grade
Upwind lines	Chain	130,00	234,00	192,50	336,31	1,44e6	R3
	Polyester	190,00	152,78	807,50	24,70	2,29e5	-
Downwind lines	Chain	95,00	171,00	181,25	179,60	7,71e5	R4
	Polyester	155,00	124,60	818,75	16,43	1,46e5	-

Table 6-15: ActiveFloat Morro Bay, TFI: Physical properties of the material used for each line of the optimized mooring system.

Table below presents the maximum values obtained from the complete analysis of DLCs 6.1 and 6.2, as well as the peak load reduction when compared to the originally optimized mooring system.

DLC61 & 62 (SOL&EOL) results	Upwind	Downwind
Maximum tension criterion (chain)	0,66	0,97
Maximum tension criterion (polyester)	0,69	0,91
Maximum tension criterion (TFI)	0,64	0,86
Maximum offset (m)	44,13	
Maximum pitch (°)	6,52	
Maximum yaw (°)	3,11	
Maximum horizontal acceleration (m/s2)	3,37	
Maximum peak load [kN]	4974	
Peak load increase	**+11%**	

Table 6-16: ActiveFloat Morro Bay, TFI: main results of start of life and end of life analysis of DLCs 6.1 & 6.2.

- **IMS-equipped mooring system**

Table below summarizes physical properties of chains and polyester used in the IMS-equipped mooring system.

Group of lines	Material	diameter [mm]	Equivalent diameter [mm]	Line Length [m]	Dry mass per meter length [kg/m]	Axial stiffness [kN]	Steel Grade
Upwind lines	Chain	135,00	243,00	200,00	362,68	1,56e6	R3
	Polyester	190,00	152,78	850,00	24,70	2,29e5	-
Downwind lines	Chain	110,00	198,00	188,75	240,79	1,03e6	R3
	Polyester	155,00	124,60	861,25	16,43	1,46e5	-

Table 6-17: ActiveFloat Morro Bay, IMS: Physical properties of the material used for each line of the optimized mooring system.

Table below presents the maximum values obtained from the complete analysis of DLCs 6.1 and 6.2, as well as the peak load reduction when compared to the originally optimized mooring system.

DLC61 & 62 (SOL&EOL) results	Upwind	Downwind
Maximum tension criterion (chain)	0,763	0,949
Maximum tension criterion (polyester)	0,786	0,975
Maximum tension criterion (IMS)	0,730	0,735
Maximum offset (m)	31,984	
Maximum pitch (°)	6,601	
Maximum yaw (°)	2,849	
Maximum horizontal acceleration (m/s2)	3,258	
Maximum peak load [kN]	5437	
Peak load increase	**+21%**	

Table 6-18: ActiveFloat Morro Bay, IMS: main results of start of life and end of life analysis of DLCs 6.1 & 6.2.

- **Conclusions**

For both TFI and IMS-equipped mooring systems, the design criteria on the maximum tensions admissible in the mooring lines is respected, as well as the constraints of maximum pitch, yaw and offset of the platform, and maximum horizontal accelerations of the RNA. Maximum yaw is quite low for DLCs 6.1 and 6.2, but are to be higher in other DLCs. To make sure that the yaw constraint would not be reached in other DLCs, the maximum

yaw criteria was set to 3° and could be achieved thanks to the mooring buoys attached on the top of the polyester sections of the lines. This is explained with more details in deliverable D2.2 [1].

Using formulas detailed in section 6.2 .3, the total costs of the optimized mooring systems have been estimated to be about 2660,1k€ with TFI, and 2586,3k€ with IMS. These costs include material costs for mooring chains, polyester, TFI or IMS systems and anchors as detailed in Table 6-19 and Table 6-20 below.

ActiveFloat Site C	Chain sections	Polyester sections	TFI	Anchors	Buoys	Total
Cost (k€)	267,0	316,4	427,8	290,8	1358,0	**2660,1**
% of total	*10,0%*	*11,9%*	*16,1%*	*10,9%*	*51,1%*	

Table 6-19: ActiveFloat Morro Bay, TFI: Cost detail of the optimized mooing system.

ActiveFloat Site C	Chain sections	Polyester sections	IMS	Anchors	Buoys	Total
Cost (k€)	297,2	332,9	290,0	308,1	1358,0	**2586,3**
% of total	*11,5%*	*12,9%*	*16,1%*	*11,9%*	*52,5%*	

Table 6-20: ActiveFloat Morro Bay, IMS: Cost detail of the optimized mooing system.

Total cost of the originally optimized mooring system had been estimated about 2220,7k€. Detail of the mooring costs is presented in the following table.

ActiveFloat site C	Phase 1	TFI	IMS
Chain sections cost (k€)	276,5	267,0	297,2
Difference (%cost of phase 1)		*-0,4%*	*+0,9%*
Polyester sections cost (k€)	290,4	316,4	332,9
Difference (%cost of phase 1)		*+1,2%*	*+1,9%*
TFI or IMS cost (k€)	0,0	427,8	290,0
Difference (%cost of phase 1)		*+19,3%*	*+13,1%*
Buoys cost (k€)	1358,0	1358,0	1358,0
Difference (%cost of phase 1)		*+0,0%*	*+0,0%*
Anchors cost (k€)	295,8	290,8	308,1
Difference (%cost of phase 1)		*-0,2%*	*+0,6%*
Total cost (k€)	**2220,7**	**2660,0**	**2586,2**
Difference (%cost of phase 1)		***+19,8%***	***+16,5%***

Table 6-21: ActiveFloat Morro Bay: Comparison of the detailed costs of the mooring systems.

With TFI attached on the top sections of the mooring lines, the total cost of the mooring has been increased of 19,8% when compared to the chain-only mooring system, for a 11% increase of the maximum peak load observed among all the load cases simulated.

With IMS attached, a cost increase of 16,5% has been reached for a 21% increase of the maximum peak load observed among all the load cases simulated.

In the TFI and IMS-equipped mooring systems, the peak load reduction systems are respectively responsible for 19,3% and 13,1% of the total cost of the mooring, representing a significant cost increase when compared to the originally optimized mooring system. A significant cost difference between both systems is observed, despite that the same number of units has been used in both moorings. Indeed, TFI cost is MBL-dependent where IMS

is not. Also, the cost increase caused by TFI and IMS cannot be compensated because of yaw stiffness limitation. Indeed, the systems have been implemented at the top of the polyester sections, just below the buoys. It had the consequence to reduce their buoyancy, resulting with higher yaw angles of the platform. It might also be the cause of having higher peak loads. It could have been compensated by increasing the number or size of mooring buoys, but also increasing the costs. Finally, it can be noted that on this site the water depth is 870m, there is no current and the mooring is a semi-taut. The behaviour of ActiveFloat platform is these conditions is not much subjected to peak loads, therefore is could explain why TFI and IMS seem not suitable at this stage for ActiveFloat on this site, in order to reduce the global costs of the mooring system.

6.4.4 WindCrete site B – Gran Canaria

The mooring system is composed of three catenary mooring lines equipped with chain from the fairleads to the anchors. At the top of the mooring system the lines are equipped with the crowfoot system (delta connection). Three types of chains are used in this system. The mooring system is design to respect design criteria established within the design basis and to avoid uplifting forces at anchors.

All three catenary lines are only composed of chain sections. Gentle environmental loads combined with higher water depth makes the use of synthetic rope or clump weights unnecessary on this site.

The following figure is a 3D view of the originally optimized mooring system as represented in OrcaFlex, in the static position, as described in deliverable D2.2 [1].

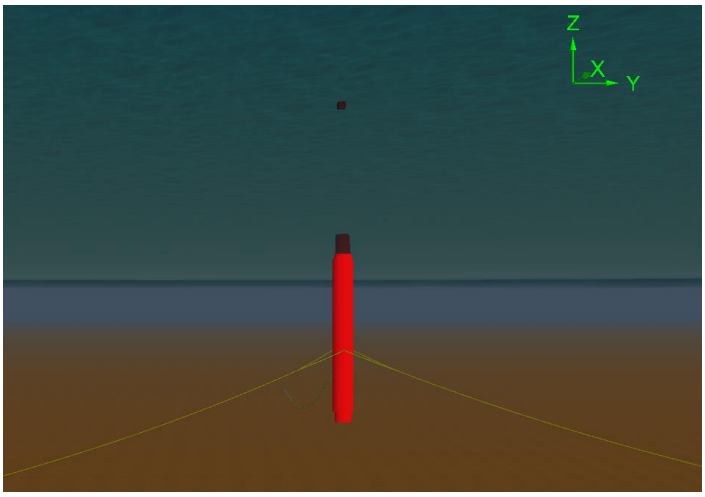

Figure 6-12: WindCrete Gran Canaria: OrcaFlex 3D view of the mooring system.

- **TFI-equipped mooring system**

Table 6-22 summarizes physical properties of chains used in the optimized mooring system featuring TFI systems on the top sections of the mooring lines (just below the delta lines).

Group of lines	Type of line	Chain bar diameter [mm]	Equivalent diameter [mm]	Line Length [m]	Dry mass per meter length [kg/m]	Axial stiffness [kN]	Steel Grade
Upwind lines	Main line	88,00	158,40	750,00	154,11	6,61e5	R3
	DeltaLines	80,00	144,00	50,00	127,36	5,47e5	R3
Downwind lines	Main Line	78,00	140,4	750,00	121,07	5,20e5	R3
	DeltaLines	80,00	144,00	50,00	127,36	5,47e5	R3

Table 6-22: WindCrete Gran Canaria, TFI: Physical properties of the material used for each line of the optimized mooring system.

Table below presents the maximum values obtained from the complete analysis of DLCs 6.1 and 6.2, as well as the peak load reduction when compared to the originally optimized mooring system.

DLC61 & 62 (SOL&EOL) results	Upwind	Deltalines	Downwind
Maximum tension criterion (chain)	0,956	0,829	0,953
Maximum tension criterion (TFI)	0,707	-	0,710
Minimum touchdown point (m)	12,00	-	17,00
Maximum offset (m)	7,993		
Maximum pitch (°)	2,148		
Maximum yaw (°)	3,843		
Maximum horizontal acceleration (m/s²)	1,576		
Maximum peak load (kN)	3471		
Peak load reduction	**47%**		

Table 6-23: WindCrete Gran Canaria, TFI: main results of start of life and end of life analysis of DLC 6.1 & 6.2.

- **IMS-equipped mooring system**

Table 6-22 summarizes physical properties of chains used in the optimized IMS-equipped mooring system.

Group of lines	Type of line	Chain bar diameter [mm]	Equivalent diameter [mm]	Line Length [m]	Dry mass per meter length [kg/m]	Axial stiffness [kN]	Steel Grade
Upwind lines	Main line	100,00	180,00	670,00	199,00	8,54e5	R3
	DeltaLines	78,00	140,40	50,00	121,07	5,20e5	R4
Downwind lines	Main Line	72,00	129,60	815,00	103,16	4,43e5	R4
	DeltaLines	78,00	140,40	50,00	121,07	5,20e5	R4

Table 6-24: WindCrete Gran Canaria, IMS: Physical properties of the material used for each line of the optimized mooring system.

Table below presents the maximum values obtained from the complete analysis of DLCs 6.1 and 6.2, as well as the peak load reduction when compared to the originally optimized mooring system.

DLC61 & 62 (SOL&EOL) results	Upwind	Deltalines	Downwind
Maximum tension criterion (chain)	0,792	0,952	0,967
Maximum tension criterion (IMS)	0,847	-	0,912
Minimum touchdown point (m)	12,00	-	12,00
Maximum offset (m)	7,260		
Maximum pitch (°)	2,132		
Maximum yaw (°)	4,323		
Maximum horizontal acceleration (m/s²)	1,574		
Maximum peak load (kN)	3593		
Peak load reduction	**45%**		

Table 6-25: WindCrete Gran Canaria, IMS: main results of start of life and end of life analysis of DLCs 6.1 & 6.2.

- **Conclusions**

The design criteria on the maximum tensions admissible in the mooring lines are respected, as well as the constraints of maximum pitch, yaw and offset of the platform, maximum horizontal accelerations of the RNA, and the minimum of 10 meters length of chain laying on the seabed required for catenary lines.

Using formulas detailed in section 6.2.3, the total cost of the optimized mooring system has been estimated to be about 813,6k€ with TFI, and 943,6k€ with IMS. These costs include material costs for mooring chains and anchors as detailed in Table 6-26 and Table 6-27 below.

WindCrete Site B	Chain sections	TFI	Anchors	Total
Cost (k€)	497,8	158,1	157,7	**813,6**
% of total	*61,2%*	*19,4%*	*19,4%*	

Table 6-26: WindCrete Gran Canaria, TFI: Cost detail of the optimized mooing system.

WindCrete Site B	Chain sections	IMS	Anchors	Total
Cost (k€)	590,4	174,0	179.2	**943,6**
% of total	*62,6%*	*18,4%*	*19,0%*	

Table 6-27: WindCrete Gran Canaria, IMS: Cost detail of the optimized mooing system.

Total cost of the originally optimized mooring system had been estimated about 1294,2k€. Detail on the mooring costs is presented in the following table.

WindCrete site B	Chain	Chain + TFI	Chain + IMS
Chain sections cost (k€)	1011,7	497,8	590,4
Difference (%cost of phase 1)		*-39,7%*	*-32,6%*
TFI or IMS cost (k€)	0,0	158,1	174,0
Difference (%cost of phase 1)		*+12,2%*	*+13,4%*
Anchors cost (k€)	282,5	157,8	179,2
Difference (%cost of phase 1)		*-9,6%*	*-8,0%*
Total cost (k€)	**1294,2**	**813,7**	**943,6**
Difference (%cost of phase 1)		***-37,1%***	***-27,1%***

Table 6-28: WindCrete Gran Canaria: Comparison of the detailed costs of the mooring systems.

With TFI attached on the top sections of the mooring lines, the total cost of the mooring has been decreased of 37,1% when compared to the chain-only mooring system, for a 47% reduction of the maximum peak load observed among all the load cases simulated.

With IMS attached, a cost reduction of 27,1% has been reached for a 45% reduction of the maximum peak load observed among all the load cases simulated.

6.4.5 WindCrete site C – Morro Bay

The mooring system is composed of four semi-taut mooring lines. At the top of the mooring system the lines are equipped with the crowfoot system (delta connection). Three types of chain are used in this system as well as two types of polyesters. The polyester used is the DeepRope polyester Acordis Polyester 855TN, developed by Bexco. The mooring system is design to respect design criteria established within the design basis.

In green are represented the polyester sections, in red the chain sections. The mooring buoys are represented in purple. Here the polyester is used for its lower weight and cost. Indeed, the water depth of 870 meters requires line lengths of at least around 900 to 1000 meters. Lines fully made of chain would have very high vertical weight and axial stiffness, inducing very high tensions.

Figure 6-13 is a 3D view of the originally optimized mooring system as represented in OrcaFlex, in the static position, as described in deliverable D2.2 [1].

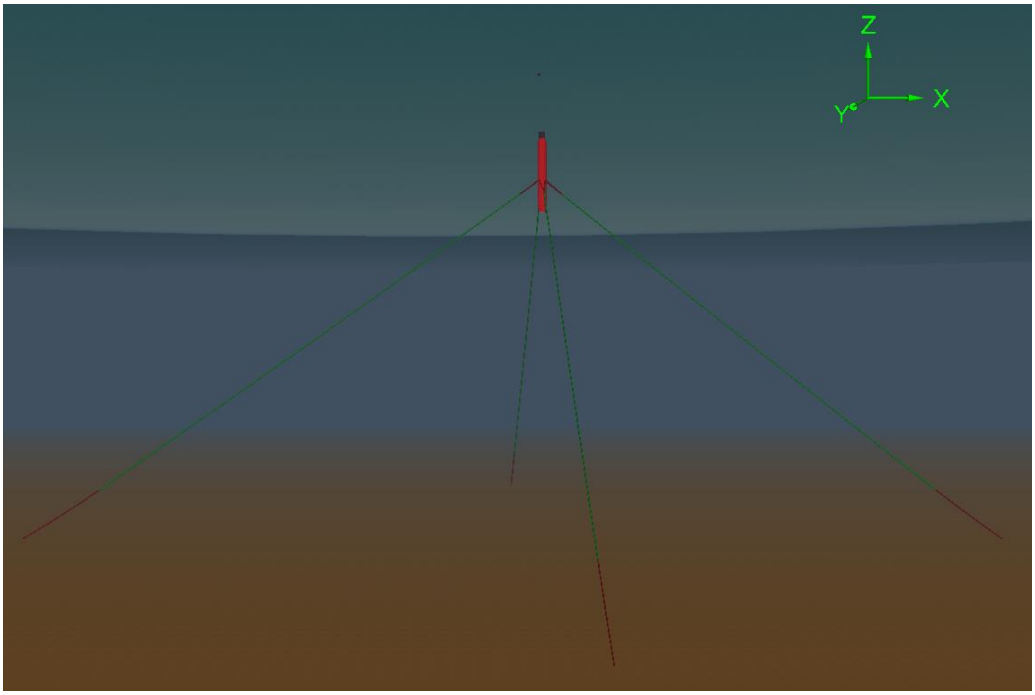

Figure 6-13: WindCrete Morro Bay: OrcaFlex 3D view of the floater and its mooring system.

- **TFI-equipped mooring system**

Table 6-29 summarizes physical properties of chains used in the optimized mooring system featuring TFI systems on the top sections of the mooring lines (just below the delta lines).

Group of lines	Type of line	Material	Diameter [mm]	Equivalent diameter [mm]	Line Length [m]	Dry mass per meter length [kg/m]	Axial stiffness [kN]	Steel Grade
Upwind lines	Main line	Chain	106,00	190,80	240,5	223,60	9,60e5	R3
		Polyester	152,00	122,22	1079,5	15,80	1,39e5	-
	DeltaLines	Chain	92,00	165,60	50,00	168,43	7,23e5	R3S
Downwind lines	Main Line	Chain	106,00	190,80	178,5	223,60	9,60e5	R3
		Polyester	158,00	127,12	1091,50	17,10	1,52e5	-
	DeltaLines	Chain	92,00	165,60	50,00	168,43	7,23e5	R3S

Table 6-29: WindCrete Morro Bay, IMS: Physical properties of the material used for each line of the optimized mooring system.

Table 6-30 below presents the maximum values obtained from the complete analysis of DLCs 6.1 and 6.2, as well as the peak load reduction when compared to the originally optimized mooring system.--

DLC61 & 62 (SOL&EOL) results	Upwind	Deltalines	Downwind
Maximum tension criterion (chain)	0,786	0,978	0,852
Maximum tension criterion (polyester)	0,977	-	0,966
Maximum tension criterion (TFI)	0,928	-	0,978
Maximum offset (m)	15,221		
Maximum pitch (°)	4,448		
Maximum yaw (°)	10,312		
Maximum horizontal acceleration (m/s²)	2,400		
Maximum peak load (kN)	4811		
Peak load reduction	**2%**		

Table 6-30: WindCrete Morro Bay, TFI: main results of start of life and end of life analysis of DLCs 6.1 and 6.2.

- **IMS-equipped mooring system**

Table 6-22 summarizes physical properties of chains used in the optimized IMS-equipped mooring system.

Group of lines	Type of line	Material	Diameter [mm]	Equivalent diameter [mm]	Line Length [m]	Dry mass per meter length [kg/m]	Axial stiffness [kN]	Steel Grade
Upwind lines	Main line	Chain	100,00	180,00	201,00	199,00	8,54e5	R3S
		Polyester	165,00	132,85	1139,00	18,67	1,68e5	-
	DeltaLines	Chain	100,00	180,00	50,00	199,00	8,54e5	R3S
Downwind lines	Main Line	Chain	100,00	180,00	189,00	199,00	8,54e5	R3
		Polyester	155,00	124,60	1071,00	16,43	1,46e5	-
	DeltaLines	Chain	100,00	180,00	50,00	199,00	8,54e5	R3S

Table 6-31: WindCrete Morro Bay, IMS: Physical properties of the material used for each line of the optimized mooring system.

Table below presents the maximum values obtained from the complete analysis of DLCs 6.1 and 6.2, as well as the peak load reduction when compared to the originally optimized mooring system.

DLC61 & 62 (SOL&EOL) results	Upwind	Deltalines	Downwind
Maximum tension criterion (chain)	0,961	0,988	0,994
Maximum tension criterion (polyester)	0,853	-	0,908
Maximum tension criterion (IMS)	0,617	-	0,571
Maximum offset (m)	14,543		
Maximum pitch (°)	4,563		
Maximum yaw (°)	11,245		
Maximum horizontal acceleration (m/s²)	2,417		
Maximum peak load [kN]	4221		
Peak load reduction	**14%**		

Table 6-32: WindCrete Morro Bay, IMS: main results of start of life and end of life analysis of DLCs 6.1 and 6.2.

- **Conclusions**

The design criteria on the maximum tensions admissible in the mooring lines is respected, as well as the constraints of maximum pitch, yaw and offset of the platform, and maximum horizontal accelerations of the RNA.

Using formulas detailed in section 6.2.3, the total cost of the optimized mooring system has been estimated to be about 1528,9k€ with TFI, and 1491,2k€ with IMS. These costs include material costs for mooring chains and anchors as detailed in Table 6-33 and Table 6-34 below.

WindCrete Site C	Chain sections	Polyester sections	TFI	Anchors	Total
Cost (k€)	451,3	479,4	260,6	337,6	**1528,9**
% of total	*29,5%*	*31,4%*	*17,0%*	*22,1%*	

Table 6-33: WindCrete Morro Bay, TFI: Cost detail of the optimized mooing system.

WindCrete Site C	Chain sections	Polyester sections	IMS	Anchors	Total
Cost (k€)	448,9	496,9	232,0	313,4	**1491,2**
% of total	*30,1%*	*33,3%*	*15,6%*	*21,0%*	

Table 6-34: WindCrete Morro Bay, IMS: Cost detail of the optimized mooing system.

Total cost of the originally optimized mooring system had been estimated about 1623,0k€. Detail of the mooring costs is presented in the following table.

WindCrete site C	Chain	Chain + TFI	Chain + IMS
Chain sections cost (k€)	529,1	451,3	448,9
Difference (%cost of phase 1)		*-4,8%*	*-4,9%*
Polyester sections cost (k€)	758,9	479,4	496,9
Difference (%cost of phase 1)		*-17,2%*	*-16,1%*
TFI or IMS cost (k€)	0,0	260,6	232,0
Difference (%cost of phase 1)		*+16,1%*	*+14,3%*
Anchors cost (k€)	335,0	337,7	313,4
Difference (%cost of phase 1)		*+0,2%*	*-1,3%*
Total cost (k€)	**1623,0**	**1529,0**	**1491,2**
Diference (%cost of phase 1)		***-5,8%***	***-8,1%***

Table 6-35: WindCrete Morro Bay: Comparison of the detailed costs of the mooring systems.

With TFI attached on the top sections of the mooring lines, the total cost of the mooring has been decreased of 5,8% when compared to the chain-only mooring system, for a 2% reduction of the maximum peak load observed among all the load cases simulated.

With IMS attached, a cost reduction of 8,1% has been reached for a 14% reduction of the maximum peak load observed among all the load cases simulated.

As for ActiveFloat on this site (see section 6.4.3), it can be noted that on this site the water depth is 870m, there is no current and the mooring is a semi-taut. The WindCrete platform in these conditions is not much subjected to peak loads, therefore is could explain why the peak loads reductions observed here were less significant than on site B Gran Canaria and site A West of Barra. Consequently, it led to less significant cost reductions and

underlines the conclusion that TFI and IMS may not be suitable at this stage for the conditions observed on this site.

6.5 Fatigue analysis of the mooring designs

In this section are presented the results of investigations regarding fatigue of the mooring systems when equipped with TFI or IMS systems. First, fatigue analyses were performed on the optimized mooring systems presented in section 6.4, and then on the optimized mooring systems not using any peak load reduction system presented in deliverable D2.2 [1].

The analysis focused on ActiveFloat site B Gran Canaria.

6.5.1 Model

A coupled model had been developed for the FLS reliability of the optimized mooring systems of task 2.2 [1] and was then used in subtask 2.3.1 to investigate potential benefits of TFI and IMS on the fatigue of the mooring systems.

The turbine object in OrcaFlex was used to build a coupled model. To do so, the IEA 15MW model provided by Orcina was slightly changed to correspond to the turbine definition described in [22].

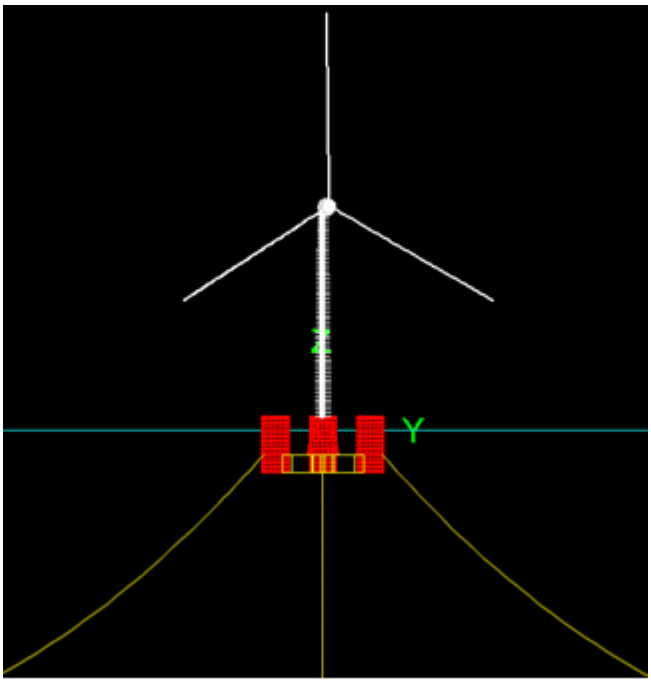

Figure 6-14: Floater and wind turbine as represented in OrcaFlex.

Then, the DLC table was established, based on the recommendation from DNVGL [17]. Assessment is performed for DLC 1.2 (for wind speeds between cut-in and cut-out wind speeds), and DLC 6.4 (for wind speeds respectively below and above these values). For each environmental sea state, the probability of occurrence is calculated.

The procedure to calculate the probabilities of occurrence of each DLC is detailed in section 7.2.2 of deliverable D2.2 [1].

The 100 most probable sea states were kept, and the probability was scaled to ensure that the sum gives 100% of occurrence. Simulations were run in OrcaFlex and fatigue assessment was calculated using the fatigue tool implemented in OrcaFlex, which is based on T-N curves and rainflow counting algorithm.

Simulations were run on 1800s and a build-up time of 2000s was considered to avoid any transient effect.

6.5.2 Results

The following tables present the results of damage and lifetime of the upwind line of each of the mooring systems analyzed. Five mooring systems are compared. Mooring A is the full chain optimized mooring presented in deliverable D2.2 [1], mooring B and C are the same mooring systems respectively with TFI and IMS implemented. For moorings B and C, the size of the peak loads reduction systems has been adapted to the ranges of tensions with the aim to reduce their amplitudes. Moorings D and E are the optimized mooring systems presented in this report, section 6.4. The arc length (in meters) is indicated as the point of the line where the maximum damage occurs, with 0m at the fairlead.

Mooring system	A	B	C	D	E
Damage over total exposure	0.14	0.13	0.14	0.34	0.42
Total exposure time (years)	1.0	1.0	1.0	1.0	1.0
Life (years)	6.9	7.6	7.2	3.0	2.4
Arc length (m)	315.8	308.4	308.8	420.5	378.1

Table 6-36: Detail of the results of the fatigue analysis of different mooring systems equipped with TFI and IMS.

Mooring system	Description
A	3 catenary chain lines, optimized
B	A + TFI of adapted size
C	A + IMS of adapted size
D	3 catenary chain lines + TFI, optimized
E	3 catenary chain lines + IMS, optimized

Table 6-37: Description of the mooring systems

Unfortunately, the results have showen that implementing TFI and IMS systems could not help to respect the fatigue criteria of five times the lifetime of 25 years required for ActiveFloat. However, adapting the size of the TFI or IMS showed that it could help to increase the lifetime when compare to the lifetime of the ULS-optimized moorings D and E.

6.6 Conclusion

In this section of the reportis investigated the potential benefits of two peak loads reduction systems: TFI and IMS, to reduce the total cost of the mooring and consequently the LCOE of floating wind. To be able to compare to the initially optimized mooring systems presented in deliverable D2.2 [1], TFI and IMS systems were implemented to the OrcaFlex models and to the optimization tool. Peak load reductions have been quantified and the total costs of moorings have been detailed and compared.

First, peak loads reduction has been possible thanks to the implementation of the systems on the top sections of the mooring lines, of almost 50% in some cases. Such peak load reduction allowed to reduce the size of the lines and consequently the cost of related materials, but it has been noted that the important price per unit of the systems could make it difficult to reduce the total cost of the mooring when compared to the initially optimized mooring systems. It was the case for ActiveFloat site A (West of Barra) for example, where the

mooring system is made of 12 mooring lines. It has also been noted differences in the magnitude of the peak load reductions depending on the nature of the site and conditions. TFI and IMS seemed to be less suitable at this stage for the conditions observed at site C Morro Bay. The largest magnitudes of peak load reductions have been observed on sites A and B of West of Barra and Gran Canaria, respectively. The largest cost reductions of the mooring system have been obtained for WindCrete on site B Gran Canaria, with 27% and 37% of reduction of the mooring system respectively with IMS and TFI.

Finally, a quick sensitivity analysis has been performed in order to investigate the potential benefits of TFI and IMS on the lifetime of the mooring of ActiveFloat site B (Gran Canaria). Unfortunately, the results were not satisfying in terms of improvement.

In the next section are presented further investigations regarding innovative solutions for mooring footprint reduction.

7 INNOVATIVE SOLUTIONS FOR MOORING FOOTPRINT REDUCTION

In this subtask, we add clump weights to the mooring lines, which are commonly utilized in offshore engineering, in order to investigate the impact of clump weights on mooring footprint and dynamic performance of the floater. The main objectives of this subtask are to propose cost-effective and low-footprint mooring configurations and to assess dynamic performances of the IEA 15MW FOWT for different mooring configurations.

Reduction in mooring costs is essential for commercial deployment of Floating Offshore Wind Turbines (FOWTs). Beyond the cost, the environmental impact of mooring systems for FOWTs on ecological systems at seabed should be considered, as more and more floating offshore wind farms are under planning. For a catenary mooring system, part of the mooring lines lay on the seabed, where the existence and the movement of mooring lines form a disrupted area.

Mooring footprint is defined as the horizontal distance between floater center at static equilibrium and anchor positions. It is an indicator of a reliable mooring configuration in both economic and environmental aspects, as it is directly linked to mooring line length and determines the disrupted area at seabed. Currently, there is no information available concerning the footprint allowances from guidelines.

7.1 Methodology

The semi-submersible floater 'ActiveFloat' is used for this study. The principal dimensions for wind turbine, floater and mooring layout as well as the specific environmental conditions are referred to the COREWIND project design basis [16] and deliverable on OpenFAST model [22]. The site is on Gran Canaria Island with a water depth of 200 m.

The mooring line properties are referred to [23] and presented in table 1. The mooring configurations are based on the equations in [24] for static equilibrium of a catenary mooring line with a clump weight. The mooring lengths and the footprints of mooring lines can be computed by in-house codes and are compared with OpenFAST static solutions.

Parameter	Unit	Value
Mooring line grade	-	Studless R4
Mass in air	kg/m	462
Mass in water	kg/m	401
Chain nominal diameter	m	0.153
Elastic stiffness	kN	3.78E06

Minimum breaking load (MBL)	kN	20156

Table 7-1: The mooring line properties

The design space for mooring configurations is explored for different pretension ratios R_t, laid down length ratios R_l and clump weights W_c. R_t is the tension ratio of mooring pretension over MBL. Three R_t values are considered for a rough range of 10% to 20 % MBL, which is commonly used in the oil and gas design practices [25]. R_l is described as ratio of laid down length over hanging length. To avoid lift-up forces, it is required to lay enough mooring lines at seabed. Three R_l values of 0.3, 0.5 and 0.7 are tested in this subtask. The total mooring line length is the sum of hanging and laid down length. The generated mooring configurations are divided into four groups, as summarized in Table 7-2. The position of added clump weight on mooring line1 is given constant value of 325m distance from fairlead along the mooring line, which is 65% hanging length (500m) without adding clump weight and leads to a range of 230m to 325m distance to anchor1 for different mooring configurations.

Group	Config nr.	R_t	R_l	W_c [t]	Length [m]	Footprint [m]
1	1	0.10	0.5	0	591	573
	2	0.15	0.5	0	750	746
	3	0.20	0.5	0	881	884
2	4	0.15	0.3	0	650	646
	2	0.15	0.5	0	750	746
	5	0.15	0.7	0	850	846
3	4	0.15	0.3	0	650	646
	6	0.15	0.34	10	650	644
	7	0.15	0.39	20	650	642
	8	0.15	0.51	40	650	638
4	4	0.15	0.3	0	650	646
	9	0.15	0.3	10	628	622
	10	0.15	0.3	20	606	598
	11	0.15	0.3	40	559	547

Table 7-2: The generated mooring configurations

Group1 corresponds to the influence of the pretension ratio effect and group2 to the influence of the mooring length ratio. Both group3 and group4 focus on the impact of adding clump weights. The comparisons of group3 and group4 can demonstrate the variances of mooring lengths and mooring footprints after adding clump weights.

With a constant pretension ratio of 0.15, by adding clump weights of 40 t, the total length and the footprint can respectively be decreased from 650 m to 559 m and from 646 m to 547 m. Static tests simulated in OpenFAST and the analytical solutions using in-house codes match well, as shown in Figure 7-1.

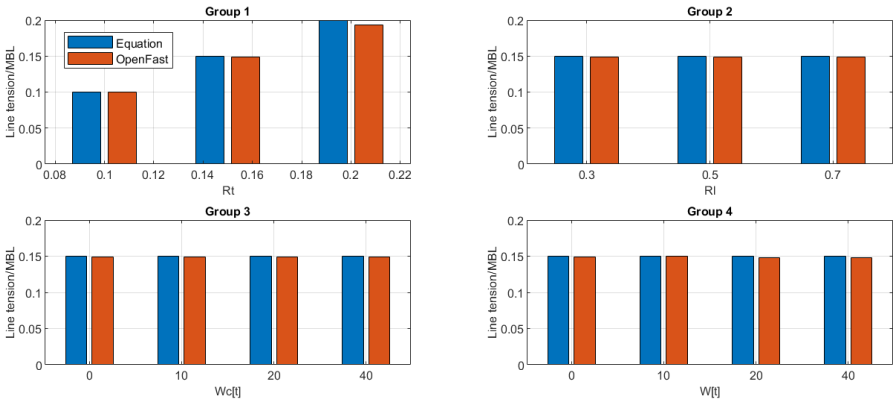

Figure 7-1: The comparisons of static mooring tension results

Three sets of tests, steady wind, ultimate limit tests (DLC6.1) and fatigue limit tests (DLC1.2) are used for evaluating the dynamic performances of different mooring configurations. The applied environmental conditions are summarized in Table 7-3.

test	Wind	Wave	Current
Steady wind	Steady wind range [4:14] m/s, with interval of 2 m/s	PM, Hs = 3 m, Tp = 8 s	
DLC6.1	EWM 50, Vs = 28.35 m/s at hub height of 135 m	JONSWAP, Hs = 5.11 m, Tp = 9 s.	50 years return period, wind induced current speed Vc = 0.57 m/s
DLC1.2	NTM, Vs range [2:12] m/s, with interval of 2 m/s	PM, Hs = 1 m & 2 m, Tp = 7 S	

Table 7-3: The applied environmental conditions

The dynamic floater motions for steady wind are illustrated in Figure 7-2. It is observed that tension ratio R_t plays a more important impact on floater peak motions compared to the rest two design parameters. In group 1 results, it is clearly shown that when tension ratio drops from 0.2 to 0.1, at wind speed of 10m/s (near rated wind turbine speed), the peak value of surge increases from 7.95 m to 19.52 m. In group 2 results, it shows that the laid down length of mooring lines has little impact on floater maximum motions, for all three length ratios R_l the motion results are similar. In group 3 and group 4 results, adding clump weight brings obvious changes in floater peak motions. Adding 40 t clump weight, the resulting rise in surge is more than 3 m.

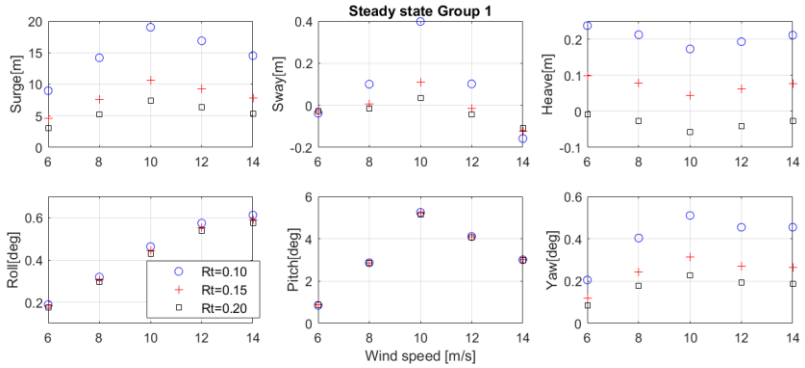

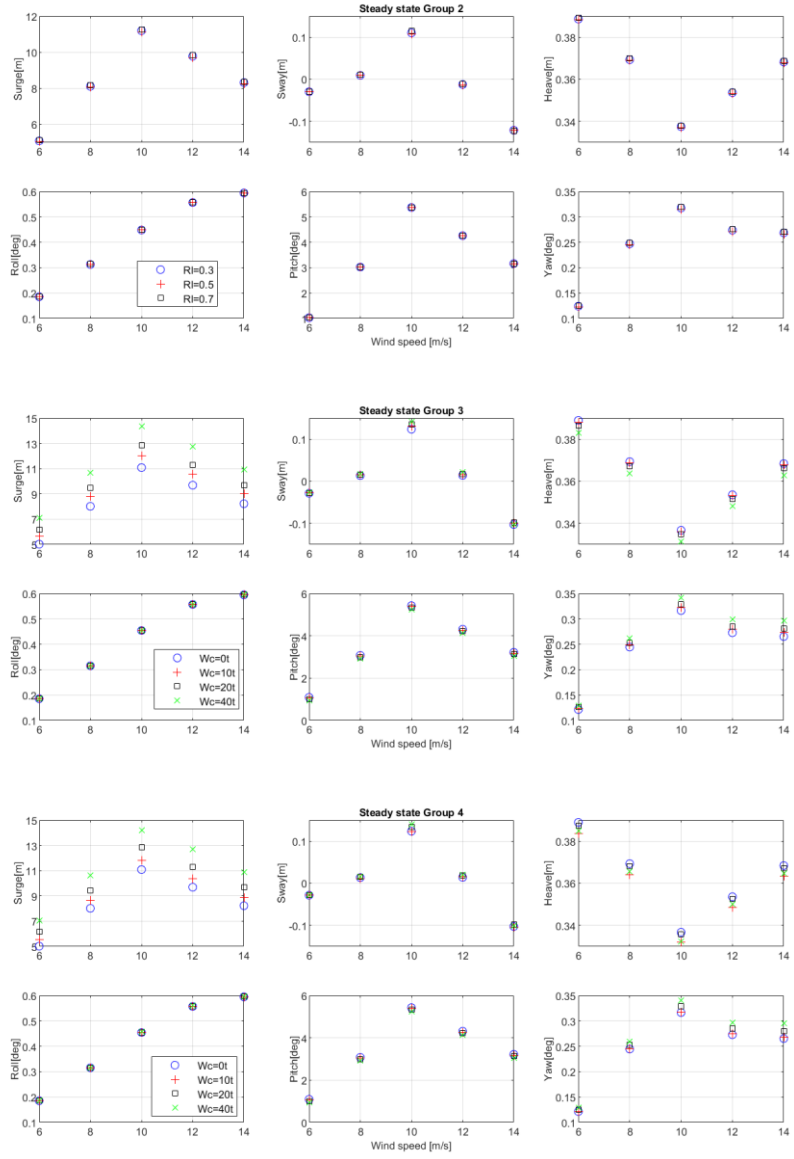

Figure 7-2: The maximum floater motions for steady wind tests

The steady wind tests prove that tension ratio plays a significant role in the peak floater motions. With larger tension ratios, the surge, heave and yaw peak values would reduce accordingly, however, the static footprint increases sharply, as Table 7-1 shows. So, the trade-off between reduction in maximum motions and controlled desired footprints asks for a balanced tension ratio. In this subtask, we choose 0.15 for further exploration on extreme mooring tensions and mooring fatigue damage.

The maximum, mean and minimum mooring tensions for DLC 6.1 tests with different clump weights are illustrated in Figure 7-3 . The idling wind turbine under 50-year extreme wind, wave and current conditions is considered in DLC6.1 tests. It is assumed that no wind-wave misalignment and no changes in the water level occur. Yaw errors of 8° are included and six wind and wave seeds are applied in 1 hour calculation for each wind speed.

The results of DLC6.1 demonstrate the impact of clump weights on mooring tensions under extreme environmental conditions. Generally, adding clump weights makes more significant reductions on maximum

mooring tensions. For the most heavily loaded mooring line, the mean and minimum values of fairlead and anchor tensions maintain stable with increasing clump weight, while the maximum mooring tension drops by 9% from 6885 kN to 6285 kN.

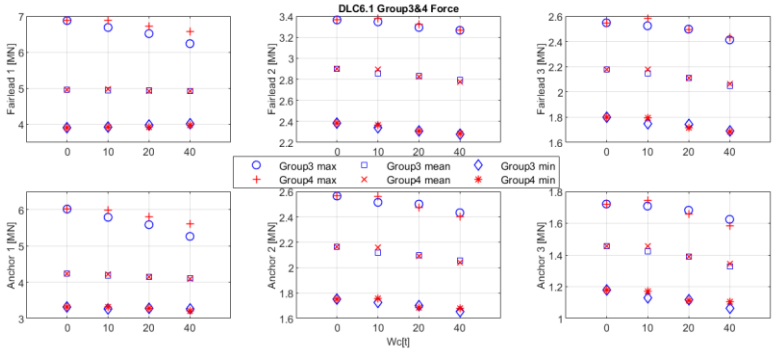

Figure 7-3: The mooring tension forces for DLC6.1 tests

The time-series of mooring tension forces for DLC1.2 are post-processed to calculate the mooring tension fatigue damage. At the early design phase of the 15MW FOWT, no available information is provided on the importance of all design relevant fatigue load cases. It is assumed in this study that mooring line design life is totally based on fatigue damage derived from DLC1.2. The purpose of this fatigue analysis is not to check the lifetime fatigue safety limit, but to quantify the influence of added clump weights to the mooring configurations.

Constant mean water level, yaw error of 10° and no wind-wave directional misalignment are assumed in the calculations. Also, no corrosion or marine growth is accounted for mooring tension fatigue damage computation. Damage is derived from S-N curve equations for studless R4 mooring line, the intercept is 6E10 and the slope of S-N curve is 3. Miner's law of linear damage accumulation is considered to add up all individual damage to total damage. Six wind and wave seeds are used and individual damage is sum up to give hourly damage for each environmental case. The occurrence probability for each sea state is presented in Table 7-4. Total mooring tension fatigue damage is the sum product of hourly damage and probability of the corresponding environmental case, as summarized in Table 7-5.

	Vs [m/s]					
Hs [m]	2	4	6	8	10	12
1	0.02	0.09	0.14	0.10	0.05	0.02
2	0.03	0.13	0.20	0.13	0.06	0.02

Table 7-4: The applied sea state probability for DLC1.2 tests

	Clump weight [t]			
	0	10	20	40
Fatigue damage	7.39E-06	7.72E-06	7.83E-06	8.25E-06
Ratio %	100	104	106	112

Table 7-5: The mooring tension fatigue damage based on DLC1.2 tests

In this study, we proposed different mooring configurations and evaluated the influence of tension ratio, length ratio and clump weights on mooring footprint, motions of floater, mooring line tensions, mooring fatigue life. The tension ratio shows a larger impact on maximum floater motions than the rest two parameters. With larger tension ratio, the mooring line length and mooring footprint increase sharply. Adding clump weights can efficiently reduce the mooring footprint and maximum mooring tensions, but induces 12% larger mooring tension fatigue damage.

8 INVESTIGATIONS OF TUNING OF THE CONTROLLER TO REDUCE MOORING FATIGUE

Mooring lines are used at Floating Offshore Wind Turbines (FOWT) for station keeping. They must withstand the hydrodynamic and aerodynamic forces acting on the turbine and the floating platform. During this task, the mooring lines show a fatigue response. The main driver of this fatigue is the aerodynamic force [1]. Low frequency thrust, e.g., through turbulent wind, plays an important role in the formation of mooring line fatigue.

The main idea of this study is to reduce the mooring line fatigue by adapting the blade pitch controller. Specifically, we used the open-source research controller ROSCO v1.0.0 [26]. As a first, computational effective measure for the mooring line fatigue, the Damage Equivalent Load (DEL) was computed. We present a PI controller gain configuration that reduces the DEL of the mooring lines by up to 6% compared to the baseline ROSCO configuration. Additionally, we show that including the nacelle fore-aft velocity in the feedback loop of the PI controller reduces the DEL of the mooring line by up to 5%.

8.1 Methodology

For blade pitch control, ROSCO implements a PI controller. As input, it takes the generator speed ω_{gen} and compares it against a reference value ω_{ref}. The error $e = \omega_{gen} - \omega_{ref}$ is then fed through the controller to calculate the control variable blade pitch θ with the formula $\theta = K_p * e + K_i * \int e \, dt$. This simple setup already leads to a stable operation if the gains K_p and K_i are well chosen. Control theory lends many tools to calculate the gains. These calculations often have the goal to maximize the power output or stabilize the dynamic behaviour of the turbine.

The main idea of this work is to adapt the PI controller to reduce low frequency component of the rotor thrust. Thereby, fatigue in the mooring lines should recede as well. We present two ways of adaption.

First, the PI controller remains unchanged in its structure and only the K_p and K_i gains are changed. The controller gains have an impact on the reaction time of the system to disturbance. A slower reaction of the blade pitch to the turbulent wind leads to less thrust in the low-frequency area. The exact calculation of the control gains is nontrivial and done by analysing the transfer function of the controller and the turbine model. For a standard PI controller, the gains are calculated as a function of the desired natural frequency and the damping ratio for the system. Analytically derived gains guarantee the dynamic stability of the system. For ROSCO, the generic calculation of stable control gains for a given turbine is laid out in [26]. We ask whether a set of K_p and K_i exists in the near vicinity of such stable gains which decreases the mooring line fatigue while maintaining dynamic stability. To investigate this, a grid search around the current operating points for K_p and K_i is conducted. This is done for K_p only, K_i only and for both variables together.

Second, the PI controller is changed to include the feed-in of the nacelle fore-aft velocity. ROSCO already provides the necessary implementation. The nacelle fore-aft velocity is multiplied with a gain $K_{p,float}$ and added on the output of the PI controller. This introduces an active counter measure against low frequency thrust. We investigate the impact of this adaption on the mooring line fatigue.

8.2 Simulation setup

Simulations are performed with OpenFAST [4]. The FOWT model consists of the IEA Wind 15MW reference turbine and the ActiveFloat floating platform [21]. Ambient conditions are set to turbulent wind and a calm sea with no waves or currents. The wind speed ranges between 10 m/s and 25 m/s. Below 10 m/s, the generator controller becomes the primary control mechanism and the blade pitch controller is inactive. The mooring design coupled to the floater is described in Table 8-1.

For each wind speed, three simulation runs are performed with different turbulent wind fields. The wind fields have the same turbulence intensity but were created with different turbulence seeds. The same set of seeds was used to create the wind fields to be able to compare the results between wind speeds. The simulated time is set to 20 minutes. From the resulting time series of the mooring line load, the Damage Equivalent Load (DEL) of all three mooring lines is calculated.

To summarize the results for wind fields with the same wind speed but different turbulence seeds, the mean DEL is calculated. This leaves us with a single mean DEL for each mooring line and wind speed, respectively. This procedure is done with the original controller setup and each new version created by the tuning process. Finally, the percentual change ΔDEL of the mean mooring line DEL compared to the baseline setup is computed.

In order to evaluate the simulations, not only the DEL of the mooring lines is taken into account. Attention is also given to the generated electrical power P_{el} and the DEL of the blades and the tower. The results presented below are chosen as a tradeoff between the reduction in mooring line DEL, generated electrical power and the DEL of the blades and the tower.

Group of lines	Chain bar diameter [mm]	Equivalent diameter [mm]	Line Length [m]	Dry mass per meter length [kg/m]	Axial stiffness [kN]	Steel Grade
Upwind lines	120.00	216.00	832.00	286.56	122.97e4	R3
Downwind lines	70.00	126.00	832.00	97.51	418.46e3	R3

Table 8-1: The mooring design of Activefloat site B

8.3 Tuning of Kp

First, only the K_p gain was tuned. Modern blade pitch controllers use different gains for different operation points. Therefore, multiple K_p gains are stored in a lookup table depending on the blade pitch and visualized as the K_p curve.

One convenient way to tune K_p around the stable operation points is to shift the K_p curve vertically Figure 8-1. The shift is done in discrete steps ΔK_p by simply adding ΔK_p to or subtracting it from each entry of the K_p lookup table. The step size is chosen as $\Delta K_p = 0.1 * \left(\max\left(K_p\right) - \min\left(K_p\right)\right)$. This guarantees a sensible magnitude of ΔK_p in relation to the given values. The new curves are therefore given by

$$K_{p,new} = K_p \pm a * \Delta K_p, \quad a \in \mathbb{N}$$

Decreasing K_p leads to a change in the respective DEL for each mooring line, but the change lacks a clear pattern: For some wind speeds, the DEL increases, for others it decreases. A clear correlation between a decrease in K_p and the change in DEL is missing. Increasing K_p leads to a decrease in the side mooring line DEL and an increase in the main mooring line DEL Figure 8-2. This holds true for a certain range around the stable operation point which is roughly $K_{p,range} \approx 3 * \Delta K_p$. Beyond this range, the main mooring line DEL increases much.

The best result of the K_p tuning was achieved at $a = 2$. The side mooring lines 2 and 3 show a decrease of DEL of 5% and 3%, respectively. However, the main mooring line 1 holding most of the aerodynamic thrust shows a DEL increase of 3%.

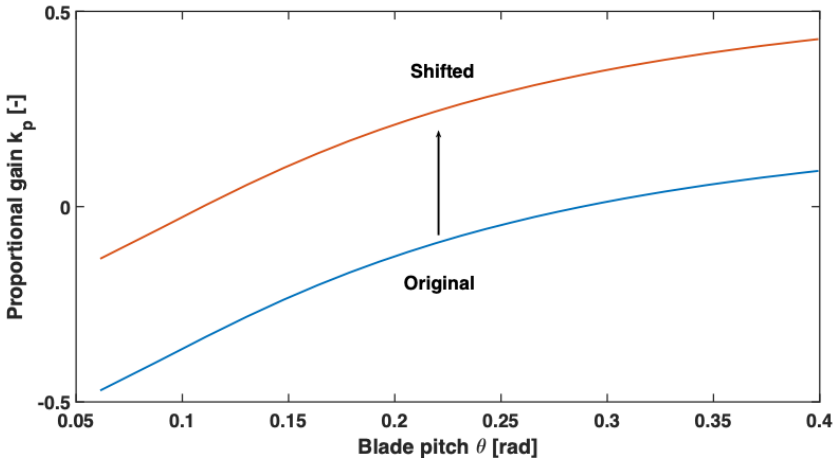

Figure 8-1: Vertical shift of the $\mathbf{K_p}$ curve. Shifts are performed in discrete steps $\Delta\mathbf{K_p}$ around the original curve.

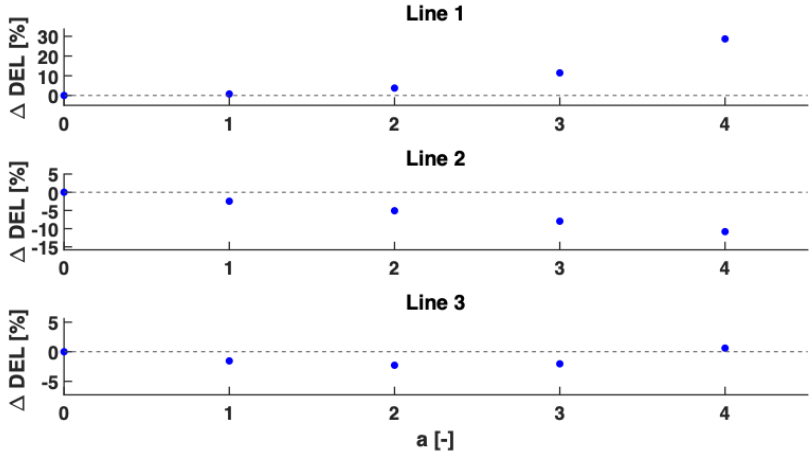

Figure 8-2 Percentual change in the mean mooring line DEL for upwards shifted $\mathbf{K_p}$ curves. Variable a in the x-axis shows how many discrete steps $\Delta\mathbf{K_p}$ were taken.

8.4 Tuning of Ki

Second, only the K_i gain was tuned. Again, the blade pitch controller uses a lookup table of K_i values for different operation points. Similar to the tuning ofK_p , the K_i curve is shifted vertically Figure 8-3 with a step size of $\Delta K_i = 0.1 * (\max(K_i) - \min(K_i))$. The new curves are therefore calculated as

$$K_{i,new} = K_i \pm b * \Delta K_i\,, \quad b \in \mathbb{N} K_{i,new} = K_i \pm b * \Delta K_i\,, \quad b \in \mathbb{N}$$

Decreasing K_i shows no clear effect on the mooring line DEL. Increasing K_i leads to a decrease in the main mooring line DEL and an increase in the side mooring line DEL Figure 8-4. Again, a certain range can be given

which marks the save area around the stable operation point. For $K_iK_i$this range is roughly $K_{i,range} \approx 7 * \Delta K_i K_{i,range} \approx 7 * \Delta K_i$.

The best result of the K_i tuning was achieved at $b = 5$. Line 1 shows a decrease in DEL of 5%. For the side lines, line 2 stays equal and line 3 shows an increase in DEL of 8%.

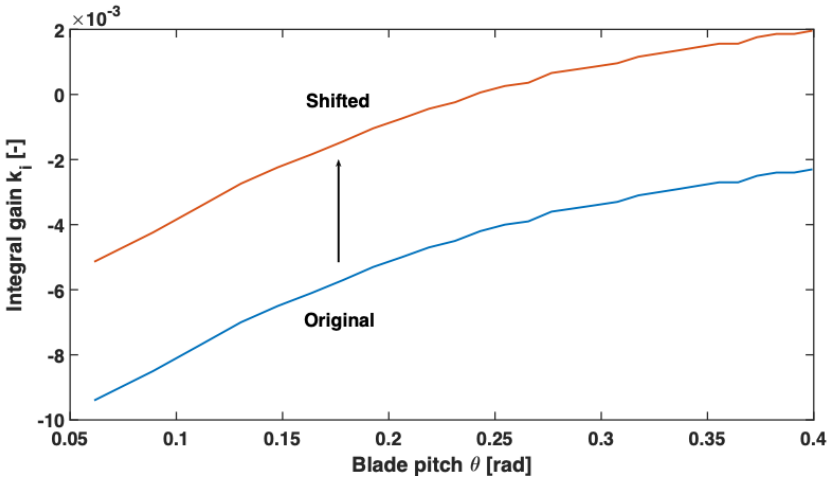

Figure 8-3*:* Vertical shift of the $\mathbf{K_i}$ curve. Shifts are performed in discrete steps $\Delta\mathbf{K_i}$ around the original curve.

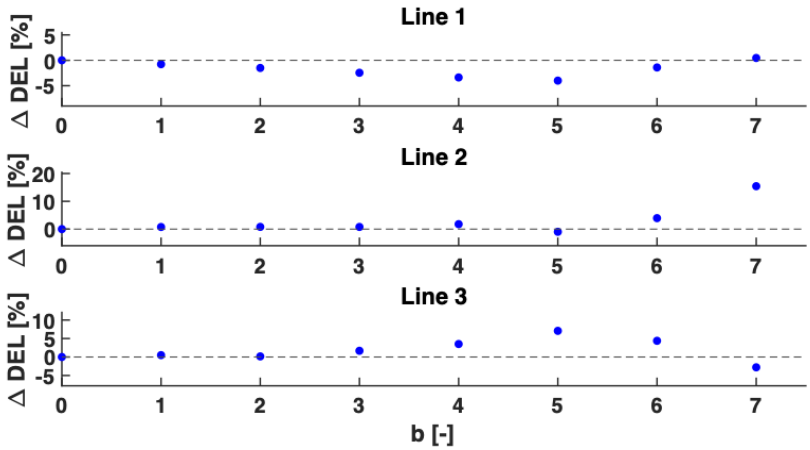

Figure 8-4: Percentual change in the mean mooring line DEL for upwards shifted $\mathbf{K_i}$ curves. Variable b in the x-axis shows how many discrete steps $\Delta\mathbf{K_i}$ were taken.

8.5 Tuning of Kp and Ki

We have seen that the separate increase of K_p and K_i show opposed characteristics. While the increase of K_p can lead to a decrease of DEL in the side lines and an increase of DEL in the main line, the opposite is true for the increase of K_i. In this case, the side line DEL increases and the main line DEL decreases. Can a combination of both approaches decrease the DEL for all mooring lines?

K_p and K_i are increased only, as decreasing them didn't deliver any favorable results in the separated simulation runs. The range of interesting steps is set to:

$$K_{p,new} = K_p + a * \Delta K_p \text{ for } \; 1 \leq a \leq 3, \; a \in \mathbb{N}$$

$$K_{i,new} = K_i + b * \Delta K_i \quad \text{for} \quad 4 \leq b \leq 7, \; b \in \mathbb{N}$$

This leads to 12 different combinations of $K_p$and K_i curves. Additionally, the set of new K_i curves are saturated to ensure $K_i \leq 0$:

$$K_{i,new} = saturate(K_i\,, 0)$$

This is necessary as a sign change in K_i changes the response of the PI controller. Especially, it leads to a bigger loss of produced electrical power P_{el}.

The results obtained with the different combinations are widespread. Many combinations reach a decrease in DEL, but also a significant reduction in the produced electrical power P_{el}. Increase in the DEL of other components such as the tower and the rotor blades was also seen. We only present the best result below.

The best result reached with $a = 1$ and $b = 4$ is a tradeoff. It doesn't represent the biggest decrease in DEL reached, but rather the best DEL reduction with acceptable power loss and low increased fatigue of other components. The results for the mooring lines in Figure 8-5 are promising. The DEL of the main line decreases for all wind speeds except 10 m/s and reaches a best reduction of 6%. The side lines show mixed results. Notably, the maximum DEL increase of any line is seen for line 3 with 4%. However, this configuration comes with a power loss of up to 7% and at least some power loss for all wind speeds Figure 8-6. The blade DEL stays neutral or decreases in both directions Figure 8-7. Only the tower DEL increases for lower wind speeds Figure 8-8.

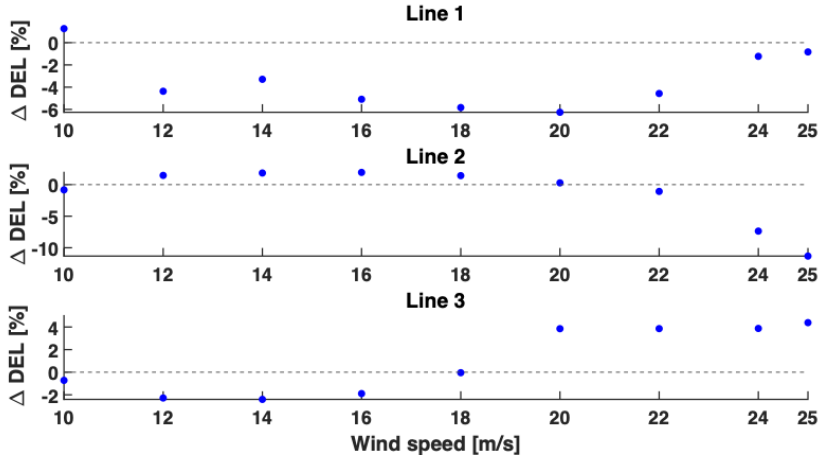

Figure 8-5: Percentual change in the mean mooring line DEL over different wind speeds for shifted $\mathbf{K_p}$ and $\mathbf{K_i}$ curves. The new curves are calculated with $\mathbf{a = 1}$ and $\mathbf{b = 4}$.

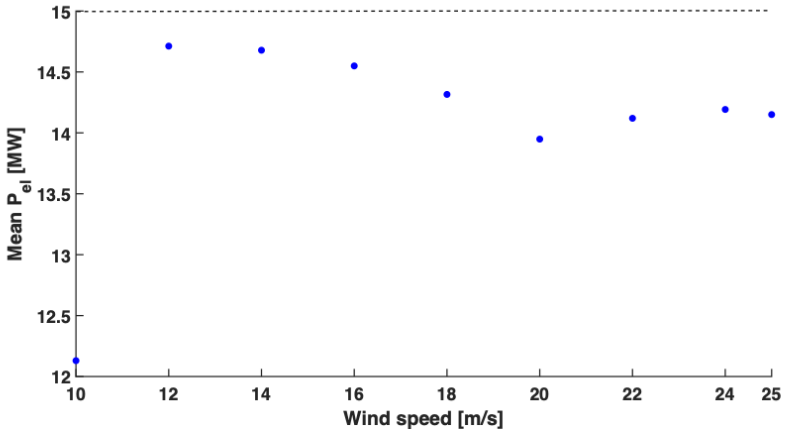

Figure 8-6:: Generated electrical power for shifted K_p and K_i curves. The new curves are calculated with $a = 1$ and $b = 4$.

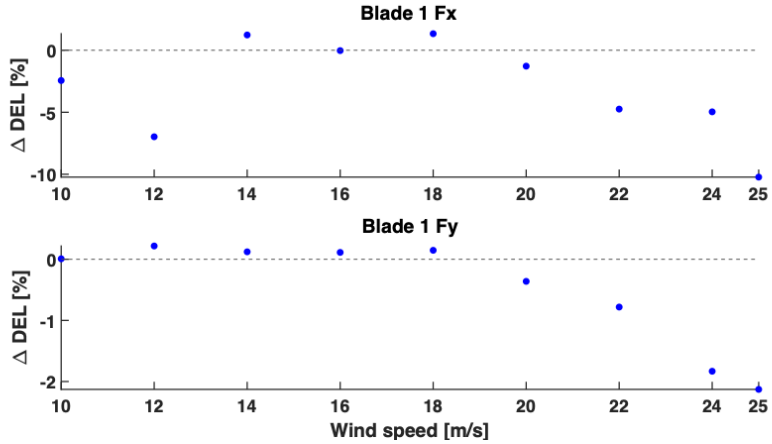

Figure 8-7: Percentual change in the mean DEL of one rotor blade over different wind speeds for shifted K_p and K_i curves. The new curves are calculated with $a = 1$ and $b = 4$.

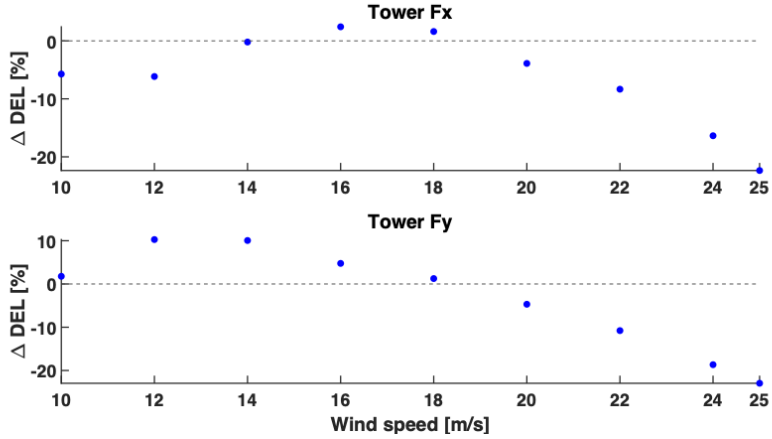

Figure 8-8: Percentual change in the mean DEL of the tower over different wind speeds for shifted K_p and K_i curves. The new curves are calculated with $a = 1$ and $b = 4$.

8.6 Tower top feedback

The last approach presented is not based on the tuning of K_p and K_i but facilitates an additional function of the ROSCO controller. The fore-aft velocity of the nacelle is measured, filtered, multiplied with a gain $K_{p,float}$ and then added on the output of the PI controller. Again, the gain was varied around the analytically derived baseline value $K_{p,float} = -9.38$. Variation was performed by inserting the following values:

$$K_{p,float} \in \{-7,\ -8,\ -9.38,\ -10,\ -11\}$$

The results show little difference between the different gain values. Therefore, the analytic solution of $K_{p,float} = -9.38$ is chosen for the following discussion. The results are compared to a control strategy with the baseline ROSCO controller without feedback of the nacelle fore-aft velocity. Including the nacelle fore-aft velocity is promising and results in a decrease of the main line DEL of up to 5% Figure 8-9. Also, the reduction is visible for most wind speeds tested and not only punctual. The side line DELs vary but most importantly don't increase above 2.5%. The generated electrical power P_{el} falls slightly by 2% for all wind speeds observed Figure 8-10. Next to the mooring line DEL, the DEL of the rotor blades and the tower was also calculated. In the blades, a slight decrease in DEL is observed Figure 8-11. In the tower, the control strategy has a stronger impact as the tower DEL drops up to 40% for the highest wind speed and decreases across all wind speeds tested Figure 8-12.

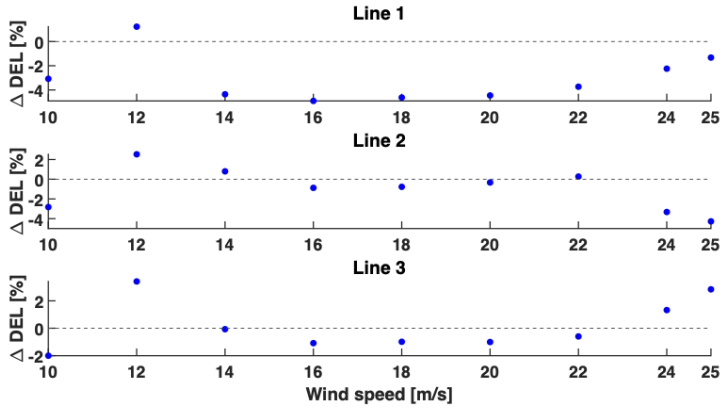

Figure 8-9: Percentual change in the mean mooring line DEL over different wind speeds for Floating Feedback control strategy. The DEL of line 1 decreases up to 5% with ongoing DEL reduction over wind speeds $v \geq 14\ \frac{m}{s}$.

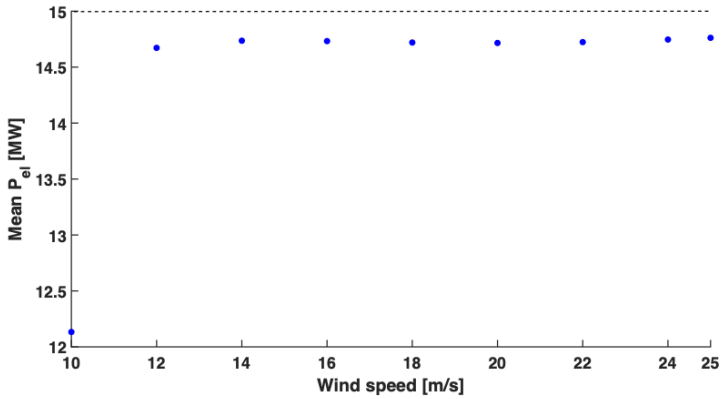

Figure 8-10: Generated electrical power P_{el} over different wind speeds for Floating Feedback control strategy.

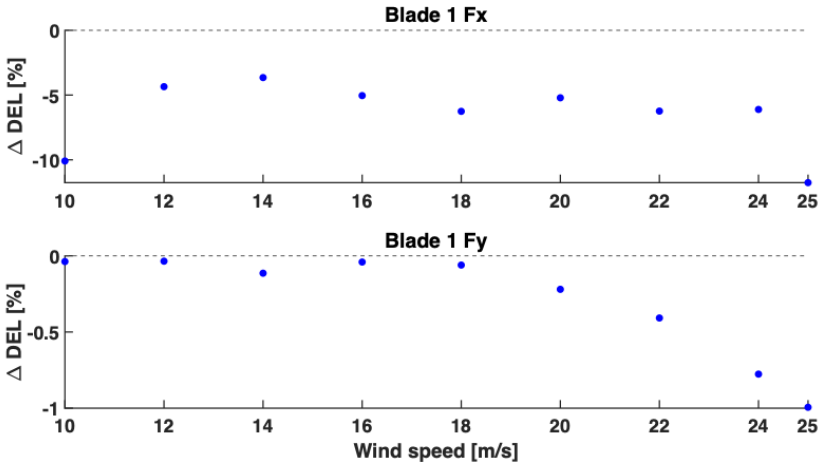

Figure 8-11: Percentual change in the mean DEL of one rotor blade over different wind speeds for Floating Feedback control strategy.

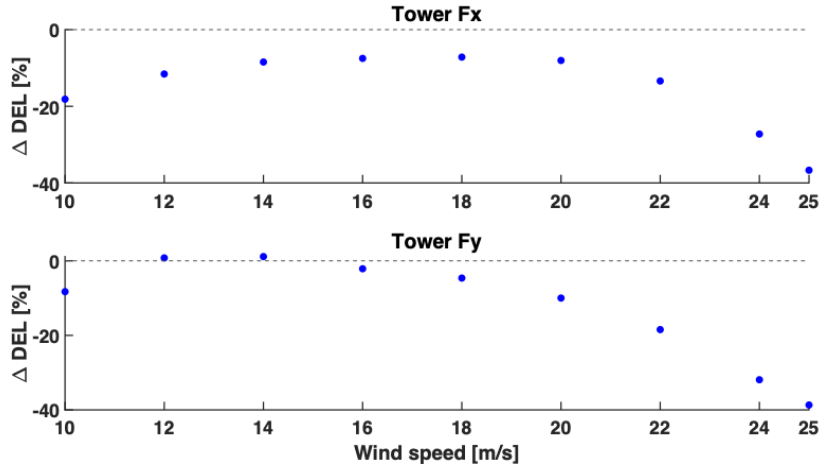

Figure 8-12: Percentual change in the mean tower DEL over different wind speeds for Floating Feedback control strategy.

8.7 Conclusion

We have seen that the blade pitch controller has a considerable effect on the Damage Equivalent Load of the mooring lines and therefore on the fatigue development. Different configurations of the pitch controller change the DEL in the mooring lines, blades, and the tower, but also the generated electrical power.

Increasing solely K_p or K_i has ambivalent effects on the DEL of the different mooring lines. Combining the adaption of both parameters is promising. The best results found was a reduction of main line DEL of up to 6% with an increase in side line DEL of up to 4% and power loss of up to 7%. Besides the variation of controller gains, the additional feed-in of the nacelle fore-aft velocity was investigated. With this method, the main mooring line DEL decreases up to 5% with the side lines increasing to a maximum of 2%. Power loss is limited to 2% as well. In general, adapting the control mechanism of the turbine to decrease mooring line fatigue is a promising path and worth further investigation.

9 DESIGN AT FARM LEVEL: STUDY OF THE COSTS BENEFITS OF SHARED ANCHORS AND SHARED MOORING LINES

9.1 Shared Anchor

The main objective of this section is to study the technical feasibility and economic impacts of shared anchors layouts.

9.1.1 Global layout

In this section, a "shared anchor layout" corresponds to a three wind turbines (WTs) layout where three mooring lines (one of each WT) are anchored at a common point at seabed level. Figure 9-1 illustrates such a layout.

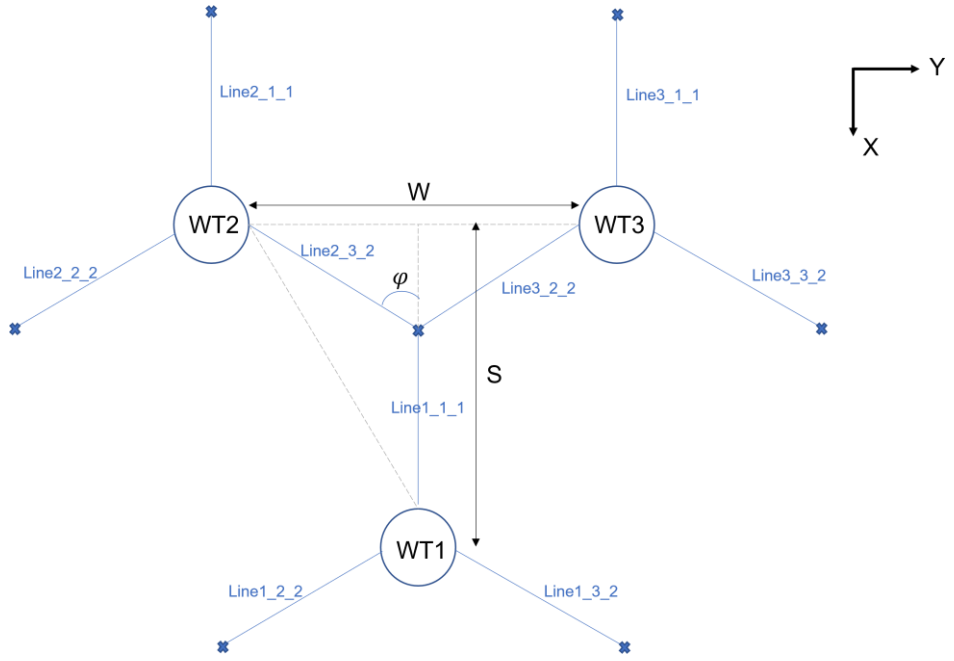

Figure 9-1: General shared anchor layout

A longitudinal spacing of 7D (with D the rotor diameter) is set between two consecutive wind turbines, as well as a lateral spacing of 4D. The spacing is imposed in order to avoid power losses due to wake effects. In the literature, the value of the spacing varies between 4D and 15D, and the value of 7D was chosen in order to be coherent with previous COREWIND work [27] .

Being inspired by the first loop of optimization conducted for the deliverable D2.2 [1], all the upwind lines of the layout will share the same characteristics (length, material, diameter etc..). In the same way, all downwind lines will be identical.

9.1.2 Approach

For each site studied, the main approach is the same. A first step consists in finding the geometrical layout that minimizes the total cumulative mooring line length. This "optimization" problem can be described as:

$$\min(6L_2 + 3L_1)$$

$$\varphi = 60°$$

$$W > 4D$$

$$S = 7D$$

Where L_1 and L_2 are the length of upwind lines and downwind lines, respectively. The other geometrical parameters can be found on Figure 9-1.

To find this layout, several shared anchor positions are tested. For each of them, WTs are positioned in order to respect geometrical constraints, and cumulative line length is then computed. The positions of the turbines correspond to initial positions, and no static analysis is conducted. Nevertheless, it has been observed that the distance between turbines in static are identical to initial distances. The layout with minimum cumulative length is chosen as basis for the second step of the study.

The second step consists in an optimization comparable to the one conducted to find the layouts presented in deliverable D2.2 [1]. The optimization tool developed for this previous study does not allow to optimize line length while keeping the anchor radius (horizontal distance between fairlead and anchor) constant. Because of the spacing constraint, we need to keep the radius constant, and thus we cannot optimize the line length. That is why the first step (geometrical optimization) is needed. Consequently, only chain and polyester diameters, as well as chain grade are optimized.

Because of important computation time, the optimization is only done on a critical DLC. This critical DLC is defined as the one resulting in the highest tension criteria in the mooring lines. The optimized layout is then tested on both DLC6.1 and 6.2 in order to check design criteria. The analysis is done in both Start of Life and End of Life condition.

No fatigue analysis has been assessed in this study.

9.1.3 Costs computation

The objective of this study is to estimate the possible economic benefits that can be obtained by using shared anchor layout instead of classic mooring layout. The mooring system prices computed here will be compared to the one presented in [1]. The following section focuses on the method used to compute the different costs

- Lines and classic anchor costs:

The lines and classic anchors costs (all the anchors except the shared one) are computed using the same formula as the one used in [1].

- Shared anchor costs:

In order to compute properly the shared anchor costs, a different method is used. Indeed, cost cannot be estimated by using the MBL of the line, because there is no unique line linked to the anchor. Moreover, the formula used until now were valid for drag-embedded anchors. Now that efforts applied on a shared anchor are multi directional, other anchor types should be considered, such as pile anchors. Consequently, the cost is estimated by the following formula [29]:

$$C_{anchor} = M.C_{material}.(1 + CF)$$

Where M is the mass of the anchor (kg), $C_{material}$ is the mass price of the anchor material (€/kg) and CF is a complexity factor, usually taken equal to 1 for pile anchor.

In order to compute the anchor volume, the American Bureau of Shipping (ABS) [28]method is used. The method enables to estimate the different characteristics of the anchor (length, diameter and thickness) once given the anchor type, the ultimate holding capacity and the soil conditions. The ultimate holding capacity of the shared anchor is defined by the following formula:

$$F_d = \gamma_{mean} . F_{mean} + \gamma_{dyn} . (F_{max} - F_{mean})$$

Where γ_{mean} and γ_{dyn} are safety factors that can be found in [16]

The force F is given by:

$$F = \sqrt{F_x^2 + F_y^2 + F_z^2}$$

With

$$F_x = \sum_{i=1}^{3} F_{x_i}, \quad F_y = \sum_{i=1}^{3} F_{y_i}, \quad F_z = \sum_{i=1}^{3} F_{z_i}$$

Where F_{x_i}, F_{y_i} and F_{z_i} are the x, y and z component of the force applied by the ith line on the anchor

- Buoys costs

The buoys used for the different layouts are selected from BALMORAL catalogue[30].An estimation of the buoy costs was provided by BALMORAL.

9.1.4 ActiveFloat site B – Gran Canaria

For this site, the layout is similar as the one presented in the first loop. The mooring system is composed of three catenary lines, fully made of chain.

Figure 9-2 illustrates this layout.

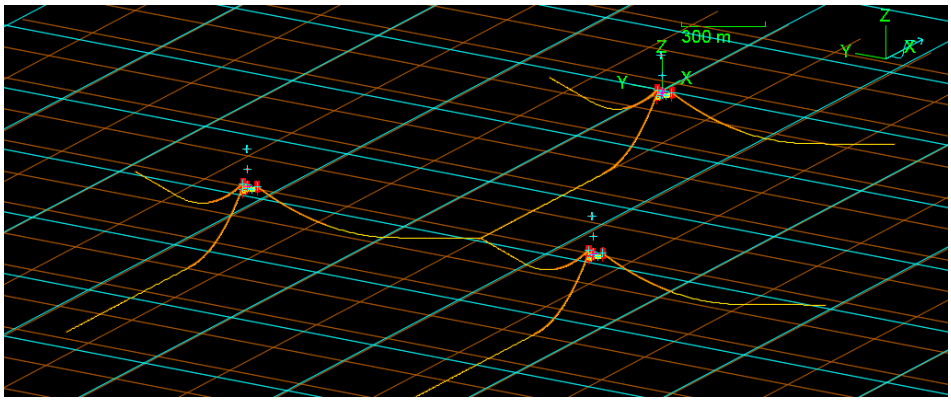

Figure 9-2: OrcaFlex 3D view of the shared anchor layout at Gran Canaria

Table 9-1 summarizes physical properties of chains and polyester used in the mooring system.

Group of lines	Material	diameter [mm]	Equivalent diameter [mm]	Line Length [m]	Dry mass per meter length [kg/m]	Axial stiffness [kN]	Steel Grade
Upwind lines	Chain	110,00	198,00	1275,00	240,8	1,03E+06	R4
Downwind lines	Chain	50,00	90,00	840,00	49,8	2,14E+05	R4S

Table 9-1: ActiveFloat site B: Physical properties of the material used in the shared anchor mooring system.

Table 9-2 below summarizes the maximum values obtain for both DLC6.1 & 6.2:

DLC61 & 62 (SOL&EOL) results	Upwind	Downwind
Maximum tension criterion (chain)	0,79	0,998
Maximum offset (m)	56,9	
Maximum pitch (°)	2,19	
Maximum yaw (°)	4,42	
Maximum horizontal acceleration (m/s²)	0,83	
Maximum vertical acceleration (m/s²)	0,53	

Table 9-2: ActiveFloat site B: Main results of the start of life and end of life analysis of DLCs 6.1 and 6.2.

- Conclusion

The design criteria on the maximum tensions admissible in the mooring lines is respected, as well as the constraints of maximum pitch, yaw and offset of the platform, and maximum horizontal accelerations of the RNA. It can be observed that the tension criteria for the downwind line is close to one. This is explained by the fact that we choose to reduce largely the diameter of the chains used for these lines.

Thanks to the formula presented in 9.1.3, the price of the complete layout is estimated at 2729 k€. Table 9-3 details the contribution of chain sections, as well as anchor costs.

ActiveFloat Site B	Chain sections	Anchors	Total
Cost (k€)	2332,3	396,9	**2729,2**
% of total	*85,0%*	*15,0%*	

Table 9-3: ActiveFloat Site B: Cost detail of shared anchor mooring system.

Those costs are compared to three times the costs of the classic layout found in the first loop. Table 9-4 summarizes this comparison:

ActiveFloat site B	Phase 1	Shared Anchor
Chain sections cost (k€)	2042,1	2332,3
Difference (%cost of phase 1)		*+14%*
Anchors cost (k€)	553,2	396,9
Difference (%cost of phase 1)		*-28,8%*
Total cost (k€)	**2595,3**	**2729,2**
Difference (%cost of phase 1)		***+5,1%***

Table 9-4: ActiveFloat Site B: Cost comparison between first loop and shared anchor layout

An increase in line costs compared to the classic layout is observed. This is due to the necessity to increase the line length in order to respect the spacing. Moreover, the criterion on the touch down point (minimum portion of line laying on seabed superior to 10 meters) added a new constraint in the geometrical optimization presented in [1]. Consequently, the line length had to be increased to respect this criterion. Conversely, thanks to the less important number of anchors, the total anchor price of the shared anchor layout decreases. Nevertheless, this decrease in anchor costs does not compensate the increase in chain costs. Consequently, the total cost of the shared anchor layout is higher than the classic layout. It is worth noting that installation costs are not included in this study, and are expected to decrease for a shared anchor configuration.

9.1.5 ActiveFloat site C – Morro Bay

For this site, the layout is similar as the one presented in the first loop. The mooring system is composed of three semi taut lines, with chain section at the top and bottom of the lines, and a polyester section in between. Buoys are added to the lines in order to increase yaw stiffness.

The following figure shows a 3D view of the layout.

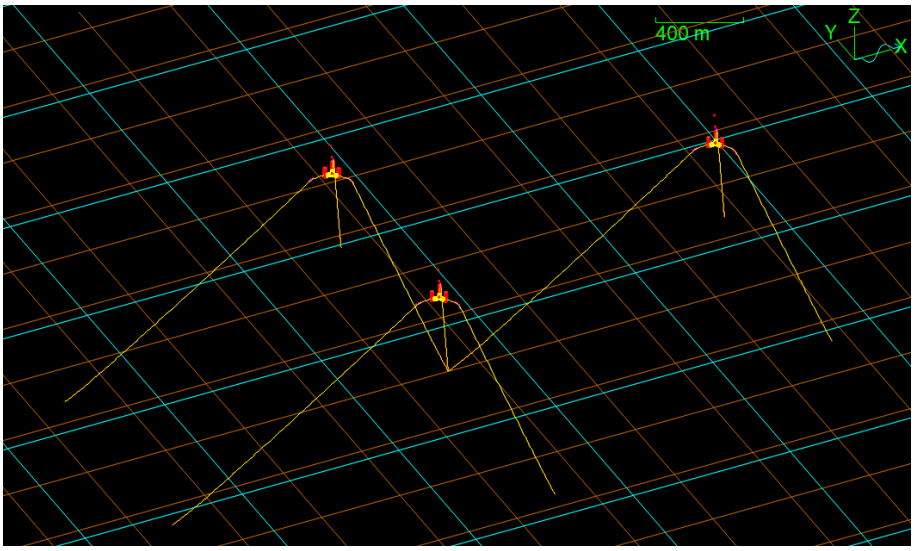

Figure 9-3: Shared anchor layout at Morro Bay

Table 9-5 summarizes physical properties of chains and polyester used in the mooring system.

Group of lines	Material	diameter [mm]	Equivalent diameter [mm]	Line Length [m]	Dry mass per meter length [kg/m]	Axial stiffness [kN]	Steel Grade
Upwind lines	Chain	105,00	189,00	275,00	219,4	9,42E+05	R3S
	Polyester	169,00	135,73	1275	19,5	1,76+05	-
Downwind lines	Chain	90,00	162,00	199,55	161,2	6,92E+05	R4
	Polyester	146,00	117,73	847,448	14,7	1,29E+05	-

Table 9-5: ActiveFloat site C: Physical properties of the material used in the shared anchor mooring system.

Table 9-6 below summarizes the maximum values obtain for both DLC6.1 & 6.2:

DLC61 & 62 (SOL&EOL) results	Upwind	Downwind
Maximum tension criterion (chain)	0,75	0,987
Maximum tension criterion (polyester)	0,651	0,948
Maximum offset (m)	44,78	
Maximum pitch (°)	6,99	
Maximum yaw (°)	3,43	
Maximum horizontal acceleration (m/s²)	4,22	
Maximum vertical acceleration (m/s²)	1,14	
Maximum pretension (kN)	1801,89	

Table 9-6: ActiveFloat site C: Main results of the start of life and end of life analysis for DLCs 6.1 and 6.2.

- Conclusion

The design criteria on the maximum tensions admissible in the mooring lines is respected, as well as the constraints of maximum pitch, yaw and offset of the platform, and maximum horizontal accelerations of the RNA.

Thanks to the formula presented in 9.1.3, the price of the complete layout is estimated at 6666,9k€. Table 9-7 details the contribution of chain sections, polyester sections, as well as anchor and buoys costs.

ActiveFloat Site C	Chain sections	Polyester sections	Anchors	Buoys	Total
Cost (k€)	811,9	1049,9	731,0	4074	**6666,9**
% of total	*12,0%*	*16,0%*	*11,0%*	*61%*	

Table 9-7: ActiveFloat Site C: Cost detail of shared anchor mooring system.

It can be observed that the buoys represent by themselves 61% of the total mooring cost, whereas only 11% of the cost is due to anchors. Even if polyester is cheaper than chain, it represents a larger part of the final costs because the cumulative polyester length (8910m) is higher than the chain one (2022m).

Those costs are compared to three times the costs of the classic layout found in the first loop. Table 9-8 summarizes this comparison:

ActiveFloat site C	Phase 1	Shared Anchor
Chain sections cost (k€)	829,53	811,9
Difference (%cost of phase 1)		*-2,1%*
Polyester sections cost (k€)	871,26	1049,9
Difference (%cost of phase 1)		*+20%*
Buoys cost (k€)	4074	4074
Difference (%cost of phase 1)		*+0,0%*
Anchors cost (k€)	887,4	731,0
Difference (%cost of phase 1)		*-17,6%*
Total cost (k€)	**6662,1**	**6666,9**
Difference (%cost of phase 1)		***+0.07%***

Table 9-8: ActiveFloat Site C: Costs comparison between first loop and shared anchor layout

As expected, a consequent increase in lines costs is observed. This is due to the necessity to increase the lines length in order to respect the spacing. Conversely, the total anchor cost decreases, due to the reduced number of anchors needed. Still, it is important to notice that the cost of a shared anchor (235,8 k€) is almost tripled compared to a classic one (≈ 85 k€). The total cost of a shared anchor layout on this site is find to be slightly superior than a classic layout. This difference is not significant because the impact of increasing length of the lines is almost compensated by the decreasing number of anchors. Nevertheless, as for Gran Canaria, this approach does not take into account installation costs, which are expected to decrease for a shared anchor layout.

9.1.6 On the possibility of using 1WT simulations

Simulations used to check design criteria on DLC6.1 and 6.2 are files with three wind turbines, which lead to greater computation time than the study with only one floater. On an indicative basis, a 3WT simulation on

Morro Bay takes approximately 23600s, whereas a 1WT simulation over the same DLC lasts 8100s. This section studies the possibility of using simulations with only one wind turbine in order to check the criteria.

All the names used in this section refer to Figure 9-1, and, for more simplicity, only 0°-wave-incidence cases have been studied.

There are two aspects in this study. First, is it possible to approximate the maximum values of the different parameters with only one wind turbine? In other words, are the maximum and mean values observed for a 1WT simulation similar to the ones observed in a full 3WT simulation?

For this subject, a comparison of mean and maximum values of design parameters between 1WT files and 3WT files has been conducted. The study was carried out on DLC6.1 simulations, for both Gran Canaria and Morro Bay sites. Table 9-9 presents the results for the floater parameters (yaw, pitch and acceleration).

ActiveFloat	Gran Canaria		Morro Bay	
	3WT	1WT	3WT	1WT
Yaw (max) [°]	4,42	4,42	3,44	3,42
Yaw (mean) [°]	0,0	0,0	0,0	0,0
Pitch (max) [°]	1,98	1,98	6,95	6,95
Pitch (mean) [°]	-0,4	-0,4	0,0	0,0
Horizontal acc (max) [m/s²]	0,83	0,83	4,22	4,22
Horizontal acc (mean) [m/s²]	0,1	0,1	0,49	0,5
Vertical acc (max) [m/s²]	0,53	0,53	1,20	1,20
Vertical acc (mean) [m/s²]	0,09	0,09	0,15	0,15

Table 9-9: Comparison between maximum and average values for the floater parameters, Gran Canaria and Morro Bay

For both sites, no significant differences are observed (maximum relative difference of 0.6%). The 1WT simulation enables a satisfactory approximation of the design criteria for those parameters.

The maximum values of utilization factor ($UF = \frac{T_d}{0.95MBL}$, where $T_d = \gamma_{mean}T_{mean} + \gamma_{dyn}(T_{max} - T_{mean})$) are presented in Table 9-10.

ActiveFloat	Gran Canaria			Morro Bay		
	WT1	WT2	WT3	WT1	WT2	WT3
Line 1 (upwind) [-]	0,79	0,76	0,76	0,76	0,77	0,77
Line 2 (downwind) [-]	0,997	0,98	0,94	0,90	0,92	0,91

Line 3 (downwind) [-]	0,92	0,90	0,85	0,95	0,95	0,93

Table 9-10: Comparison of the utilization factors of each lines, Gran Canaria and Morro Bay

Differences can be noticed between the three turbines. A maximum difference of 8% is observed between line 3 of WT1 and WT3. Nevertheless, the maxima are in a large majority observed on WT1, which means that the 1WT-approach seems conservative. Moreover, those differences can be lowered thanks to the second part of the study.

The second aspect relates to the computation of the force applied on the shared anchor. Indeed, if only one wind turbine is considered, two of the three lines usually used to compute this force are missing. Consequently, it is necessary to find a way to approximate the efforts applied by the missing lines through the efforts given by the downwind lines of the turbine considered.

When we look at the signal of effective tension of a downwind line connected to WT1 (L_1_3_2), we observed that it has the same general behaviour as the one observed in L_2_3_2 and L_3_3_2, but with a certain lag. This result can be highlighted by computing the cross correlation between the two signals. The cross correlation between two signals s_1 and s_2 is defined by:

$$\rho_{s_1 s_2}(\tau) = \lim_{T \to \infty} \frac{1}{T} \int_0^T \frac{s_1(t_i) s_2(t_i + \tau)}{N_t}$$

This measure allows to evaluate the similarity between the two signals as a function of the lag between them.

Figure 9-4 shows the cross correlation between the two time-series of effective tension, as a function of the time lag. The correlation is normalized by dividing the signals by their standard deviation

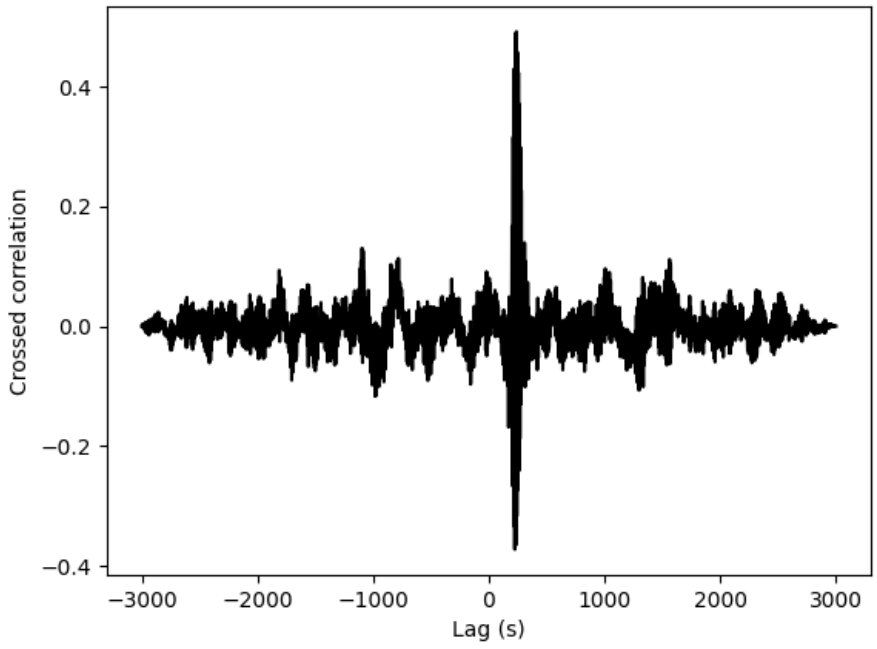

Figure 9-4: Crossed correlation between two signals of effective tension (L1_2_3 and L2_2_3)

We can observe a correlation peak around a particular lag τ (In this example, taken from Gran Canaria site, τ = 237,2s). The maximum value of correlation is approximately equal to 0,49. Therefore, we can conclude that if the first signal is shifted by τ, the two signals will be at 49 % identical. Ideally, a correlation peak greater than 0.6 would be wanted to be fully satisfied. Nevertheless, we observed that the correlation at $lag = 0$ is largely lower ($\approx$ 0,02) than the one at τ. Consequently, shifting the signals of the downwind lines linked to the shared anchor before summing them up is expected to give more coherent results than a simple summation on the unshifted signals.

The behaviour observed on that particular case has been observed on all the DLCs studied. Consequently, the conclusion derived above can be extended. Nevertheless, in this computation time-saving approach, the 3WT simulation, and therefore the correlation analysis, are not available. An estimation of τ has to be derived. A first approximation of τ can be made by estimating the group velocity of the waves. T_p is taken as a reference period, and a deep-water hypothesis is made. Therefore, by using the dispersion relation, we have:

$$c_g = \frac{T_p . g}{4\pi}$$

The distance between WT_i and WT_j , projected in the wave propagation direction, is noted d_{ij}. Because the actual positions of the turbines are not available in 1WT files, this distance is estimated through the static positions. The lag can be estimated as:

$$\tau_{approx} = \frac{d_{ij}}{c_g}$$

In order to estimate the efficiency of this approach, the force applied on the shared anchor was computed for several cases (all with a 0° wave orientation for more simplicity) by using three method:

- Computation with the three wind turbines (F_{ref})

  Computation with only one wind turbine, unshifted (F_{1WT})
  Computation with only one wind turbine, shifted by τ_{approx} ($F_{1WT,shift,approx}$)

The results of this study are available on Figure 9-5.

Gran Canaria		Morro Bay	
3WT/1WT	3WT/1WT,shift,approx	3WT/1WT	3WT/1WT, shift, approx
1.5%	0.7%	0.2%	3.8%
2.2%	0.1%	3.8%	4.9%
2.5%	1.0%	0.9%	2.7%
1.9%	1.2%	1.0%	1.6%
2.8%	0.8%	4.6%	0.6%
0.0%	1.9%	1.4%	0.8%
2.4%	1.9%	6.1%	4.2%
2.2%	1.7%	4.9%	2.5%
0.5%	6.8%	7.6%	2.5%
5.1%	1.5%	3.1%	1.6%
3.9%	2.1%	0.9%	1.2%
3.0%	0.5%	3.5%	4.5%
1.7%	0.8%	0.3%	3.9%
2.4%	0.2%	5.6%	5.3%
2.8%	1.1%	1.3%	4.1%
2.1%	1.2%	3.1%	1.2%
3.0%	0.8%	4.8%	0.4%
0.0%	2.0%	2.5%	1.2%
2.4%	2.1%	5.7%	2.9%
0.8%	6.7%	6.7%	0.9%
5.3%	1.6%	4.4%	0.0%
4.2%	2.2%	0.1%	1.1%
3.2%	0.4%	5.0%	4.4%

Figure 9-5: Comparison between F_{ref}/F_{1WT} and $F_{ref}/F_{1WT,shift,approx}$ for Morro Bay and Gran Canaria

For each site, in the first column, the relative difference between F_{ref} and F_{1WT} can be found, while in the second column, the relative difference between F_{ref} and $F_{1WT,shift,approx}$ can be found. Each line corresponds to a DLC. The green boxes correspond to cases where $F_{1WT,shift,approx}$ gives better results than F_{1WT} . We can observe that, for Gran Canaria, the shifting improves the results in 83% of the cases. For Morro Bay, an improvement is observed for 60,1% of the cases. The deteriorated results compared to the unshifted situation could be explain by the fact that wind loads are applied through an identical time series for the three turbines, without shifting it. A comparison between $F_{1WT,shift,approx}$ and $F_{1WT,shift}$ (which corresponds to the force computed by shifting the signals by the lag τ obtained through the correlation analysis) shown that the results are similar in the two cases. Moreover, we can observe that even without shifting the signal, the relative difference with the reference does not exceed 7.6 %. It can therefore be concluded that a study with a 1WT simulation gives a satisfactory approximation of the force applied on the anchor.

It is possible to generalize this approach to every DLC and every shared anchor layout. Indeed, for a given wave direction θ, the distance between each turbine, projected in the wave direction, can be approximated from the initial position of each turbine. Once this distance is known, the different lags can be computed using the method described above.

Another thing to consider is the total simulation time. Indeed, if we want that all the 3WT see the same waves, the simulation time must be increased by 2τ (where τ is the greatest lag needed).

To conclude, this study has demonstrated that interesting time savings could be achieved by using models with only one wind turbine instead of three. Indeed, a good approximation of the maximum values of design parameters, as well as a satisfactory estimation of the force applied on the shared anchor can be derived from the three lines of a 1WT simulation.

9.1.7 Conclusion

For the both sites studied, it seems possible to find a shared anchor layout that respects the design criteria. However, the costs of such layouts are roughly identical to the one of classic layouts. This is mainly due to the fact that the decrease in anchor costs is compensated by an increase in line length (in order to respect spacing and touch down point criteria), and consequently in line costs. Nevertheless, several aspects shall be considered in order to improve these results. First, as mentioned earlier, the installation costs are not taken into account in this study. Those costs are expected to decrease in a shared anchor layout. Moreover, improvement can be made in material costs for Gran Canaria, by using the optimization tool. Indeed, the optimization has been "handmade" for this site, due to time constraints. Finally, spacing hypothesis can be discussed. More advanced studies on wake effect and turbine positions relatively to one other could be carried out in order to potentially reduce the spacing, and consequently line lengths.

9.2 Shared Mooring Lines

The main objective of this section is to study the technical feasibility and economic impacts of shared mooring lines layouts.

9.2.1 Global layout

In this section, a "shared mooring lines layout" corresponds to a three wind turbines (WTs) layout where three mooring lines (one of each WT) are linked to a common buoy. The buoy is linked to the seabed through a vertical mooring line. Figure 9-4 illustrates such a layout.

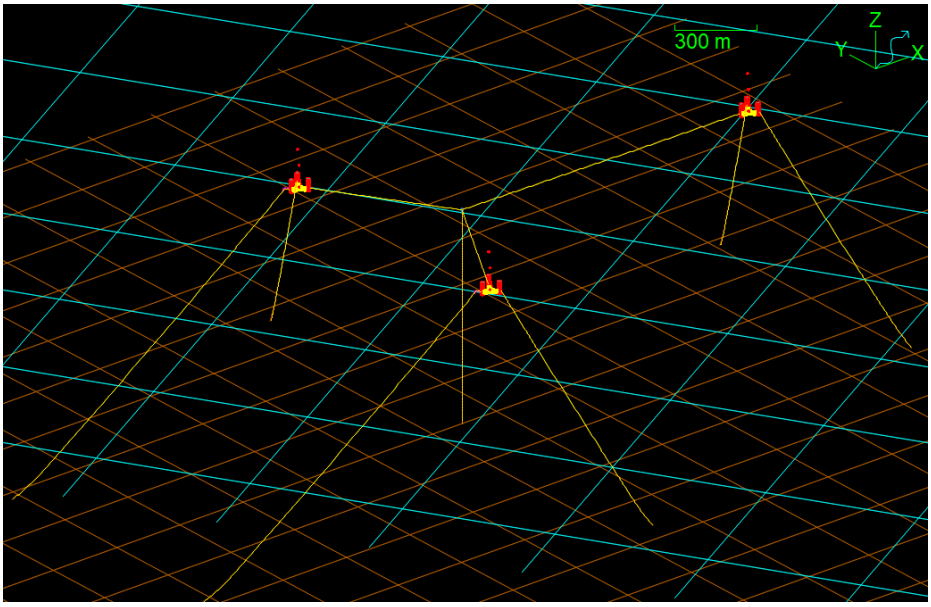

Figure 9-4: Shared mooring lines layout at Morro Bay

This layout is a first simple configuration in order to evaluate the feasibility of shared mooring line systems on a reduced scale farm. Indeed, in this model mooring lines that are not linked to the central buoy are directly anchored to seabed, as a classic mooring. A whole wind farm based on shared mooring line anchorage will be much more complex to model, and this first configuration allows to study the possibility to gather wind turbines by islet of three.

For the reasons exposed in 9.1.1, a longitudinal spacing of 7D, along with a lateral spacing of 4D are fixed.

9.2.2 Approach

The global approach exposed in 9.1.2 remains identical for the shared mooring lines study. The geometrically optimized layout is found by using the layout established for the Morro Bay shared anchor configuration (see 9.1.5). Indeed, for identical WT and anchor positions, a shared mooring lines layout allows to reduce the total line length compared to a shared anchor one.

The buoy vertical position and buoyancy are new parameters to take into account in the optimization. Nevertheless, by comparing several configurations with various depth for the buoy, the most interesting layout (in term of tension in the lines) was found to be the one with a surface buoy.

9.2.3 Site C - MorroBay

In this layout, six of the mooring lines are semi taut, with a chain section at the top and the bottom of the line, and a polyester section in-between. The three lines linking the wind turbines to the central buoy are composed of a chain section attached to the fairlead, the rest of line being made of polyester. The vertical line is mainly composed of polyester. Chain composes the last 10 meters of the line close to the seabed. The buoys used in order to increase yaw stiffness, as well as the one used to link the shared lines, are similar to the one used in 9.1.5.

Table 9-11 summarizes physical properties of chains and polyester used in the mooring system. The shared lines are referenced as “Shared” and the classic semi taut as “Classic”.

Group of lines	Type of line	Material	Diameter [mm]	Equivalent diameter [mm]	Line Length [m]	Dry mass per meter length [kg/m]	Axial stiffness [kN]	Steel Grade
Upwind lines	Shared	Chain	92,00	165,6	10,00	168,43	7,73E+05	R4S
		Polyester	126,00	101,54	1235,00	10,90	9,15E+04	-
	Classic	Chain	128,00	230,4	200,00	326,04	1,40E+06	R4
		Polyester	190,00	152,78	1376,00	24,70	2,29E+05	-
Downwind lines	Shared	Chain	92,00	165,6	10,00	168,43	7,73E+05	R4S
		Polyester	126,00	101,54	535,00	10,9	9,15E+04	-
	Classic	Chain	97,00	174,6	181,25	187,2	8,04E+05	R4S
		Polyester	166,00	133,7	860,00	18,9	1,70E+05	-
Vertical line		Chain	92,00	165,6	10,00	168,43	7,73E+05	R4S
		Polyester	126,00	101,54	840,00	10,90	9,15E+04	-

Table 9-11: ActiveFloat site C: Physical properties of the material used in the shared mooring lines layout.

Table 9-12 below summarizes the maximum values obtain for both DLC6.1 &6.2:

DLC61 & 62 (SOL&EOL) results	Upwind	Downwind
Maximum tension criterion (chain)	0,529	0,94
Maximum tension criterion (polyester)	0,823	0,863
Maximum offset (m)	29,13	
Maximum pitch (°)	6,80	
Maximum yaw (°)	3,23	
Maximum horizontal acceleration (m/s²)	4,39	
Maximum vertical acceleration (m/s²)	1,24	
Maximum pretension (kN)	2126,7	

Table 9-12: ActiveFloat site C: Main results of the start-of-life and end-of-life analysis of DLCs 6.1 and 6.2.

The design criteria on the maximum tensions admissible in the mooring lines is respected, as well as the constraints of maximum pitch, yaw and offset of the platform, and maximum horizontal accelerations of the RNA.

Thanks to the formula presented in 9.1.3, the price of the complete layout is estimated at 3425,0 k€. Table 9-13 details the contribution of chain sections, polyester sections, as well as anchor and buoys costs.

ActiveFloat Site C	Chain sections	Polyester sections	Anchors	Buoys	Total
Cost (k€)	668,4	1178,6	695,7	887,3	**3425,0**
% of total	*19,0%*	*34,0%*	*20,0%*	*26,0%*	

Table 9-13: ActiveFloat Site C: Detailed costs of shared mooring lines layout.

Those costs are compared to three times the costs of the classic layout found in the first loop. Table 9-14 summarizes this comparison:

ActiveFloat site C	Phase 1	Shared Anchor
Chain sections cost (k€)	829,53	668,4
Difference (%cost of phase 1)		*-19,4%*
Polyester sections cost (k€)	871,26	1178,6
Difference (%cost of phase 1)		*+35%*
Buoys cost (k€)	4074	887,3
Difference (%cost of phase 1)		*-78,2%*
Anchors cost (k€)	887,4	695,7
Difference (%cost of phase 1)		*-21,6%*
Total cost (k€)	**6662,1**	**3425,0**
Difference (%cost of phase 1)		***-48,6%***

Table 9-14: ActiveFloat Site C: Cost comparison between first loop and shared mooring lines layout

As expected, an important increase of the polyester section costs is observed. Indeed, lines length had to be increased in order to respect spacing. Here, the choice has been made to increase the polyester section in priority, in order to limit the costs. A large reduction of buoys cost is also observed. This is explained by the fact that this layout allows to verify yaw design criteria without using as much buoys as the optimized layout found in deliverable D2.2 [1]. Moreover, the cost of the anchors is also reduced, due to the lower number of anchors. In this case, the cost of the central anchor (15k€) is almost negligible compared to the cost of the other classic anchors (between 98,3k€ and 143,7 k€ each). Indeed, the effort applied to the central anchor by the vertical line is very low compared to the one observed for a classic anchor. This leads to a global cost decrease of almost 50%.

9.2.4 Accidental Limit State

The objective of this section is to study the impact of the loss of one of the shared mooring lines. Indeed, a shared mooring lines configuration implies the interdependence of several wind turbines. Therefore, the failure of a wind turbine's mooring line can have consequences on all the turbines linked to the turbine. Different cases are studied, each one corresponding to the failure of a particular line. Only a Start-of-Life analysis is conducted. It was also checked that permanent state was reached, to make sure that transient effects were avoided.

Transient accidental state is not studied here, the failure being considered from the beginning of the simulation. DLC 7.4 is used, following recommendations from [14]. Three yaw error (0°, -8°, 8°), as well as three wind-wave misalignments (0, 30°, -30°), are considered. The studied is carried out for two wave peak periods (12s and 16s), which correspond to the minimum and maximum T_p for a one year-return period. The corresponding H_s is equal to 6m [16]. Wind speed is taken equal to 24.77 m/s, which corresponds to the one year return period wind speed at Morro Bay REF design basis [16]

The coefficient γ_{mean} and γ_{dyn} used to compute the tension design criteria (see Corewind design basis [16]) are modified in keeping with the requirement of DNVGL-ST-0119 [17] for ALS analysis.

- Upwind Shared Line

In this case, the upwind shared line (L1_1_1, see Figure 9-1) is supposed to be lost. The maximum values of the design parameters are given in Table 9-15.

DLC7.4 (SOL) results	Upwind	Downwind
Maximum tension criterion (chain)	0,214	0,331
Maximum tension criterion (polyester)	0,132	0,382
Maximum offset (m)	321,6	
Maximum pitch (°)	4,37	
Maximum yaw (°)	47,07	
Maximum horizontal acceleration (m/s2)	2,29	
Maximum vertical acceleration (m/s2)	0,58	
Maximum pretension (kN)	405,26	

Table 9-15: ActiveFloat site C: Main results of the start of life for DLC 7.4, failure on the upwind line.

We observe that the damaged layout still respects the tension criteria, as well as the pitch, acceleration and pretension criteria. Nevertheless, the maximum yaw is far beyond the design criteria. A similar conclusion can be drawn for the offset. The maximum values of yaw and excursion are obtained for the turbine linked to the failed line. Indeed, the yaw stiffness, as well as the restoring force created by the shared lines do no longer exist when a line break. Nevertheless, considering the distances between the turbines, and the fact that the wind turbine won't be producing during this phase, those behaviours will not represent important risks for the farm. It is worth noting that, for several lines, a portion of line lies on the seabed, which is not suitable for a semi taut mooring with synthetic. Nevertheless, the length of this section is never superior to the bottom chain section length. Consequently, there is no risks of abrasion of the polyester sections.

- Downwind Shared Line

In this case, the downwind line L3_2_2 has failed. The maximum values of the design parameters are given in Table 9-16.

DLC7.4 (SOL) results	Upwind	Downwind
Maximum tension criterion (chain)	0,271	0,136
Maximum tension criterion (polyester)	0,161	0,153
Maximum offset (m)	387,4	
Maximum pitch (°)	3,84	
Maximum yaw (°)	37,29	
Maximum horizontal acceleration (m/s2)	2,23	
Maximum vertical acceleration (m/s2)	0,62	

Maximum pretension (kN)	296,1

Table 9-16: ActiveFloat site C: Main results of the start of life for DLC 7.4, failure on a downwind line.

As observed before for the upwind shared line, only the yaw and offset criteria are unverified. This time, those maximum values of yaw and excursion are obtained for WT3, which is linked to the failed line. The conclusion about the laying-on-seabed portion of line remains identical as the one derived for the upwind shared line.

- Vertical Line

In this case, the vertical line, which links the central buoy to the anchor, is supposed to be lost. The maximum values of the design parameters are given in Table 9-17

DLC7.4 (SOL) results	Upwind	Downwind
Maximum tension criterion (chain)	0,266	0 ,399
Maximum tension criterion (polyester)	0,53	0,463
Maximum offset (m)	19 ,23	
Maximum pitch (°)	3,56	
Maximum yaw (°)	2,46	
Maximum horizontal acceleration (m/s2)	2,27	
Maximum vertical acceleration (m/s2)	0,59	
Maximum pretension (kN)	1953,9	

Table 9-17: ActiveFloat site C: Main results of the start of life for DLC 7.4, failure of the vertical line.

We observe that all the criteria are respected. The different maximum values are even relatively low compared to the design criteria. In this case, there is no portion of line lying on seabed. We can conclude that the loss of this particular line would not represent a significant risk for the farm.

- Conclusion

This ALS study enabled to estimate the risks of a shared mooring line failure. The three cases studied led to similar conclusions: even if several parameters, such as yaw and offset, reach especially high values, the risks for the farm will remain limited. Indeed, the values of tension in the remaining lines indicate that there will be no domino effect if one line fails. Moreover, portions of line are expected to lay on the seabed, but considering the length of the portions, no risks of abrasion has been spotted. Nevertheless, transient cases where a line breaks during the simulation shall be considered in order to properly conclude.

9.2.5 Modal Analysis

The objective of this section is to realize a modal analysis of the system formed by the three wind turbines and their mooring systems. The results are obtained thanks to the modal analysis available on OrcaFlex. This study will be limited to the description of the first modes, along with a comparison between mode frequencies and external excitation such as wave frequencies or 1P frequencies.

For n > 25, the nth mode corresponds to a mooring line mode, and consequently does not impact the whole system. Among the first 25 modes, there are also few line modes. The study will then be reduced to the only modes corresponding to non-line modes.

The different modes are computed from the static analysis. The environmental conditions are taken into account in OrcaFlex statics, so waves and thrust at tower top will be considered here. Nevertheless, the same study had been carried out with all the environmental conditions set to zero, and also with only the waves set to zero (wind still considered). The three cases gave very similar results in term of modes frequencies, so it was decided to reduce the study to the only case with wind and waves.

The graph presented on Figure 9-6 shows the different frequencies of interest for this study. The blue curves represent the waves spectra for $T_p = 16$s (dark blue) and $T_p = 18$s (light blue). The green triangles represent the natural frequencies of an individual floater and its mooring. The 1-P region is represented in grey. This region corresponds to the range of blade passing frequencies, for wind speed going from cut in speed to cut out speed. Finally, the orange cross are the shared lines layout's mode frequencies.

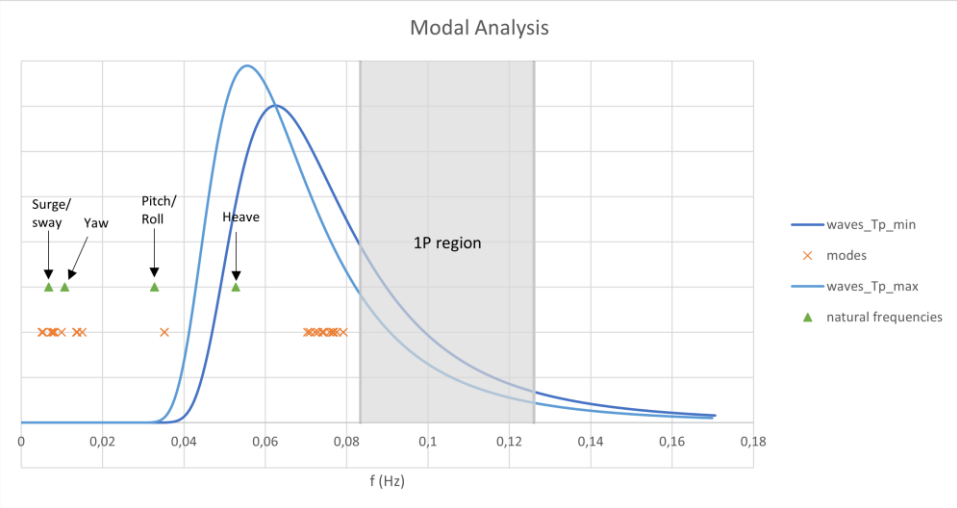

Figure 9-6: Shared mooring lines mode frequencies, along with individual floater natural frequencies and exterior loads frequencies

The first modes ($f \in [0{,}0051\ Hz\ ;\ 0{,}01Hz]$) are surge and sway modes for the different turbines. Several modes concern all the turbines, while others are individual turbine modes. The three modes around f = 0,014Hz correspond to the yaw modes of each turbine. The group of frequencies between f = 0,07Hz and f = 0,08Hz correspond to roll and pitch modes. It is worth noting that even if there are no mode frequencies in the 1P region, the shared lines layout adds new roll and pitch modes whose frequencies are in the wave frequencies range.

This type of analysis could, in the future, be a first step in designing that type of layout. Indeed, we observed that a shared mooring lines configuration can impact the natural frequencies of the system, and, consequently, a modal analysis can be a first screening tool in the design of the layout.

9.2.6 Conclusion

This study enabled to find a shared mooring lines layout that respects the design criteria. Moreover, noteworthy costs reductions (almost 50%) had been reached thanks to a decrease in the number of buoys needed. As for shared anchor, installation costs were not taken into account, and could lead to greater cost diminution. Nevertheless, practical aspects such as access and manoeuvrability around the turbines shall be taken into account. Indeed, a surface buoy was for now chosen to link the shared lines together, and consequently the latter are close to the sea surface. This could impact the navigability around the turbines, and make maintenance operations more complex.

10 DTU – OPTIMIZATION OF SHARED MOORING LINE DESIGN

This section presents the design optimization of a shared mooring line system by means of a surrogate model. The surrogate model is generated using HAWC2 simulation results, with different design parameters. The shared mooring line design in Morro Bay is selected for optimization, and the details of the baseline design can be found

in ([31],[32],[33]). First, the shared mooring line design in Morro Bay is introduced briefly and then HAWC2 results for different design parameter results are given. Subsequently, the surrogate model generation and its use for design optimization are presented together with the optimization results.

10.1 Shared mooring line design

The shared mooring line dynamic and loads are investigated by HAWC2 and published in ([31],[32],[33]). In [31], the dynamics of shared mooring line designs in Morro Bay and Grand Canaria sites were investigated. Natural frequencies and mode shapes of shared mooring line designs were computed and compared with single turbine designs. The effect of shared mooring line length on natural frequencies were also investigated in that study. It is found that shared mooring design in Morro Bay which has 870 meters water depth with taut mooring lines has better performance with shared mooring line than the design in Grand Canaria site with catenary lines.

In [32], response of shared mooring line design in Morro Bay site was computed for DLC1.6 load case according to IEC standards [34] and effect of second order wave load effects were investigated. Results of the study show that second order wave loads are important even in deep water conditions that are typical for floating wind turbines. Furthermore, the shared mooring farm response is significantly different than individually moored turbines, to the extent that the maximum mooring line loads are increased by 21%.

In [33], the dynamics of shared mooring lines were presented for both Morro Bay and Grand Canaria sites, and some load case analysis with different wind and wave conditions were performed for shared mooring line design in Morro Bay site. The study showed that the turbines in shared mooring line design had similar response and performance under steady waves and wind, the upstream mooring line had about 30 % higher loads than the single turbine. Furthermore, the upstream turbine's surge displacement was almost double compared to the downstream turbine and to the single turbine.

In this report, the optimization of shared mooring line design in Morro Bay site is presented. Figure 10-1 shows the single turbine design, the HAWC2 coordinate system, the general dimensions and the mooring line sections for Morro Bay site. The water depth in the site is 870 meters and the turbine is IEA WIND 15 MW turbine with 240 meters rotor diameter. The design has a spar buoy floater with four mooring lines whose sections and connection to the floater are shown in the figure.

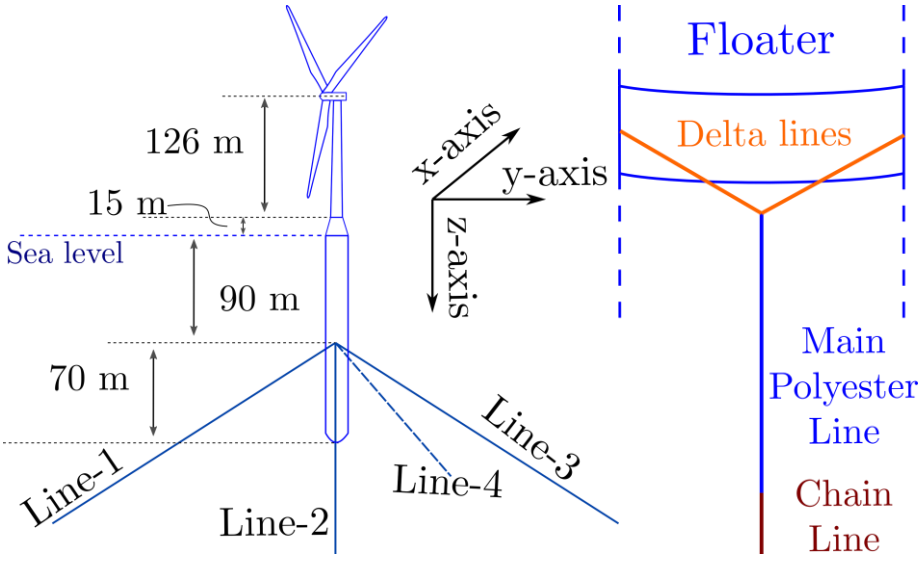

Figure 10-1: Single turbine design with 4 mooring lines and mooring line sections at Morro Bay

Table 10-1 shows the properties of the delta lines, the main polyester lines and the chain sections of the mooring lines. In the vicinity of connection points at floater and the seabed, there are chain sections. However, their lengths are very small compared to the polyester section which are very elastic compared to the chains.

	Delta line	Main polyester	Chain line
Length [m]	50.0	1020.8	183.7
Diameter [mm]	90	205	85
Equivalent D [mm]	162	164	171
Dry mass [kg/m]	161.0	28.6	179.6
Axial stiffness [kN]	6.92e5	2.68e5	7.71e5

Table 10-1: Properties of mooring line sections at Morro Bay

Figure 10-2 shows the shared anchor design between two turbines for the Morro Bay site. The initial distance between the turbines is 1680 meters which is equivalent to 7 rotor diameters of the IEA WIND 15 MW. The lines have the same properties as for the single turbine case except for Line-1, Line-7 and Line-9. Line-1 and Line-7 have delta lines on the floater side whose properties are identical to the Delta line properties of other mooring lines. After the Delta line sections, the polyester section starts and Line-9 consist of only polyester section. The polyester section length of Line-1 and Line-7 is 783.4 meters whereas Line-9 has 600 meters length.

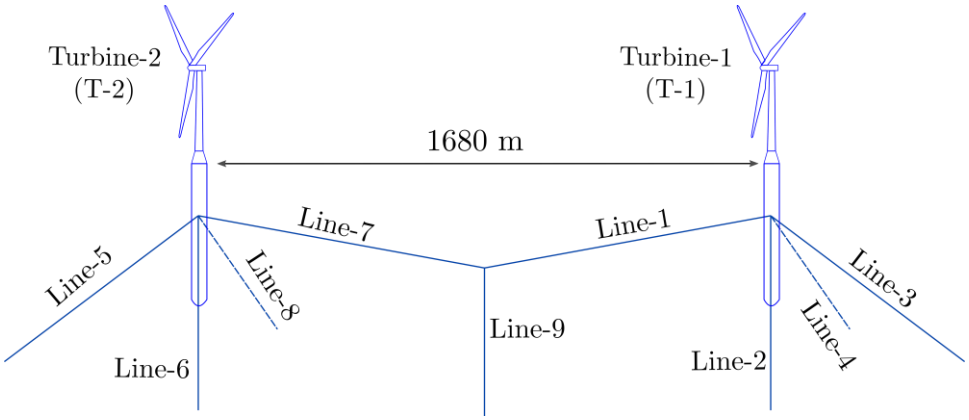

Figure 10-2: Shared anchor design with 2 turbines in Morro Bay site

10.2 HAWC2 analysis

The length of Line-1 and Line-7 is chosen as single design parameter and both line lengths are changed from 833.4 meters to 733.4 meters which corresponds to 50 meters longer and shorter line lengths compared to 783.4 meter which is the original design length of the lines.

First equilibrium point of the system without any wave or wind load is determined and compared with respect to the shared mooring line (Line-1/7) length change. Additional damping forces are applied as external forces which are function of the floater velocity in the equilibrium analyses, so the analysis time is shortened significantly. The turbine system together with mooring lines are released from initial points which are shown

in Figure 10-2 and simulated for 500 seconds with external damping forces. The surge, sway, pitch and yaw motions from the initial state for both turbines are shown below. The x-axis of the plots shows the length change of Line-1 and Line-7. Shared mooring lines lengths are changed by 50 meters so that the lines become 50 meters shorter and 50 meters longer than their original lengths. Sway and yaw motions are mostly insensitive to Line-1/7 lengths, even there are some nonzero values for these channels after 35 meters longer version of the shared lines, these values are very small compared to surge and pitch. The main effect of shared mooring line length is in surge and pitch directions. Floaters stay at their initial position when the Line-1/7 are 6 meters longer than their original lengths. As Line-1/7 get longer, the distance between turbines increases.

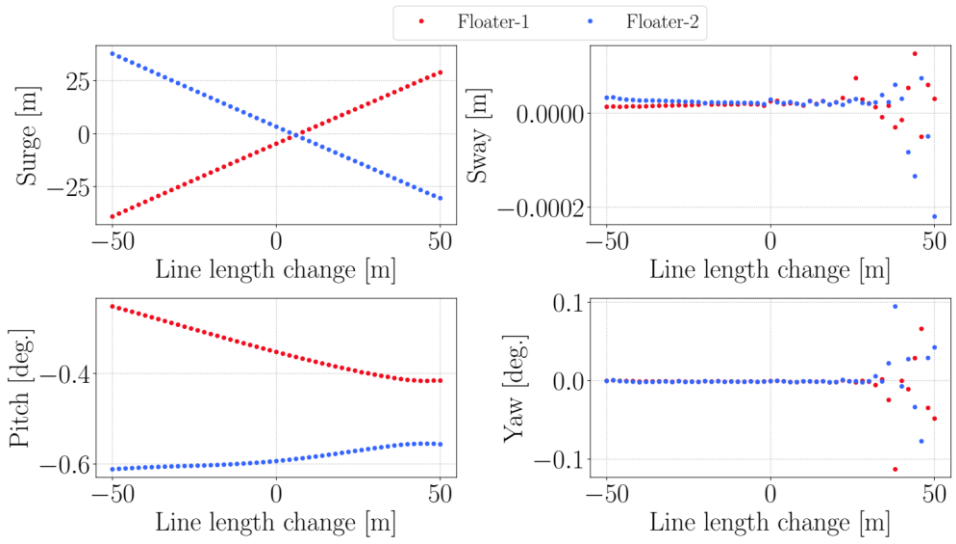

Figure 10-3: The surge, sway, pitch and yaw motions of both turbines (floaters) for different length of shared mooring lines (Line-1/7)

Figure 10-4 shows mooring line tension forces at the equilibrium points for different lengths of Line-1/7. The tension forces at side mooring lines (Line-2/4/6/8) change from 5 MN to 6 MN forces as Line1/7 gets longer. On the other hand, fore and aft mooring line (Line-1/3/5/7) forces decrease more than 10 MN from the shortest version to the longest version of Line-1/7. Line-9 tension force also decreases more than 4 MN from short case to long case of shared lines. Line-5 and Line-3 tension forces become more than 12 MN when the shared mooring lines are 50 meters shorted that their original length.

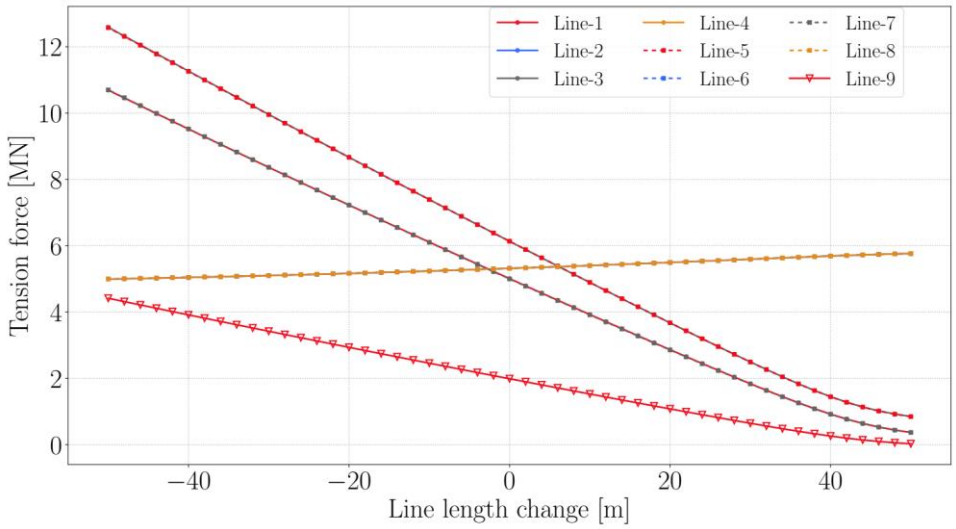

Figure 10-4: Mooring line tension forces for different lengths of shared mooring lines

Equilibrium results showed that the length of Line-1/7 has significant effect on surge/pitch direction and the tension forces of fore-aft mooring lines. On the other hand, sway direction and side mooring lines are almost insensitive to the lengths of Line-1/7.

After the equilibrium analysis, response of the system is computed for steady wind at rated wind speed (11 m/s) and irregular waves which are shown in Figure 10-5. The power spectrum of irregular waves is also given in Figure 10-6. The total simulation time for response analyses are 800 seconds where the first 200 seconds are taken as initialization period by applying external damping forces. The maximum and mean floater motions from their equilibrium points are computed together with maximum mooring line tensions for generating the surrogate model. The results of these outputs are given in the next Section 10.3 together with the results of surrogate model.

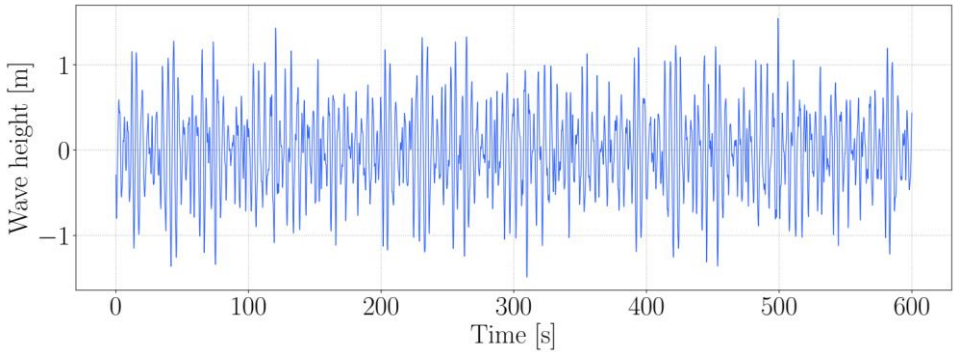

Figure 10-5: Time series of wave heights at Floater - 1

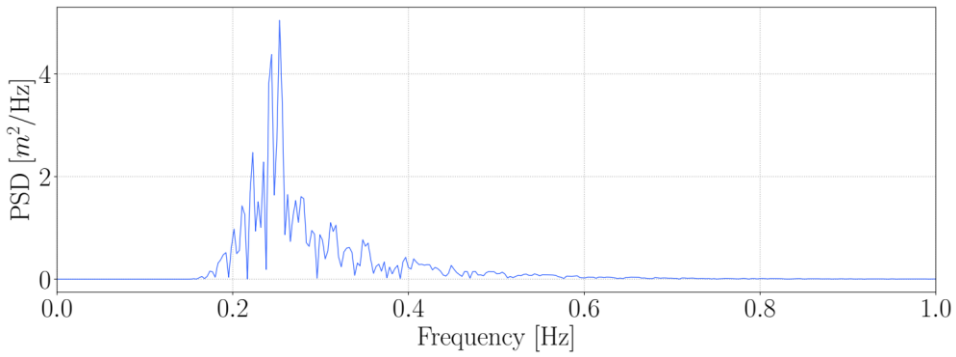

Figure 10-6: Power spectrum density of wave heights at Floater-1

10.3 Surrogate model

In this section we describe the procedure followed to generate a surrogate model of the two wind turbines systems shown above in Figure 10-2. Through the surrogate model, it will be possible to optimize the design of the two wind turbine systems efficiently, without the need of running expensive hydro-aero-servo-elastic simulations with HAWC2 within the design optimization analysis. In fact, HAWC2 is used to generate a dataset, which in turn is used to train a surrogate model. Several types of surrogate models are available and have been used in the literature. Herein, we will rely on a neural network.

First the data base is generated. As mentioned above, we consider at this stage one design parameter, even though the proposed methodology can be extended to several design parameters. This parameter is the length

of the mooring lines number 1 and 7 (see Figure 10-2). In particular, we consider a variable elongation or shortening of the mooring lines with respect to the reference baseline design. As a result, we vary the length of the mooring lines 1 and 7 by adding an elongation dL, such that the total mooring line length is L+dL. The variable dL varies between –50 m and +50 m with steps of 2 m, i.e. dL = -50 : 2 : +50 m. The data base consists of several response quantities, evaluated for the different values assumed by dL. These response quantities are the maximum values of the six displacements of the tower bottom (surge, sway, heave, roll, pitch, yaw) and the maximum tensions in the nine lines composing the shared mooring system.

Once the data base has been generated, it is used to train a neural network. For this purpose, we rely on the python library TensorFlow, which is an open-source library for machine learning. The neural network consists of an input layer with only one input parameter (dL), and an output layer with 21 parameters (the six displacements of each wind turbines plus the nine tensions in the associated mooring lines). The neural network has also three hidden layers densely connected with 10, 30, and 20 neurons, respectively. The ReLu activation function is considered for all of the hidden layers. The training is performed over 2500 iterations using as optimizer the Adam algorithm, with a learning rate set to 0.001. During the optimization analysis for training the model, the function minimized is the mean squared of error between data and model predictions. For training and testing the neural network model we split the data base in two parts. 90% of the data base is used for training, and 10% is used for testing the neural network model on data that the model has not seen during training. The figure below shows the evolution of the loss function during the optimization analysis performed for training the model.

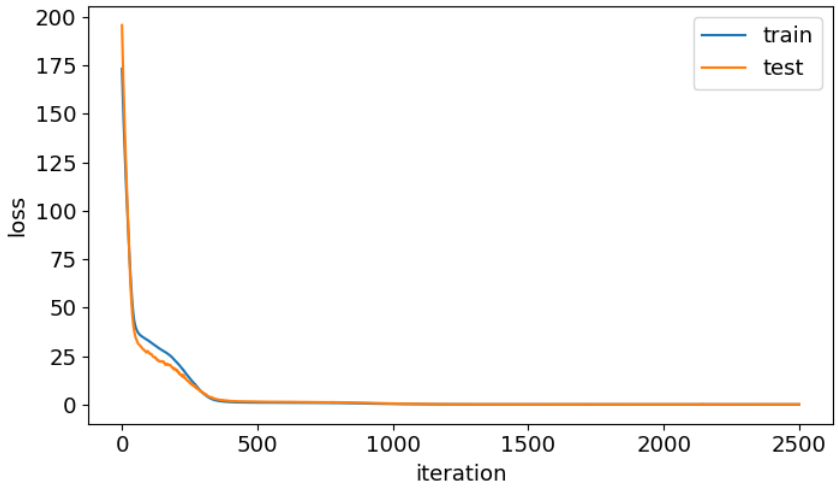

Figure 10-7 Evolution of the error function during the optimization analysis performed to train the neural network surrogate model. The error (loss) is evaluated with two sub-sets of the dataset, the training set and the test set

Once the model has been trained, we compare the prediction of the two wind turbine system response of the neural network against the response obtained with the HAWC2 model (I.e. the values in the data base). For the sake of brevity, in the following we show the comparison for the surge response of the two wind turbines, and for the tension in the mooring lines number 1, 7, 9, 5.

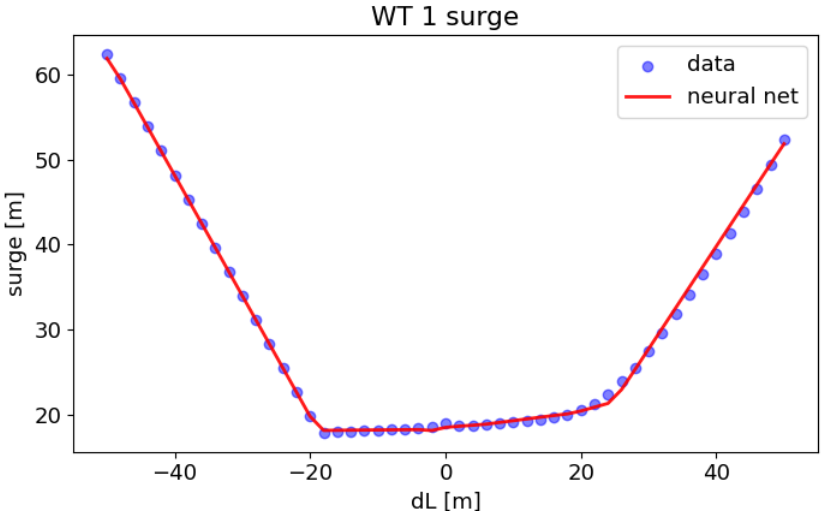

Figure 10-8: Surge displacement of wind turbine 1 for the sampled values of the design variable dL. Comparison of the estimated values of the trained neural network with the response evaluated with HAWC2

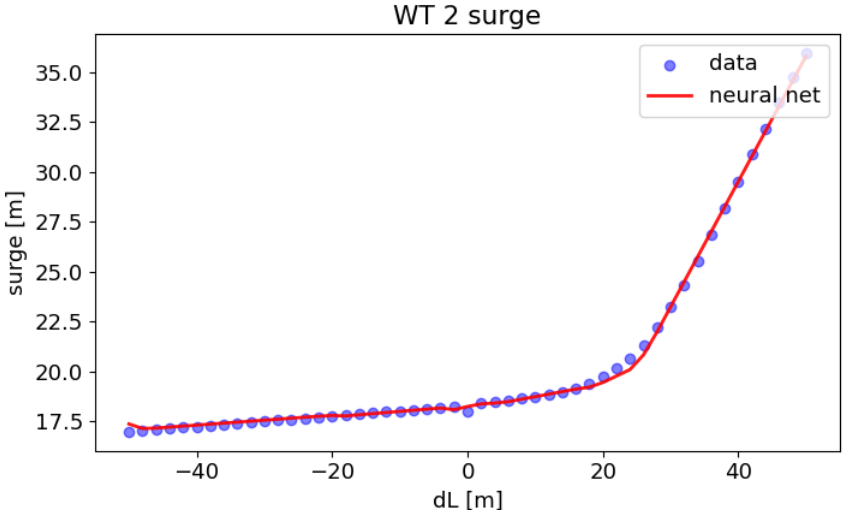

Figure 10-9: Surge displacement of wind turbine 2 for the sampled values of the design variable dL. Comparison of the estimated values of the trained neural network with the response evaluated with HAWC2

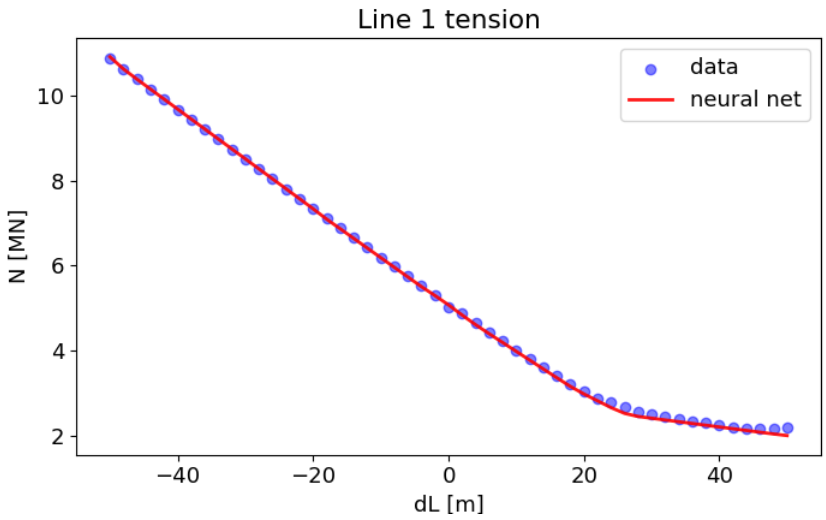

Figure 10-10: Tension in the mooring line 1 for the sampled values of the design variable dL. Comparison of the estimated values of the trained neural network with the response evaluated with HAWC2

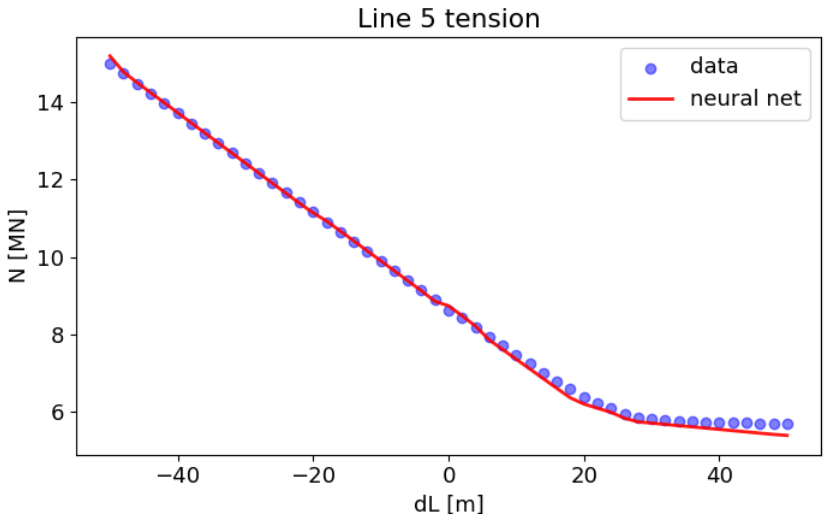

Figure 10-11: Tension in the mooring line 5 for the sampled values of the design variable dL. Comparison of the estimated value of the trained neural network with the response evaluated with HAWC2

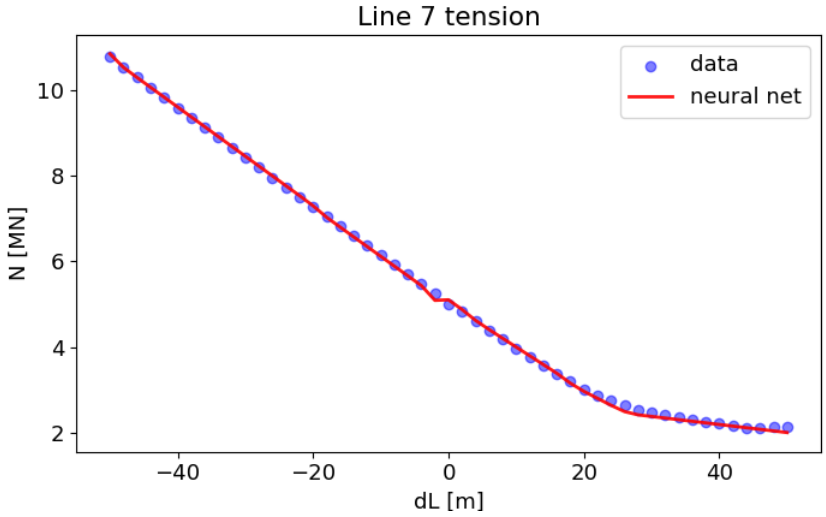

Figure 10-12: Tension in the mooring line 7 for the sampled values of the design variable dL. Comparison of the estimated value of the trained neural network with the response evaluated with HAWC2

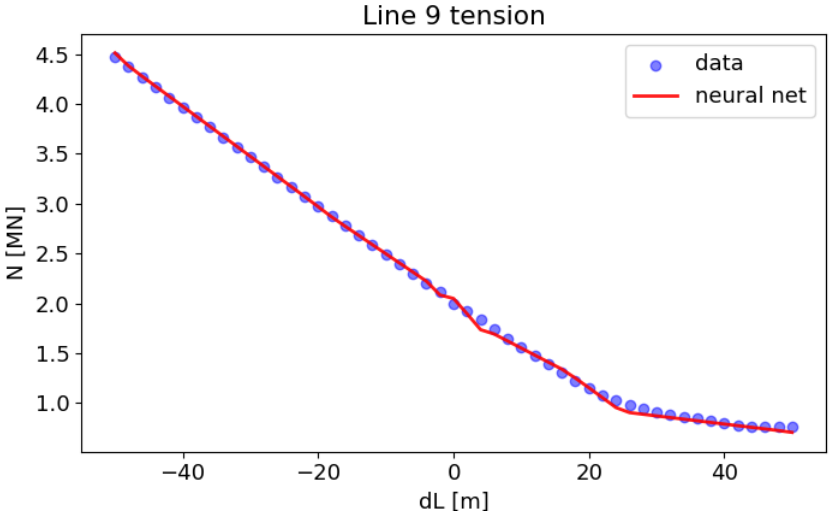

Figure 10-13: Tension in the mooring line 9 for the sampled values of the design variable dL. Comparison of the estimated value of the trained neural network with the response evaluated with HAWC2

10.4 Design optimization of shared mooring system

In this section we present the problem formulation and the results for the design optimization of the shared mooring line system depicted in Figure 10-2. We consider one design variable, dL. As it has been mentioned it defines an elongation or a shortening of the original length of the mooring lines number 1 and 7. We seek to minimize the length of the mooring lines 1 and 7, with constraints on the maximum surge of the two wind turbines and of the maximum tension in the mooring line number 5. The optimization problem is stated as follows:

$$\min dL$$
$$s.t.\ g_1 = u^1_{max} - \overline{u} \leq 0$$

$$g_2 = u_{max}^2 - \overline{u} \leq 0$$
$$g_3 = T_{max}^5 - \overline{T} \leq 0$$
$$-50\,m \leq dL \leq +50\,m$$

where $u_{max}^1$is the maximum surge of the first wind turbine in time, $u_{max}^2$is the maximum surge displacement in time of the second wind turbine, $\overline{u}$ is the maximum allowed value of surge set here to 30 m, $T_{max}^5$is the maximum tension value in the mooring line number five, and $\overline{T}$is the maximum accepted value of tension in the mooring line number five set here to 10 MN. For optimization, we use the gradient-based algorithm SLSQP implemented in the SciPy library, which is an open-source python library for scientific computing. We provide the analytical gradients of the constraint functions to SLSQP (i.e. ∇g_1, ∇g_2, ∇g_3), by using the automatic differentiation capabilities available in TensorFlow neural network models. In this way, the optimization algorithm is capable of performing the numerical design optimization relying on accurate first-order information of the surrogate model considered. The design variable dL is initialized to +50 m, and the optimization converges in 7 iterations. The output produced by the SLSQP algorithm at the end of the optimization analysis is the following:

```
Optimization terminated successfully (Exit mode 0)
            Current function value: -11.079041449218876
            Iterations: 7
            Function evaluations: 9
            Gradient evaluations: 7
x = [-11.07904145]
f = -11.079041449218876
```

As it can be seen, the final optimized value of the design variable is dL=-11.08 m. That is, a shortening of 11.08 m with respect to the initial length of the mooring lines 1 and 7 is prescribed. The figure below shows the evolution of the objective (dL) and constraint functions during the optimization iterations. It should be noted that the values have been normalized to allow for a joint representation.

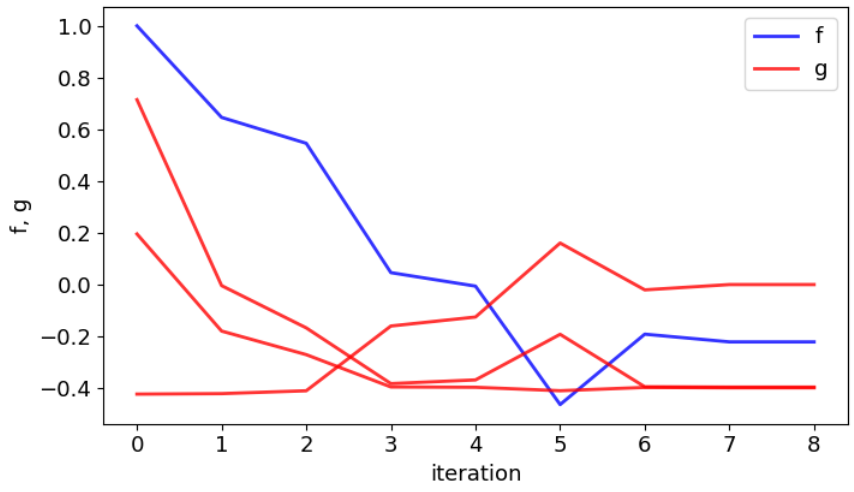

Figure 10-14: Evolution of normalized objective function and constraint functions during the design optimization analysis with the surrogate model

Above, in Figure 10-14 it can be observed that in correspondence of the final optimized design point all the constraint are satisfied, that is, their values are less or equal to zero. At the end of the optimization, the active constraint (the one governing the design) is the one on the maximum tension in the mooring line number five.

10.5 Conclusion

In this study, optimization of shared mooring line was carried out with one design parameter. The shared mooring line design at Morro Bay was used and length of shared mooring lines were selected as design parameter. HAWC2 analysis were performed for different design parameters and the results are used to generate a surrogate model which is used in optimization process. Results show that surrogate model is very accurate and suitable for optimization. The optimization results give the optimum design with 11.08 meters shorter shared mooring line length than the original design. Since the current setup is working for optimization purposes, it is planned to use it with multiple design parameters in the future for optimization of shared mooring lines.

11 CONCLUSION AND OUTLOOK

This report presents results of the exploration of innovations and breakthroughs of station keeping systems for FOWT. Several aspects have been investigated to reduce mooring system costs.

In deliverable D2.2 is described the optimization screening tool developed for mooring systems optimizations regarding the total costs of materials. Its efficiency has been proven, except for harsh environments. In the present report, a study is presented on two peak load reduction systems, TFI and IMS, as part of the subtask 2.3.1. These systems act respectively as a spring and a hydraulic damping system. They have been implemented to the optimization screening tool in order to be able to optimize TFI and IMS-equipped mooring systems. Their MBL and unit number were the optimization parameters, in addition to the line materials and anchors. TFI and IMS costs functions were provided by the owners. This has resulted in more complex and time-consuming optimizations, but whose efficiency could be proven. However, the optimization tool continued having difficulties to show good results in harsh environments. Regarding the benefits of TFI, the system was able to reduce the peak loads in the mooring lines of site B Gran Canaria by 28% with ActiveFloat platform and by 47% with WindCrete, which reduced the mooring cost by 18% and 27% respectively for ActiveFloat and WindCrete. IMS showed reductions in the same ranges for this site. For site C Morro Bay, the results showed smaller peak loads reductions with WindCrete, of 14% with IMS and 2% with TFI, and even showed peak load increase with ActiveFloat. Indeed, this site has a water depth of 870 meters and no current, resulting in different loading and behaviour of the platform when compared to the other sites, and the use of peak loads reduction systems showed to be less relevant at this stage. For site A West of Barra, TFI helped reducing the peak loads by 32% but without any benefit to the total cost of the mooring system due to the high number of units used (24), consequence of the large number of mooring lines (12). No results could be presented with IMS on this site because of the increase of surge that they induced to the platform, leading to increasing offsets.

Within the objective to reduce overall mooring lines costs, subtask 2.3.2 investigated various solutions to reduce mooring footprint. Different mooring configurations have been proposed, and were evaluated the influence of tension ratio, length ratio and clump weights on mooring footprint, motions of floater, mooring line tensions and mooring fatigue life. The tension ratio showed a larger influence on maximum floater motions than the two remaining ratios. Indeed, larger tension ratio led to increasing the mooring line length and consequently, the mooring footprint. Adding clump weights showed that it could efficiently reduce the mooring footprint and maximum mooring tensions but induced 12% larger mooring tension fatigue damage.

To reduce the total anchor costs, subtask 2.3.4 investigated innovative layouts such as shared anchor and shared mooring lines configurations. The study has been conducted on sites B Gran Canaria and C Morro Bay. For both sites, the overall costs of shared anchors layouts obtained were roughly identical to the one of classic layouts. Indeed, anchors costs decreased, but line lengths increased in order to respect spacing and touch down point criteria. Regarding shared mooring lines layouts, costs reductions of 50% for ActiveFloat Morro Bay have been reached thanks to a decrease in the number of buoys needed. Nevertheless, the installation costs were not considered in this study and are expected to decrease when compared to classic layouts, for both shared anchors and shared mooring lines configurations. It has been noted in the case of share mooring lines that practical aspects such as access and manoeuvrability around the turbines shall be accounted. Also, more advanced studies on wake effect and relative turbine positions could be carried out to potentially reduce the spacing. Finally, it should be reminded that no fatigue analysis was conducted during this study, and regarding the results of Report D2.2, fatigue might be driving for the design of this layouts.

In sight of the conclusions about the fatigue of the mooring systems in deliverable D2.2 [1], investigations on fatigue analysis of the mooring systems of ActiveFloat at Gran Canaria site have been conducted and showed that TFI and IMS have an insignificant influence on the lifetime of the mooring lines, even when their size (MBL)

was adapted to the ranges of tensions observed in the fatigue load cases. In addition, subtask 2.3.3 investigated the benefit of tuning of the controller, to reduce mooring fatigue. The study showed that the blade pitch controller has a considerable effect on the DEL of the mooring lines and therefore on the fatigue development. Adapting the gain Kp and Ki of the blade pitch controller has led to a promising result of 6% reduction of the DEL of the main line, for a power loss of up to 7%. The additional feed-in of the nacelle fore-aft velocity was also investigated and led to a DEL decrease up to 5% for power loss limited to 2%. In general, adapting the control mechanism of the turbine to decrease mooring line fatigue is a promising path and worth further investigation.

Therefore, the present work, with the detailed results of the investigations on the benefits of peak loads reduction systems, solutions to reduce mooring footprint, shared mooring lines and shared anchors layouts, and the benefits regarding fatigue analysis of peak loads reduction systems and controller tunning, provides a number of reference cases and design improvements that each contribute to reduced cost of energy for floating offshore wind technology.

12 REFERENCES

[1] Deliverable 2.2 Design analysis and optimization of mooring & anchoring system for FOWT, Corewind consortium, 2020.

[2] Deliverable 2.1, Review of the state of the art of mooring and anchoring designs, technical challenges and identification of relevant DLCs, Corewind consortium, 2020.

[3] Orcina, [Online]. Available: https://www.orcina.com/. [Accessed 08 2022].

[4] NREL, "OpenFast," [Online]. Available: https://www.nrel.gov/wind/nwtc/openfast.html.

[5] NREL, "GitHub: OpenFast," [Online]. Available: https://github.com/OpenFAST. [Accessed 05 2022].

[6] Torben J. Larsen and Anders M. Hansen. How 2 HAWC2, the user's manual. Tech. rep. DTU Wind, 2020.

[7] Madsen, H. A., Larsen, T. J., Pirrung, G. R., Li, A., and Zahle, F.: Implementation of the blade element momentum model on a polar grid and its aeroelastic load impact, Wind Energy Science, 5, 1–27, https://doi.org/10.5194/wes-5-1-2020, 2020.

[8] Li, Ang, Georg Raimund Pirrung, Mac Gaunaa, Helge Aagaard Madsen, and Sergio González Horcas.: A computationally efficient engineering aerodynamic model for swept wind turbine blades, Wind Energy Science 7, 1, https://doi.org/10.5194/wes-7-129-2022, 2022

[9] Shabana, A. A.: Dynamics of multibody systems, Cambridge University Press, Cambridge, 2013.

[10] CH Lee. Wamit Theory Manual. Tech. rep. 95-2. Massachusettes Institute of Technology Department of Ocean Engineering, 1995.

[11] V.Thorey, Benderopt library, [Online]. Available: https://pypi.org/project/benderopt/. [Acessed 08 2022].

[12] V.Thorey, Python GUIs for humans, [Online]. Available: https://pypi.org/project/PySimpleGUI/. [Accessed 08 2022].

[13] H. T. N. B.-F. J. Ocean Engineering 206, "Large-scale testing of a hydraulic non-linear mooring system for floating offshore wind turbines", 2020.

[14] DNVGL-ST-0437 Loads and site conditions for wind turbines, DNVGL, 2016.

[15] Banque de France, "Taux de change (parités quotidiennes)," [Online]. Available: https://www.banque-france.fr/statistiques/taux-de-change-parites-quotidiennes-23-mars-2020. [Accessed 06 2022].

[16] Deliverable D1.2 Design Basis, Corewind consortium, 2020.

[17] DNVGL, "DNVGL-ST-0119 Floating wind turbine structures," 2021.

[18] DNVGL, "DNVGL-OS-E301 Position mooring," 2018.

[19] Bridon, "Bridon Fiber Rope Catalogue, Fibre".

[20] Bexco, "DeepRope Manual 2004: Polyester & Dyneema mooring ropes manual 2004," 2004.

[21] Deliverable 1.3 Public design and FAST models of the two 15MW floater-turbine concepts, Corewind consortium, 2020.

[22] C. (USTUTT/UPC/COBRA/ESTEYCO/DTU), "Public design and FAST models of the two 15MW floater-turbine concepts," 2021.

[23] Stenlund, Tiril. *Mooring system design for a large floating wind turbine in shallow water*. MS thesis. NTNU, 2018.

[24] Smith, Russell J., and Colin J. MacFarlane. "Statics of a three-component mooring line." Ocean Engineering 28.7: 899-914, 2001.

[25] Ma, Kai-Tung, et al. *Mooring system engineering for offshore structures*. Gulf Professional Publishing, 2019.
[26] Controller: ROSCO. Version 1.0.0, https://github.com/NREL/ROSCO, 2020.
[27] Deliverable 1.4 Methods for multiple floaters and dynamic cables at farm level, Corewind consortium, 2021.
[28] Offshore Anchor Data for Preliminary Design of Anchors of Floating Offshore Wind Turbines, ABS, 2013.
[29] Deliverable 4.6 Framework for the prediction of the reliability, economic and environmental criteria and assessment methodologies for Moorings and Foundations, DTOCEAN consortium, 2015.
[30] Balmoral product brochure, 2021.
[31] Gözcü O. and Kontos S. and Bredmose H. and Bailey T. and Borisade F., Methods for multiple floaters and dynamic cables at farm level, Corewind D1.4, 2021.
[32] García R. N. and Horcas S. G. and Jurado A. P. and and Kontos S. and Gözcü O. and Bredmose H. and Özinan U. and Mahfouz M. Y. and Fontanella A. and Facchinetti A. and Belloli M., Methods for nonlinear wave forcing and wakes, Corewind D1.5, 2022.
[33] Gözcü O. and Kontos S. and Bredmose H., Dynamics of two floating wind turbines with shared anchor and mooring lines, J. Phys.: Conf. Ser. 2265 042026, 2022.
[34] IEC 61400-3. International Electro technical Committee IEC 61400-3: Wind Turbines part 3: Design Requirements for Offshore Wind Turbines. Edition1, Geneva, 2009.